



Art restoration and archaeological material study are inseparably related to scientific investigation and scientific data processing of the information. This reality makes the mentioned field of the most attractive one and a very generous one for professional development.

The e-proceeding, published by INTEGRA NATURA ET OMNIA - INOE, brings together a large part of the contribution to The Third Balkan Symposium on Archaeometry organized in Bucharest on 29 and 30 October 2012, and is following the close related volume that was published by The Kultur Intitute University from Istanbul. The biennial event gathers scientists, conservators, restorers, architects, companies, decision-makers, professors and students involved in projects on all aspects of archaeometry, the application of modern experimental methods and techniques used in investigation, identification and dating of ancient artifacts, as well as related fields of archaeology and art history. Appreciated researchers from multidisciplinary groups, not only from Balkans, have been invited to contribute with keynote speeches and to support the dissemination of recent results. The event continues the tradition of previous symposiums, the first being held in Ohrid - Republic of Macedonia in 2008 and the second in Istanbul – Turkey in 2010.

Special support for present e-proceeding publishing have been received from Dr. eng. Roxana Savastru – general manager of INOE, who was sustaining all initiatives of the Center for Restoration by Optoelectrical Techniques and who permanently, and who generously offers her experience and professional skills.

The editors wish to remind to all participants to The Third Balkan Symposium on Archaeometry that the devoted specialist and initiator of the Balkan Network on Archaeometry – permanently close to each edition organization- is Prof. Prof. Biljana Minceva-Sukarova from Institute of Chemistry, Faculty of Natural Sciences and Mathematics "SS. Cyril & Methodius" University, Republic of Macedonia.

Proceedings of the 3rd Balkan Symposium on Archaeometry

29-30 October 2012
Bucharest, Romania



Editors:
Roxana Radvan
Sevim Akyuz
Monica Simileanu
Vivian Dragomir

TABLE OF CONTENTS

TRAINING WITHOUT BORDERS: ON-LINE OPEN PLATFORMS FOR TRAINING IN SCIENTIFIC INVESTIGATION FIELD <i>ROXANA RĂDVAN</i>	3
STUDY AND CONSERVATION OF A GLASS VASE EXCAVATED IN DURRES <i>IRIS BAKIRI AND FREDERIK STAMATI</i>	5
SPECTRAL DATABASE OF RENAISSANCE FRESCO PIGMENTS BY LIBS, LIF AND COLORIMETRY <i>V. SPIZZICHINO, L. CANEVE, F. DE NICOLA AND R. FANTONI</i>	9
PRELIMINARY STUDY OF SOME IRON SLAGS FROM NORTHERN AND CENTRAL ALBANIA <i>EDLIRA DUKA, OLTA ÇAKAJ, ZAMIR TAFILICA, ILIR GJEPALI, FREDERIK STAMATI, NIKOLLA CIVICI, TEUTA DILO</i>	17
STUDY OF VULNERABILITY AND CHARACTERIZATION OF STONE COLUMNS FROM SEVILLE (SPAIN) <i>R. ORTIZ, P. ORTIZ, J.M. MARTIN, M.A.GOMEZ-MORÓN, T. CORDERO, M.A. VÁZQUEZ, M.P. MATEO, G. NICOLAS</i>	23
MULTISPECTRAL IMAGING - A FAST AND ACCURATE FOR ARTWORKS' DOCUMENTATION <i>LUCIAN RATOIU, LAURENȚIU ANGHELUȚĂ</i>	28
THE COMBINED USE OF ARCHAEOMETRIC TECHNIQUES FOR NON-INVASIVE ANALYSIS OF PAINTINGS: THE STUDY OF ALBANIAN ICONS BY ONOUFRI <i>ENRICO FRANCESCHI, DION NOLE AND STEFANO VASSALLO</i>	35
NON-DESTRUCTIVE INVESTIGATION USING RAMAN SPECTROSCOPY OF STONE ARCHAEOLOGICAL ARTIFACTS FROM APESOKARI - CRETE <i>G. FLOUDA, G. VAVOURANAKIS, TH. KATSAROS, TH. GANETSOS AND B. TSIKOURAS</i>	45
ACTIVE FAULTS AND ANCIENT ROMAN SETTLEMENTS IN AEGEAN REGION <i>MUSA TOKMAK</i>	52
PRELIMINARY INVESTIGATION OF SOME COPPER ALLOY MEDIEVAL OBJECTS FROM THE NORTHERN ALBANIA <i>OLTA ÇAKAJ, EDLIRA DUKA, ZAMIR TAFILICA, FREDERIK STAMATI, NIKOLLA CIVICI, TEUTA DILO</i>	58

CHEMICAL AND MINERALOGICAL STUDY OF A YAMUR FROM THE THIRTEEN CENTURY	
<i>M.A. GÓMEZ-MORÓN, R. ORTIZ, P. ORTIZ, J.M. MARTIN, R. BAGLIONI AND A. BOUZAS</i>	65
DOCUMENT PAPER TREATED WITH NANOPARTICLES INVESTIGATED BY ATOMIC FORCE MICROSCOPY	
<i>SANDA MARIA DONCEA, RODICA MARIANA ION AND JACOBUS F. VAN STADEN</i>	69
COPPER BROMIDE LASER IN CULTURAL HERITAGE MONUMENTS RESTORATION	
<i>V.ATANASSOVA, K.DIMITROV, M.GROZEVA, M.SIMILEANU & R.RADVAN</i>	74
MICRO-RAMAN SPECTROSCOPY FOR PIGMENTS IDENTIFICATION IN A 19TH CENTURY MANUSCRIPT FROM BUKOVINA	
<i>CRISTINA MARTA URSESCU, ELENA ARDELEAN AND LAURA URSU</i>	79
CONSERVING AND INVESTIGATING A HISTORIC TEXTILE WITH A PREVIOUS ADHESIVE TREATMENT	
<i>E. P. TSVETKOVA</i>	84
NEW DATABASE MAPPING SYSTEM (NDMS) – A NON-DESTRUCTIVE METHOD OF BUILDING STONES’ ANALYSIS USED IN THE STUDY OF THE HISTORICAL CITY WALL OF CLUJ-NAPOCA, ROMANIA	
<i>P.C. RĂCĂȚĂIANU</i>	88
GAMMA IRRADIATION - A CHANCE FOR TEXTILE AND LEATHER CULTURAL HERITAGE ARTIFACTS’ CONSERVATION	
<i>CORNELIU PONTA, VALENTIN MOISE, MARIA HAIDUCU, MARIA GEBĂ, LUCRETIA MIU, IOANA STANCULESCU</i>	96
THE STUDY OF ARCHAEOLOGICAL CERAMIC SAMPLES FROM SATU MARE COUNTY, ROMANIA	
<i>BEÁTA KOCSIS, EMŐKE NAGY, RÉKA BARABÁS, MÁRTA GUTTMANN ZSOLT KOVÁCS-MOLNÁR</i>	102

Training without Borders:

On-line open platforms for training in scientific investigation field

Roxana RĂDVAN

National Institute of Research and Development for Optoelectronics INOE 2000

Bucharest, România

A huge amount of knowledge has been accumulated due to advanced scientific research addressed to any domain. While today we accept that the presence of the modern equipment that assists physician procedure next to the patient can have its own healing merits, but nevertheless it is impossible to have advanced laboratory and expert medical practitioners to be present wherever their expertise is needed. In spite of a very similar development in respect with the methods and instrumentation for *monitoring – investigation-diagnosis* and *intervention* for cultural heritage goods, energies towards their use on larger scale are lower because of several prejudices, like: high costs, limited access to such infrastructure, high-technological skills required. Almost all the scientific equipment and installations are now accessible and controlled by dedicated computers. In this category there are many important and already recommended fast techniques of investigation based on non-contact, non or micro invasive methods, which do not request samples' preparation and do not involve long time processes.

The huge popularity of various e-learning means and programs takes them out from un-conventional. All forms of electronically supported learning and teaching are known, accepted and tested in almost all corners of the world. The certain success of the e-learning is one of the most solid reasons for the development of the e-training on new research skills and for on-line access to infrastructure addressed to artwork investigators, restorers, and conservators.

Nowadays, running projects for new instrumentation building, for data processing and simulation have at least several activities for demonstrations and must assure large access for potential users. Common international structures, programs and protocols are desired and permanently updated.

The advanced preoccupation developed by INOE, that became an appreciated running project in 2012, is focused on the design and construction of a complex system that will offer access to research infrastructure for cultural heritage investigation.

WWW *wATCH* - "Worldwide Open Workshop With Advanced Techniques for Cultural Heritage" - An open laboratory, or an open restoration workshop (studio) that benefits by updated technical and scientific assistance is a huge step simultaneously forward:

✓ a modern and harmonized education and training – it is less productive to allow any longer the fact that several European regions do not have yet the necessary resources to add updated laboratory to each main university, and obviously such laboratories will miss out the best maintenance staff and the chance to be constantly updated;

✓ a platform for early stage common experiments, involving invited well-known groups contribution to online experimental conditions setup, with experts counseling for experimental data interpretation and/or supervising – usually, the major concern of all scientific investigator facing new methods and techniques is related to collected experimental data interpretation. Any new method

beginning is raising scientific setup issues and data interpretation issues. The first are solved much faster and are not enough to guarantee the best data interpretation quality;

✓ an effective exploitation of the scientific infrastructure;

✓ an extended user-network and an instrument for know-how transfer in European and in extra-European regions;

✓ a catalyzer for high-specialized services commitments, particularly in extra-European areas – an extension of this collaborative multidisciplinary model is expected for immediately identified specific aims: European network of certified laboratories; an international database for material and procedures identifications; common anti-malpraxis procedures and self-control methods etc;

✓ a higher visibility of specialized research teams – it is an aspect of maximum interest according research groups access to EC R&D Programs; also for universities classification factor improving; and last but not least restoration groups/firms/specialists could apply their competences and could open on international restoration yards.

✓ best feedback for scientists and engineers – a very important observation from all projects for multidisciplinary domains is the correct identification of the demands from application practice and less useful to create a scientific solution to a theoretical issue.

“Worldwide Open Workshop With Advanced Techniques for Cultural Heritage - *WWW wATCH*” is the project that has been generated by the stringent necessity to promote the methods developed through disparate advanced researches and to apply these results in current practice, in complementary with the traditional methods, aiming to define their applicability limits from scientific and economic efficiency point of view.

In strong collaboration with many universities, museums, galleries, the project is already presenting the structure of the open laboratory and the operational resources correlation - informational, scientific and human resources and first Informational

and scientific infrastructure completion and detailed justification of each ensemble role, access technical conditions and definition of safe operation (limitations and protocols).

The first uploaded tutorials, courses, demonstrations and the first user clusters are available to <http://certo.inoe.ro/watch/index.html>.

The first groups of beneficiary of this open laboratory are students coordinated by Dr. Hamada Sadek Kotb from *Fayoum University, Department of Conservation* and will become active on second half of November 2012. Other active representatives of the research cluster belong to Bulgarian Academy of Science, Institute of Solid State Physics, particularly dr. Margarida Grozeva and dr. Peter Vassiliev.

The calendar of the on-line open workshop, including the real-time monitoring of the current on-site intervention, will be posted 2 months before each summer campaign. The first open workshop will be coordinated by Dr. Maria Dumbravician from National Arts University from Bucharest and, in 2013, will follow the activity from Tismana Monastery, Romania.

This project is delivering a significant part of the complex workstation for high education, training and early research stages on cultural heritage conservation topics, it is a platform of collaboration which will generate scientific “profit” based on collected feed-backs, and could become an important and strong portal for international services towards universities, museum, galleries etc.

The involved consortium strongly emphasize that the workstation principles are available for many other sorts of industries and research domains, i.e. medical and pharmaceutical laboratory, food industry, forensic investigation and others – opening opportunities for by-products or services, and finally more turnover capital.

ACKNOWLEDGEMENT

The presented activities are part of the national project *World Wide Open Workshop with Advanced Techniques for Cultural Heritage*, funded by ANCS, CNDI – UEFISCDI, Partnerships in priority domains, project number: PN-II-PT-PCCA-2011-3.2-0356.

Study and conservation of a glass vase excavated in Durres

Iris Bakiri

University of Tirana, Center of Applied Nuclear Physics, Tirana, Albania

Frederik Stamati

Conservator, Tirana, Albania

Abstract: The goal of this paper is to present a short study on the conservation of a glass vase excavated in the city of Durres. The amassment of glassware consisted on 249 pieces. The fragments of the glassware were studied with optical microscopy and x-ray florescence method. After the different examination there were found two kind of colored glass. The rebuilding of the vase was very difficult. The reconstruction of the vase run into a lot of difficulties related to a further deterioration due to erosion of broken surfaces. In the end of the conservation it was revealed that we were dealing flower vase with a height of 51cm and 20cm diameter is the biggest and most beautiful vase excavated in Albania.

1 INTRODUCTION

In early 2002 an amassment of glassware (Photo 1) reached the laboratory of Conservation and Archaeometry of the Institute of Folk Culture. The amassment of glassware consisted on 249 pieces of glassware and the pieces seemed to belong to one individual vase.

The remained pieces of the vase were excavated close to Byzantine wall of the foundations of the administration offices of the Sandjak of Durres built in 1088. The study and the restoration of this vase posed different kind of problems.



Photo 1: *The amassment of glassware consisted on 249 pieces*

2 METHODS

2.1 *Visual examination*

The work started with an optic examination and documentation of all the fragments of the vase. This was necessary for both examination of the conditions of the glassware and the future reconstruction of the vase. The examination showed that we were dealing with a vase worked with a complicated technology.

Fragments from the inner side of the vase are made up of colorless glass and with no decorative applications. After cleaning it from the mud it turned out that the glass of this side was well preserved, despite some isolated cavities and we also noticed a slight iridescence in this part of the vase.

The view appears different in the outer side of the vase. Fragments of this side were covered by mud and underneath it were possible to notice surfaces colored in brown and two filigree of white and opaque glass.

The layer colored in brown appears to be unattached and comes down easily revealing an iridescent and a stratified stable sub layer with different coloration especially in the breakdown. The

brown color can be dissolved in water whereas iridescence vanishes by washing to reappear again after water evaporation.

One of the white glass filigree looks like an artificial filament twisted from a thin wisp of glass fibers (*Photo 2*).



Photo 2

Both filaments are attached to the surface of a vase by heating which is characteristic of the decoration “*vetro filigrana*”, used since 1527-1529 in Murano. In some parts of the vase due to the distention of the glass and the fine-drawn, the decoration dilates and seems to expand on the glass and it looks like a white opaque glass “*lattimo*” or the type “*vetro a fili*” (*Photo 3*).



Photo 3

2.2 Analytical examination

Small colorless fragments from the inner side, fragments from the white filigree glass and the brown color material were analyzed to determine the elemental composition. First the samples were measured by x-ray fluorescence method at the Center of Applied Nuclear Physics in Tirana. The results obtained by these measurements showed the

presence of manganese in the sample of brown color, while lead and tin were present at the samples from the white filigree.

However, to obtain information on the composition of the narrow areas of the samples, they were analyzed by SEM-EDS in the Laboratory of Solid Body of the Department of Physics in the “Aristotle” University of Thessaloniki.

The results of the analyses are as follows.

Table 1. Elementary composition of glassware samples..

Elements	Glasware inner side	White glass ware filigree	Brown color glasware
Na ₂ O	12.78		
MgO		1.40	1.91
Al ₂ O ₃		3.78	6.35
SiO ₂	79.62	28.35	35.34
P ₂ O ₅		5.70	6.34
K ₂ O	2.51	1.38	3.82
CaO	5.09	6.35	18.57
MnO		3.38	15.43
Fe ₂ O ₃		3.14	6.49
SnO		40.69	
PbO		5.33	5.31

3 RESULTS

A. The glassware colored in brown is composed from a manganese compound which most probably should be the pyrolusite which was also used as a pigment. The brown layer is contaminated due to the long time passed underground. It was hard to clean it because of its fragility and its accelerated state of degradation. For this reason it was quite impossible to do further measurements by X-ray diffraction to determine the mineralogical composition. Thus we couldn't find out if the percentage of aluminum, calcium, phosphorus and silica were related to the composition of the soil or to the decomposition of the glassware.

B. The lines of the white glass filaments which form the filigree have been well preserved. This is because of the presence of phosphorus and aluminum typical of some medieval glass¹. The percentage of the oxides of these two elements has been carefully studied and witnesses a rich experience of the manufacturers. The presence of these oxides protects glass from decomposition due to the elimination of unbound oxygen in the crystalline system. Practically, it is formed a layer of

alumina-silicate upon a layer of silica and also a layer of calcium phosphate. Initially this layer was formed in high velocity to slow down soon afterwards. Due to the stability in acid conditions as well as in basic one, this layer has conserved the lines of filigree irrespective of the burial conditions.

Another group of compounds that have positively influenced in the preservation of the filigree were a small quantity of CaO which forms a layer of hydroxyapatite and also a small amount of PbO.

However, the main contribution in its preservation is by tin (SnO - 40.69). Tin has a dual role as a dyer and as a conservator.

Along the lines of the filigree are visible some yellow stripes, which should be caused by the migration of the sodium ions.

Under the brown layer it can be noticed an iridescent layer in silver color and it is made of superposed layers. The water has infiltrated into the soil and has reacted with the present oxygen in the glassware forming hydroxyl compounds in. The glassware in question is relatively rich in sodium and potassium and the hydroxyl ions have migrated along with the respective alkaline ions, at first with a parabolic rate with a subsequent decrease. Thus the alkaline ions during wet periods are replaced by proton. As a result of the small volume of protons in comparison with the alkaline cations, the surface has been reduced and shrunk. Such a phenomenon characteristic of silicon-rich surfaces has led to a micro porosity of the upper layer.

This stratified layer impoverished in alkaline elements and can hardly be protective. It can be easily penetrated by water vapors, leading to in a further deterioration due to the accumulation of alkaline ions and increase of pH to 9 which attack the silica system. Therefore we can conclude that the glassware in study is not protected and the deterioration will proceed depending on conservation or exhibition conditions.

The inner side of the glassware is relatively well preserved. This is due to the presence of the potassium, which together with sodium forms the effect of the alkaline mixture. The presence of sodium and potassium in this glassware appears to be in very good proportions that can also double its

sustainability. This proves the rich experience of the artisan who mounded the glassware. However in some areas of the inner side can be noticed cavities as a consequence of the loss of sodium and silica.

Having carefully reviewed this situation a question can arise: why the glassware is well preserved in the inner side, but it has been eroded in the brown color area? The answer to this question requires more complete analytical data. However based on the current knowledge, we can assume two reasons associated to the technological effect. First in the course of applying brown color which is not baked as it should and second the presence of calcium in the brown color that might have led the glass attachment. Unless we're dealing with two types of glass glued to each other. However, this phenomenon should be explained through further studies and detailed analysis.

Conservation of the vase was very difficult and lasted more than a year.

First the glassware fragments and the inner part of many fragments of the vase were cleaned with ethanol. The outer part was cleaned mechanically.

Plastogen EP was used to attach the glassware fragments, which is a epoxy resin, Bisphenol A Diglycidyl Ether is mixed with dibutyl ftalat, whose rigid element is an aliphatic amine. In order to speed up the kinetic reaction, during the gluing process was used the ratio 3:2. The benefit of this adhesive is the strong bind with the glass and stability to light, particularly UV radiation.

The attachment of the glassware fragments was made one by one without creating links of bridges shapes between the fragments. We were obliged to do so to avoid further damages of the brown surface, which could come as a result of the use of cyanoacrylate adhesives used to fix the connecting bridges.

The way used to conserve the vase preserved the brown surface, but could not avoid the distortions arisen as a result of the alterations of the vase dimensions due to the adhesive layers placed between the glassware fragments.

The reconstruction of the vase run into a lot of difficulties related to a further deterioration due to erosion of broken surfaces. The siliceous layers detached along with glue, especially at the thin

fragments in the convex area of the vase (nearly 0.5 mm thick). Another difficulty is related to the absence of many glassware fragments, especially in the convex area. Therefore the vase could not stay erected without a support. For this reason inside the vase were placed translucent Plexiglas stripes glued with the same adhesive. A black granite pedestal on which was mounted a stainless steel bar 6mm diameter was used as a support to the vase. This bar perforates the inside of the vase in a part where glassware fragments are missing while on top of it was mounted a nut Plexiglas.

For the iridescent layer was not used any kind of alloy or reinforcing substance, since the treatment with Paraloid B72, butyric polyvinyl etc. recommended in these cases, even though it strengthens the glass, it eliminates the iridescent appearance. Our reviews have shown that during such operations can fade away the object "nobility" and the surface would look like wet. Moreover, in our case the iridescent layer and the brown color of the fragments do not accept such treatments.

The case of this vase conservation cannot be considered closed just by laboratory intervention presented in this paper, but it must be accompanied by other protective measures during exposure. So it should be kept in environments with relative humidity levels lower than that of hygroscopic compounds that are created on the vase surface.



Photo 4

Picture 4 presents the vase after conservation. This flower vase with a height of 51cm and 20cm diameter is the biggest and most beautiful vase excavated in Albania.

REFERENCES

Neton R, & Davison S. 1989. Conservation of Glassware.

Spectral database of Renaissance fresco pigments by LIBS, LIF and colorimetry

V. Spizzichino, L. Caneve and R. Fantoni

UTAPRAD – ENEA, Frascati, Italy

F. De Nicola

Student, Italy

Abstract: A set of about 70 fresco samples made with pigments and binders typical of the Renaissance period in Rome has been characterized by LIBS, LIF and colorimetric measurements in order to build an as much as possible complete database. Aiming at providing the restorers and art historians with a useful tool for the study of ancient frescoes, the samples have been prepared in agreement with the Cennino Cennini recipes for both materials and procedures. Afterward, the obtained spectral data have been processed by means of multivariate analysis methods in order to find the most significant features that can help in fast characterization and recognition of real unknown specimens.

1 INTRODUCTION

The fast analysis and recognition of fresco pigments by optical methods that are fully non destructive or present a very low invasiveness is an important issue. In fact, the more information on surface materials of a fresco are given to the restorers, the better the restoration works can be carried out. In particular, the used pigments, the followed procedure and eventual successive application of consolidants or modern pigments are the most enquired queries that chemists and physicists receive from art historians, archaeologists and restorers for dating, assignment and investigation of ancient artworks.

During the last decade laser techniques, as Laser Induced Breakdown Spectroscopy (LIBS) and Laser Induced Fluorescence (LIF), have been recognized as unique tools for Cultural Heritage study mainly due to the offered advantages relevant to in situ applicability, capability of remote analysis, minimal or absent invasiveness, and as far as LIBS is concerned, possibility to perform stratigraphic analysis with high sensitivity for a very large number of elements, including light atoms [*Osticioli et al 2009, Caneve et al 2010, Colao et al 2007, Colao et al 2008*].

In the present work, a set of about 70 fresco specimens prepared with pigments and binders typical of the Renaissance period in Rome has been characterized by LIBS, LIF and colorimetric measurements in order to build as much as possible a complete database. Aiming at providing the restorers and art historians with a useful tool for the study of ancient frescoes, the samples have been prepared in agreement with the Cennino Cennini recipes for both materials and procedures. In particular, much attention has been paid to the geographic origin and chemical composition of plaster (*intonachino*) and pigment components. LIBS measurements have been carried out at 1064 nm, while LIF ones have been performed using two wavelengths (355 and 266 nm), in order to compare the different induced fluorescence emissions. Afterward, the obtained spectral data have been processed by means of multivariate analysis methods in order to find the most significant features that can help in fast characterization and material recognition of real unknown specimens. The simultaneous use of these various diagnostic techniques is fundamental in order to obtain a sharper interpretation of the results, as for instance, the certain recognition of different pigments related to their chemical classes that a colorimetric response

couldn't definitely give by itself. Moreover, the concurrent optic techniques have given the possibility to extract the various spectral responses either due to the interaction between pigments and binders, or due to the mix of the same pigments at several concentrations.

2 SAMPLES

The knowledge of the materials and the methodologies originally adopted by Michelangelo for the Sistine Chapel frescoes has been necessary to reproduce in laboratory about 70 samples (*Fig. 1*) comparable to real mural paintings belonging to the Renaissance period in Rome.

The mortar constituting the samples has been produced using the slaked lime matured for 48 months, together with the gray pozzolana from Bracciano, in the same Sabatini Volcanic District where Michelangelo provided himself for his frescoes, aimed at the pre-existing tufaceous masonry constituting the Sistine Chapel (Burrigato & Gabrielli 1990). The rougher side of a square clay tile, 3 cm long and 0,4 cm thick, has been chosen to prepare the substrate of each sample. The surface has been scratched with a metal file and the entire tile has been wetted to saturation with distilled water. The tile has been covered with the *rinza*, a thin layer that has been made in this case of small splashes of mortar, obtained by mixing 1 part per volume of slaked lime and 3 parts of fine pozzolana, made almost liquid by the addition of distilled water. Afterwards, a layer about 0,5 cm thick, called *arriccio*, has been spread on the dry *rinza*. The *arriccio* has been made of mortar mixed in the proportions of 1 part per volume of slaked lime and 2 parts of pozzolana, characterized approximately by grains of size between 0,5 and 3 mm. Subsequently, the *arriccio*, still humid, has been covered by the ultimate layer, the plaster, originally called *intonachino*, characterized by a thickness of about 5 mm and consisting of 1 part per volume of slaked lime and 2 parts of finer pozzolana, previously sifted until it has reached a final grain size less than 0,5 mm (Colalucci 1990).

The chosen pigments include, in addition to the ones laid with successive repaintings,

Michelangelo's colour palette, such as: *Bianco San Giovanni* i.e. Lime White; Mars Brown and Yellow; Earth Umbers; Sienna Earths; Yellow and Red Ochres; Green Earths; Ultramarine Natural Blue; Smalt; *Morellone* i.e. ferric oxide; Ivory Black; Vine Black (Gabrielli & Morresi 1990); Cinnabar; Minium (Gabrielli 1994); *Giallolino* i.e. Lead Tin Yellow; Azurite; Red Lake; Malachite (Mancinelli et al. 1992). Most of these pigments, suitable for fresco painting, as the earth pigments, have been dissolved in little distilled water and then spread on the plaster still wet (hence the name of this technique, *a fresco*). Other types of pigment instead, as Minium, Malachite, Copper Resinate (Mancinelli 1994), Flame Black (Conti 1986), Azurite, Red Bole, and Van Dyke Brown require proper binders and have to be spread therefore on dry plaster, previously covered by a layer of the same binder (Cennini 1859; Vasari 1568). Binders used are: linseed oil (Mancinelli et al. 1994); rabbit skin glue (Colalucci 1992); albumen and yolk (Cennini 1859; Vasari 1568).

Both pigments and binders have been prepared in agreement with the Cennino Cennini recipes, proper procedures were followed accordingly. In particular, pigments mix as *Cinabrese*, *Verdaccio* and the preparatory coating for Azurite have been made utilizing the components and the proportions recommended by Cennini (Cennini 1859). Several concentrations have been tested in some cases, as for instance for *Verdaccio*.

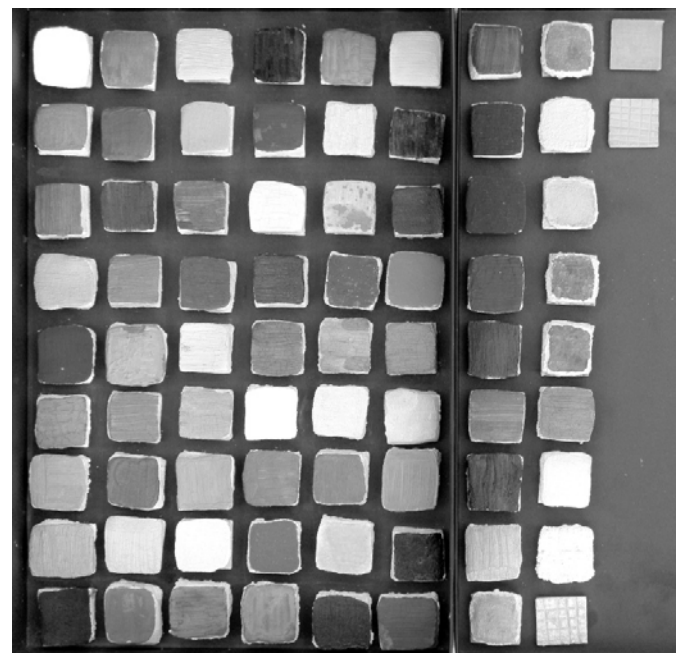


Figure 1: *Fresco samples*

3 EXPERIMENTAL

All samples have been analyzed by LIF, colorimetry and LIBS (LIBS measurements have been carried out after performing other two measure sets). In following sections brief descriptions of the systems used are reported.

3.1 LIF set up and measurements

LIF measurements have been carried out with a scanning lidar fluorosensor experimental apparatus developed at the Diagnostic and Metrology Laboratory of the ENEA center of Frascati. The light sources are two compact pulsed, diode pumped, solid state lasers, emitting in the UV @ 355 nm and @266 nm. A set of optics (mirrors, lens and quartz fiber optic) allows to transmit the exciting radiation and to receive the scattering and fluorescence signals from the investigated target.

Two filters (HR @ 355 nm and HR @ 266 nm, respectively) were used to filter out unwanted laser light, nevertheless a portion of the 532 nm still remains in the output laser beam. This residual radiation can be used as an additional channel to evaluate the target reflectance in the green. The coaxial transmitter/receiver scheme was obtained by using a holed mirror, through which the laser beam passes in order to reach the scanning mirror, used also for collecting the radiation emitted by the sample. The latter mirror is actuated by two rotating servo controls operating at high accuracy.

The fluorescence and backscattered radiation is optically driven to a collecting lens and focused at the entrance of a fiber optic, linked to a compact spectrometer. The CCD detector in the spectrometer permits to record the overall spectral emission with 2.5 nm resolution in the range from 200 nm up to 900 nm.

For every sample 16 measurements have been acquired in different points of the surface in order to take into account material and color inhomogeneities. For the acquisition 1 s long, no temporal delay has been applied, while laser energy was set at 1 mJ for the laser at 266 nm, and at 5 mJ for laser at 355 nm.

The measurements have been performed at an average daytime temperature of 26,3°C and relative humidity 50,8 %.

3.2 Colorimetry measurements

Colorimetric measurements have been carried out by the ColorLite sph850 spectrophotometer.

The samples have been illuminated with D65 standard illuminant. The measurement geometry was characterized by a circular illumination at 45° and measurement at 0° according to the DIN-Norm 5033. The system has been firstly calibrated with a reference measurement, using the BAM white (certificated by the Federal Institute for Material Research and Testing), in order to determinate the spectral properties of the instrument. The standard spectral properties are subject to change in the course of time, and the results can be hence influenced by strong fluctuating working conditions, as temperature fluctuations. Then, the white calibration has been made at regular intervals during these large series of fresco samples measurements.

The instrument has been furthermore set for performing a single measurement cycle, however repeated 5 times in 5 different surface points, in order to determine the averaged color values of each sample. In order to exactly positioning the probe head onto a chosen point of the sample surface and rotate it during the measurement, the automatic probe head trigger has been also switched off. Moreover, the stray light compensation has been applied, in order to measure any surrounding light in case its head opening was not completely closed due to the sample surface irregularities. Afterwards, the sample of *intonachino* without the ultimate pigment coating has been measured as a standard to be used as reference for every later measurements of the other fresco samples.

The outputs of such measurements consisted in $L^*a^*b^*$ data and in reflectance spectra in the range 400-700 nm with a spectra resolution of 10 nm.

The measurements have been performed at an average daytime temperature of 25,1 °C and a relative humidity of 53,6 %.

3.3 LIBS set up and measurements

LIBS experiments have been carried out by a Nd:YAG laser (Handy Quanta System) working at the fundamental wavelength of 1064 nm and a repetition rate of 10 Hz. The pulse duration was of 8

ns for all considered pulses and the total energy was kept below 0.2 J. The plasma emission was collected by suitable receiver optics and the optical signal was carried by an optical fiber to the entrance slit of a 550mm monochromator (Jobin Yvon model TRIAX550) equipped with three different gratings: 3600, 2400, 1200 grooves/mm. In the present experiments the 2400 grooves/mm was utilized, achieving a resolution of 0.05 nm at 532 nm. A multichannel analyzer based on a gated ICCD, model Insta Spec IV, recorded LIBS spectra; by means of the utilized grating, sections of 10 to 20 nm were acquired depending on the spectral range considered.

The temporal interval for recording emission spectra was selected after measuring kinetic series on a selected pigment sample. Finally, the delay was set at 2000ns and the width at 5000 ns in order to have plasma in LTE conditions. To reduce as much as possible the number of shots on the pigment coatings, only spectral ranges which features interesting to atomic composition have been selected and analyzed. In particular the intervals centered at 235 nm, 253 nm, 286 nm, 326 nm, 354 nm, 388 nm, 399 nm, 501 nm, 535 nm, 604 nm, 611 nm, 692 nm have been chosen. For every sample single shot measurements have been acquired and repeated 15 times in every spectral range selected.

The measurements have been performed at an average daytime temperature of 27,6°C and a relative humidity of 43,8%.

4 DATABASE BUILDING

Thanks to measurements performed by the three techniques presented a spectral database has been built in order to have for every studied pigment as much as possible a complete information on composition and aspect (color). In Table 1 samples studied are listed. For mix the recipe used for the preparation is given. In total 46 pure pigments, 4 binders, 10 mix have been analyzed.

Table 1: *Fresco samples are listed together with specifications on ingredients and preparation. Acronyms used are: LO (linseed oil); RSG (rabbit skin glue); A (albumen); Y (yolk); PPV (part per volume).*

Sample	Binder	Notes
1 Plaster	-	-
2 Cyprus Ochre	-	-
3 Ultramarine Blue	-	-
4 Cobalt Blue	-	-
5 Egyptian Blue	-	-
6 Brentonico Green Earth	-	-
7 Red Earth	-	-
8 Madder Lake	-	-
9 Raw Sienna Earth	-	-
10 Vine Black	-	-
11 Red Ochre	-	-
12 Preparatory coating for Azurite	-	2 ppv of n. 11 + 1 ppv of n. 10*
13 Morellone	-	-
14 Deep Azurite	RSG	Spread on Morellone coating (see n. 13)
15 Deep Azurite	RSG	Spread on preparatory coating (see n. 12)
16 Lime White paste	-	-
17 Burnt Sienna Earth	-	-
18 Golden Ochre	-	-
19 Ivory Black	-	-
20 Pozzuoli Red	-	-
21 Warm Green Earth	-	-
22 Ultramarine Natural Blue	-	Afghan Lapis Lazuli pigment (first rate quality)
23 Caput Mortuum	-	-
24 Yellow Ochre	-	-
25 English Red	-	-
26 Pale Yellow Ochre	-	-
27 Flame Black	-	-
28 Ercolano Red	-	-
29 Dark Verdaccio Earth	-	-
30 Raw Umber Earth	-	-
31 Lead Tin Yellow	-	-
32 Deep Malachite Green	-	-
33 Mars Black	-	-
34 Mars Yellow	-	-
35 Mars Orange	-	-
36 Mars Red	-	-
37 Mars Brown	-	-
38 Red Bole	A	-
39 Copper Resinate	LO	-
40 Minium	LO	-
41 Van Dyck Brown	LO	-
42 Smalt	-	Spread on preparatory coating composed of 1 ppv slaked lime + 1 ppv smalt
43 Antique Green Earth	-	-
44 Burnt Umber Earth	-	-
45 Natural Sanguine	-	Ground chalk powder
46 Deep Ochre	-	-
47 Deep Cinnabar	-	-
48 Cinabrese	-	2 ppv of n. 11 + 1 ppv of n. 50*
49 Italian Warm Ochre	-	-
50 Lime White powder	-	-
51 Linseed oil	LO	Layer of binder on the plaster
52 Rabbit skin glue	RSG	Layer of binder on the plaster
53 Incarnato	-	1 ppv of n. 11 + 1 ppv of n. 50 + 1 ppv of n. 43

		**
54 Incarnato	-	1 ppv of n. 11 + 1 ppv of n. 50 + 1 ppv of n. 29 **
55 Incarnato	-	1 ppv of n. 11 + 2 ppv of n. 50 + 1 ppv of n. 43 **
56 Incarnato	-	1 ppv of n. 11 + 2 ppv of n. 50 + 1 ppv of n. 29 **
57 Verdaccio	-	1 ppv of n. 46 + 1 ppv of n. 50 + hint of n. 10 + hint of n. 48 *
58 Verdaccio	-	1 ppv of n. 46 + 2 ppv of n. 50 + hint of n. 10 + hint of n. 48
59 Incarnato	-	2 ppv of n. 11 + 6 ppv of n. 50 + 3 ppv of n. 43 **
60 Incarnato	-	1 ppv of n. 11 + 6 ppv of n. 50 + 2 ppv of n. 43 **
61 Albumen	A	Layer of binder on the plaster
62 Deep Malachite Green	A	-
63 Yolk	Y	Layer of binder on the plaster
64 Flame Black	Y	-
65 Flame Black	RSG	-
66 Red Bole	LO	-
67 Smalt	-	Spread on the plaster consisting of a different slaked lime
68 Red Bole	RSG	-
69 Verdaccio	-	1 ppv of n. 46 + 1 ppv of n. 50 + hint of n. 10 + hint of n. 48 *, spread on the plaster consisting of a different slaked lime
70 Red Ochre	-	4 coatings on the plaster

*(Cennini 1859)

** (Gabrielli 1994)

For every sample the database is composed by:

- *LIF*: averaged spectrum normalized on the background intensity picked in a range free from emission bands.

- *Colorimetry*: averaged reflectance spectrum, L*a*b* data and XYZ values.

- *LIBS*: presence/absence of the selected emission lines (reported in table 2) as a file containing 0 (absence) and 1 (presence). Intensity values of these lines normalized by background intensity picked in a range free from emission lines.

All data are in ASCII format, easy to consult and to handle. An example is presented below.

```
red ochre sample id
0 binder (0 none, 1 linseed
oil, 2 rabbit glue, 3 albumen, 4 yolk)
```

```
7 number of blocks
3 channels block 1 (XYZ)
5 average on block 1
3 channels block 2 (L*a*b*)
5 average on block 2
31 channels block 3
(reflectance 400-700/10 nm)
5 average on block 3
278 channels block 4 (LIF 266
nm 200-890/2.5 nm)
16 average on block 4
278 channels block 5 (LIF 355
nm 200-890/2.5 nm)
16 average on block 5
-999 channels block 6
(presence atomic lines 0 absence, 1
presence)
15 average on block 6
-999 channels block 7
(intensity atomic lines/bck)
15 average on block 7
START
13.7512
10.3532
4.1424
ALT
START
38.454
27.922
26.398
ALT
START
3.718
3.724
3.844
3.512
3.622
3.828
3.944
3.916
4.274
...
ALT
```

Table 2: Database of lines free from overlapping and self-absorbing for LIBS analysis.

Fe II	26	2343.50	Ca	20	3933.66
Fe II	26	2348.12	Al	13	3944.01
As	33	2349.84	Ti	22	3948.67
Cd	48	2508.91	Al	13	3961.52
Mn	25	2572.76	Ca	20	3968.47
Cd	48	2580.11	Mn	25	4030.76
Sn	50	2863.32	Mn	25	4033.07
Si	14	2881.57	Mn	25	4034.49
Co	27	2886.44	Ti	22	4991.07
Ni	28	2907.45	Ti	22	4999.51

Cu	29	3247.54	Cr	24	5345.81
Sb	51	3267.51	K	19	5359.57
Zn	30	3302.60	Cr	24	5409.79
Cu	29	3524.23	S	16	6052.66
Pb	82	3572.73	Ba	56	6142.10
Mg	12	3832.30	Hg	80	6934.00
Mg	12	3838.29			

5 RESULTS AND DISCUSSION

A very large amount of data is present in the database built. Several interesting information can be extracted from row data. However it has to be noticed that the most important results can be obtained only comparing the three techniques. In fact, for example, LIF spectra give information mainly on used binders. As it is possible to see in figure 2, thanks to the LIF analysis at 2 different wavelengths, rabbit glue, albumen, yolk, linseed oil, can clearly distinguished.

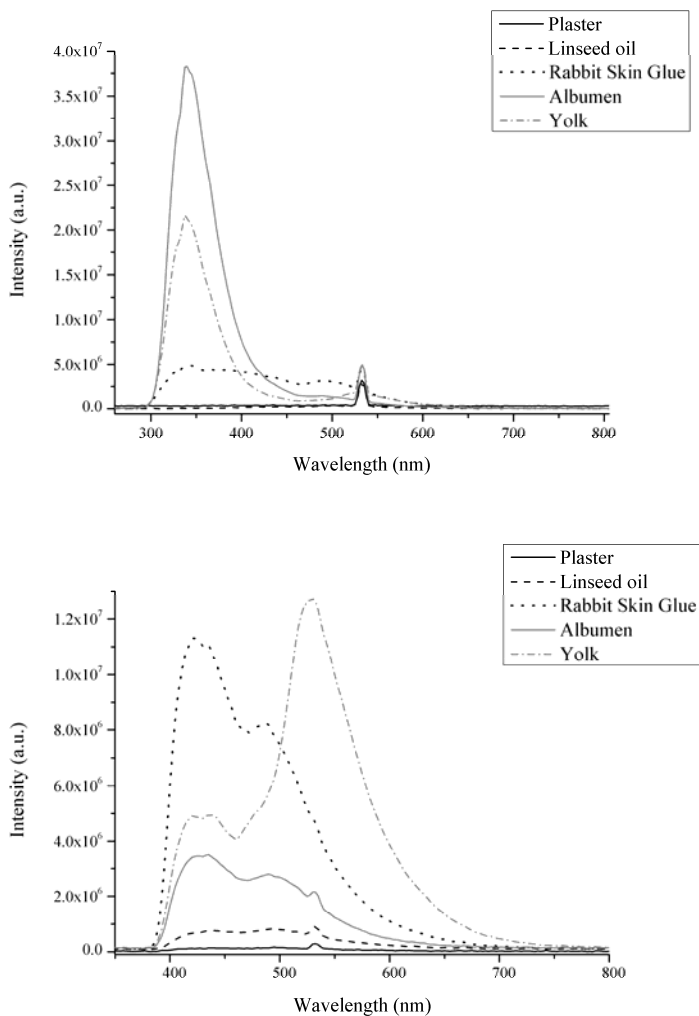


Figure 2: LIF spectra for plaster and binders on plaster at 266 nm (above) and at 355 nm (below).

Instead, colorimetric measurements cannot help to this purpose, as well shown in figure 3 for the case of flame dark, while are obviously useful in the classification of the pigments depending on their color. Moreover colorimetry can give some interesting information on the used technique, as presented for the flame black in figure 3 and revealed also for other pigments, the reemission intensity is quite different if a pigment has been spread “a fresco” or with a undetermined binder.

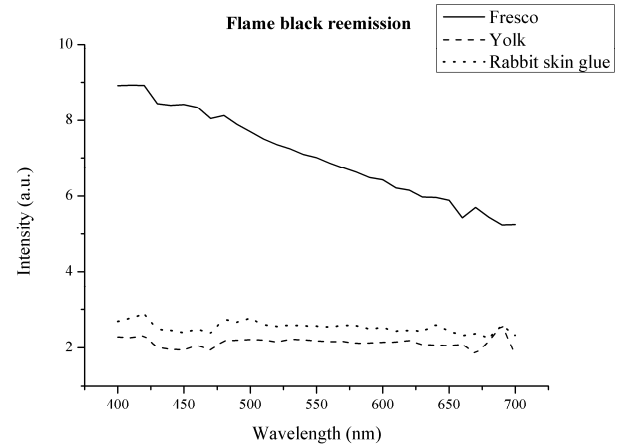


Figure 3: Reemission spectra by colorimetric measurements on flame black pigment.

Besides, with LIBS measurements, the pigment recognition can be improved thanks to its ability to perform an elemental analysis of the surface material.

This very huge and etherogeneous quantity of information collected in the database requires, therefore, techniques of data mining to extract useful information and allow unambiguous material recognition. In the last past years the Principal Component Analysis (PCA) has been applied with good and encouraging results to solve problems related to the analysis of complex data sets deriving from many different optical experimental systems [Baumgartner et al 2000, Sarmiento et al 2011].

On a selected set of pigments a test of the performance of multivariate analysis has been carried out. In particular PCA has been applied on data relevant to presence/absence of the database lines in LIBS spectra. The first results show the capability of such approach to group the pigments in agreement with their origin (mineral pigments, earths, synthetic, ...), and not with similar colors.

In fact, as shown in Figure 4, in the plane

individuated by PC1 and PC2, starting from the axes origin, it is possible to notice directions along which groups of pigments with common features are distributed. In the plane individuated by PC2 and PC3 artificial chemical based pigments are even better grouped and isolated. Moreover, in this plane, it can be observed a disposition of the points depending on the importance of the substrate contribution to the relative experimental spectra (presence of mixes, thick or thin pigment layers).

This interesting result confirms the choice of combining in the database the colorimetric measurements and the LIBS data, that seems to be complementary. Finally the database is completed by the presence of LIF spectra, that provide, instead, information on binders and media, not achievable from LIBS and colorimetry.

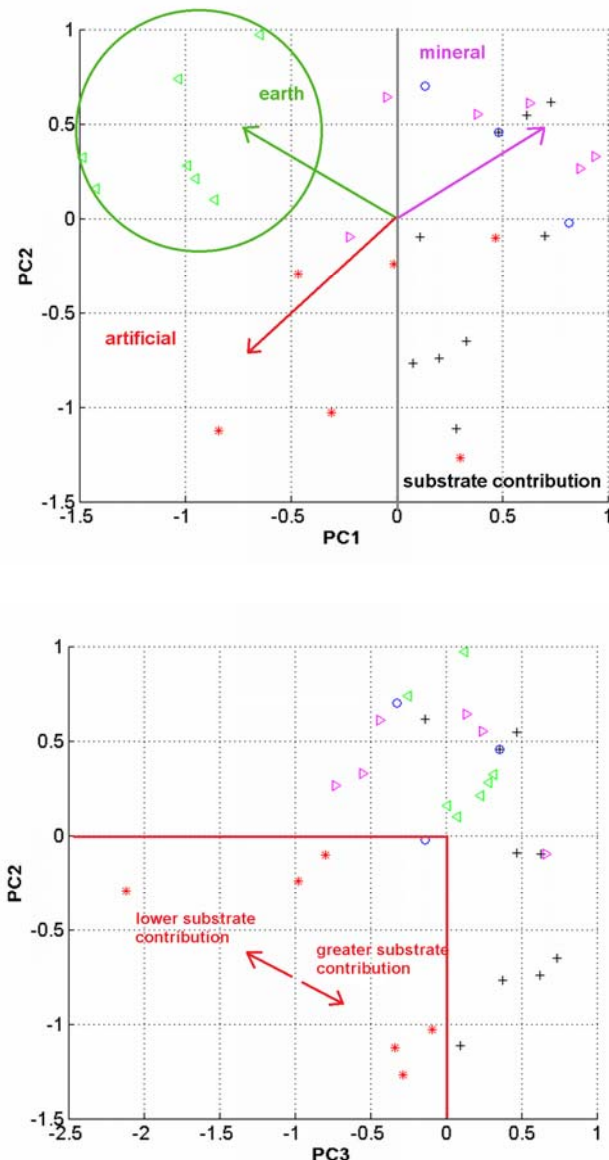


Figure 4: above PC1 vs PC2, below PC3 vs PC2.

6 CONCLUSIONS

The results obtained support the choice of combining in the database colorimetric measurements, LIBS data and LIF spectra at two different excitation wavelengths. Such data, in fact, are demonstrated to be complementary among them. Moreover, the results found on applying a multivariate analysis method on data extracted from LIBS spectra prove the necessity and the utility to use multivariate analysis method to correctly interpret experimental data and to find out from these the most important features for clustering and material characterization. In particular these outcomes suggest to use statistical approaches in the analysis of all the acquired data of the database for a smart and quick characterization, that can help in on field analysis of historical frescoes.

REFERENCES

- Baumgartner, R., Ryner, L., Richter, W., Summers, R., Jarmasz, M., and Somorjai, R. 2000. Comparison of two exploratory data analysis methods for fMRI: fuzzy clustering vs. principal component analysis. In *Magnetic Resonance Imaging*, vol. 18: 89-94. Burrigato, F. & Gabrielli, N. 1990 (printing 1991). *Gli intonaci della volta*. In *Michelangelo e la Sistina: la tecnica, il restauro, il mito : 27 aprile-28 luglio 1991, Isola di San Giorgio maggiore, Venezia*: 122-123. Roma: F.lli Palombi.
- Caneve, L., Diamanti, A., Grimaldi, F., Palleschi, G., Spizzichino, V., Valentini, F. 2010. Analysis of fresco by laser induced breakdown spectroscopy. *Spectrochimica Acta B* 65: 702-706.
- Cennini, C. 1859 (first thus). *Il libro dell'arte, o Trattato della pittura / di Cennino Cennini ; di nuovo pubblicato, con molte correzioni e coll'aggiunta di più capitoli, tratti dai codici fiorentini, per cura di Gaetano e Carlo Milanese*. Firenze: Felice Le Monnier.
- Colalucci, G. 1990 (printing 1991). *Stato di conservazione*. In *Michelangelo e la Sistina: la tecnica, il restauro, il mito : 27 aprile-28 luglio 1991, Isola di San Giorgio maggiore, Venezia*: 91-113. Roma: F.lli Palombi.
- Colalucci, G. 1992. *Gli affreschi della volta sistina. La tecnica di esecuzione*. In De Vecchi, P. (ed). *La Cappella Sistina : la volta restaurata: il trionfo del colore*: 24-45. Novara: Istituto geografico De Agostini.
- Colao, F., Fantoni, R., Fiorani, L., Palucci, A. 2007. *Dispositivo portatile a fluorescenza per la scansione spaziale di superfici, in particolare nell'ambito dei beni culturali*. Patent RM2007A000278.
- Colao, F., Caneve, L., Palucci, A., Fantoni, R., Fiorani, L. 2008. *Scanning hyperspectral lidar fluorosensor for fresco diagnostics in laboratory and field campaigns*. In Ruiz, J., Radvan, R., Oujja, M., Castillejo, M., Moreno P., (Ed.s). *Lasers in the Conservation of Artworks (LACONA VII)*: 149-155. CRC Press..

- Conti, A. 1986. Michelangelo e la pittura a fresco : tecnica e conservazione della volta sistina. Firenze: La casa Usher.
- Gabrielli, N. & Morresi, F. 1990 (printing 1991). Ricerche tecnico scientifiche sugli affreschi di Michelangelo. In *Michelangelo e la Sistina: la tecnica, il restauro, il mito: 27 aprile-28 luglio 1991, Isola di San Giorgio maggiore, Venezia*: 115-121. Roma: F.lli Palombi.
- Gabrielli, N. 1994. Ricerche tecnico scientifiche sugli affreschi di Michelangelo. In Mancinelli, F. (ed). *Michelangelo, la cappella Sistina: documentazione e interpretazioni. II: Rapporto sul restauro della volta*: 361-365. Musei Vaticani; Tokyo; Novara: Istituto Geografico De Agostini.
- Gabrielli, N. 1994. Gli affreschi della volta della cappella Sistina. Analisi di laboratorio : schede. In Mancinelli, F. (ed). *Michelangelo, la cappella Sistina: documentazione e interpretazioni. II: Rapporto sul restauro della volta*: 369-424. Musei Vaticani; Tokyo; Novara: Istituto Geografico De Agostini.
- Mancinelli, F., Colalucci, G., Gabrielli, N., 1992. Il Giudizio e il suo restauro. Note di storia, tecnica, conservazione. In De Vecchi, P. (ed). 1992. *La Cappella Sistina : la volta restaurata: il trionfo del colore*: 236-255. Novara: Istituto geografico De Agostini.
- Mancinelli, F. 1994. Tecnica e metodologia di Michelangelo sulla volta della Cappella Sistina. In Mancinelli, F. (ed). *Michelangelo, la cappella Sistina: documentazione e interpretazioni. II: Rapporto sul restauro della volta*: 9-22. Musei Vaticani; Tokyo; Novara: Istituto Geografico De Agostini.
- Mancinelli, F., Colalucci, G., Gabrielli, N. 1994. Michelangelo: il Giudizio Universale, *Art Dossier* 88: 10-14. Firenze: Giunti.
- Osticioli, I., Mendes, N.F.C., Nevin, A., Gil, F.R.C., Becucci, M., Castellucci, E. 2009. Analysis of natural and artificial ultramarine blue pigments using laser induced breakdown and pulsed Raman spectroscopy, statistical analysis and light microscopy. *Spectrochimica Acta A* 73: 525-531.
- Sarmiento, A., Perez-Alonso, M., Olivares, M., Castro, K., Martinez-Arkarazo, I., Fernandez, L. A., Madariaga, J. M. 2011. Classification and identification of organic binding media in artworks by means of Fourier transform infrared spectroscopy and principal component analysis. *Analytical and Bioanalytical Chemistry* 399 (10): 3601-3611.
- Vasari, G. 1878 (1st edition 1568). Introduzione di messer Giorgio Vasari pittore aretino alle tre arti del disegno. Della Pittura. In Vasari, G., Milanesi, G. (ed). *Le Vite de' più Eccellenti Pittori, Scultori ed Architettori*. I: 111-172. Firenze: Sansoni.

Preliminary study of some iron slags from northern and central Albania

E. Duka and O. Çakaj

FIM&IF, Polytechnic University of Tirana, Albania

Z. Tafilica

Archeological Department, Historical Museum of Shkodra, Albania

I.Gjepali and F. Stamati

Centre of Albanological Studies, Tirana, Albania

N.Civici

Centre of Applied Nuclear Physics, University of Tirana, Tirana, Albania

T. Dilo

Faculty of Natural Sciences, University of Tirana, Tirana, Albania

Abstract: Important elements of the ancient fortified settlements were melting furnaces used for the production of tools and objects. In this preliminary study slag samples from different areas of Albania were investigated. These slag samples were discovered from archeologists during excavations in Mërqi (north of Lezha), in Varosh (north east of Lezha), in Hajmel (south east of Shkodra), all three areas are located in the northern Albania and in Qukës (south east of Librazhd) located in the eastern Albania.

Different analytical methods were used to study the slags such as optical microscopy (reflected and polarized light) for micro structure investigations, X ray diffraction / X ray fluorescence to define the qualitative and quantitative phase and chemical elements content. The densities of the slag samples were measured; most of the samples were magnetic.

1 INTRODUCTION

A slag can represent a simple compound consisting of just one single slag mineral or phase after solidification, but more often slags are complex mixture of many constituents with a wide range composition. From the analyses of such slags can be deduced an indication of the temperature of the fire that caused the destruction, as derived from the formation temperatures of the slag minerals (*Bachmann, 1982*). So how did iron production realized and how did it evolve in Albania? How was it embedded in society? Recently excavated early production finds of iron smelting at Mërqi, Varosh, Hajmel and Qukës present an exceptional opportunity to start answering such questions. The

main goal was to obtain a preliminary, general view of metallurgical production at this site. The study of traditional iron-smelting practices stems from several important roots. The earth science and engineering approach are the two most predominant – investigating the chemical and mineralogical compositions of iron, slag and other physical residues (*Bachmann H-G, 1982*). Factors such as melting technical ceramics, fuel ash and potential fluxes, in addition to variable furnace operating parameters, play a crucial role in slag formation and thus in the slag composition. Many of these slags are no longer seen as residues merely to be discarded, but as potential economic sources of metals, or as useful byproducts in their own right (*Jones R.T, 2004*).

Iron has been a valuable commodity since the Iron Age and was utilized to create an array of objects. The main method of smelting iron ores in premodern times was the so-called “direct” or “bloomer” method, in which the ore is processed in a furnace with carbon-rich fuel at temperatures around 1200 °C. In this process the iron never reaches the molten state, but as iron oxides are reduced, they coalesce as a solid mass of metal or “bloom”. This bloom can subsequently be refined and shaped into the required forms by hot working or smithing (Pleiner R, 2000.)

2 LOCATION AND EXCAVATION HISTORY

Historical sources of foreign ancient authors claim that during the Iron Age the territory of Albania was inhabited by the Illyrians, one of the largest populations of ancient time was spread all over the western part of Balkan peninsula. In essence, the Iron Age is characterized by marked changes in many areas of the economy, in developed quality exchanges, in the growth of social wealth, the formation of tribal federations as a form of political organization, etc. Systematic excavations during the Iron Age have been run in parallel with research on the Bronze Age, for the fact that the same settlements and necropolis have continued to live and were used in both these historical epochs. Age of Bronze and Iron is represented by a collection of objects: weapons, tools, earrings, fibulae, etc. (Cabanes .P et al 2008, Ceka N 2000). Slags have been found in different town areas in Albania (Fig.1). Hajmel is one of the towns where the slags are found. Hajmel is a place with a very small population in the region of Shkoder. Even to this day, in Hajmel area there are some ruins of such workshops where parts of weapons were produced. Lezha (Lissus-Lyssos) is said to have been founded by the year 385 BC. Lezha area and its surrounding areas are rich in minerals and archeological finds. Merqi and Varosh are places with a very small population in the region of Lezha, Albania.

Qukes is a locality in the Librazhd district, Elbasan County, in Eastern Albania. Qukes

has a very old history which starts from the Iron Age, till Middle Age. Because of this it is very hard to find the production time of slags and iron objects. This area was known for producing weapons and iron objects. It was also in the vicinity of the road connecting Albania with other Balkan countries, which was known in Prehistory by the name Kandavia and was afterwards called Egnatia. During the Middle Age, its name was Royal Road.



Figure 1: Location map of iron slags in Albania

3 MATERIALS AND METHODS

3.1 Samples description

Most of the investigated slags can be ascribed to the iron production chain. All iron slags from Albania so far analyzed are smithing slags.

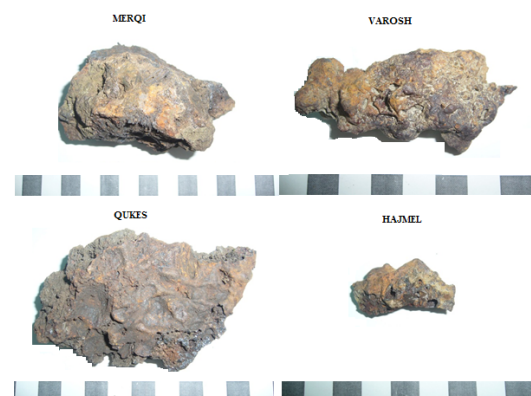


Figure 2: Frontal views of slags from Albania. (Each square on the scale =1 centimeter)

Slags are heterogeneous materials and it is important to take enough samples so that it reasonably represents the whole artifact - 100 milligrams is deemed as a standard amount. From each section are taken considerable amounts of sample.

Macroscopic investigation of samples allowed us to recognize different types of plane-convex slags on the basis of their general characteristics: (Bachmann, 1982) Due to their high content of iron silicates, slags from metal smelting tend to be black or dark grey on freshly exposed surfaces. This is a characteristic that we see from our sample (Fig.3).



Figure 3: Image of slag found in Merqi

Some of our slags show flow textures, resembling volcanic lava. Other samples are striated or layered. All samples are porous in various degrees. (Fig.4).



Figure 4: Inclusion like sand grain found in the Varosh slag

Another characteristic of our slags are inclusions like mineral grains, fragments of charcoal, globules or veinlets of pure metals or sulphides sand grains from the slag bed, and similar elements. This is most characteristic for the slag found in Varosh (Fig.4).

Many slag minerals, especially iron silicates are resistant to weathering, even under humid climates and retain their color.

3.2 Samples sizes and densities

Slag diameters vary from 3 to 15 cm, while their thickness is 1.5 to 7 cm (Fig. 2). Samples were cut into 2 big pieces and afterwards one of them was cut in 4 pieces of approximately 1 to 2 cm in diameter. Densities were measured according to Archimedes principle.

Table.1 Densities value

	<u>Densities</u> gr/cm ³			
	Merqi	Hajmel	Varosh	Qukes
Sample 1	3.54	3.20	2.36	5.54
Sample 2	3.14	3.46	2.08	5.75
Sample 3	3.72	3.70	2.79	5.90
Sample 4	2.91	3.95	2.05	5.60

After having calculated the densities, we notice that the value of the Qukës sample is higher than the others. This is thought to happen due to metal grains which came out during milling. Presence of iron metallic) grains in those samples shows that they are antic, because modern slags do not contain iron metallic grains.

3.3 Samples preparation

All the samples were cleaned using water and a brush. Afterwards they were polished in different parts using silicon carbide paper 120, 220, 320, 500, 1000, 1200 and 4000. The abrasive paper may be mounted on the surface of a flat, horizontally rotating wheel and the metallographic specimen held against it. At the present time the abrasive extensively used for the rough polishing operation is powdered diamond dust, with particle size 3 microns and 6 microns.

Each half type of sample has been made into powder for XRF analysis with the help of a ball mill.

3.4 Samples' examination

The analysis of the artifacts from Albania required the use various equipment.

These include optical microscopy (reflected light, Kozo XJP300). For smaller magnification images the XTL6445 stereomicroscope was used. Pictures were taken using a Sony TCC-8.1 camera and TS View Version 1.0.0.1 software for all the microscopic observations.

Mineralogy and phase transformation were determined by XRD: Major and trace elemental composition of slags detected by XRF.

The XRF system is composed of a tube excitation system (Philips PW 1729 X-ray generator and PW 2215/20 Mo anode X-ray tube), an X-Ray spectrometer with a Si (Li) detector and spectrum acquisition system (Canberra mod 2024 fast spectrometry amplifier, Mod 8076 ADC, Mod 3105 high voltage power supply and Genie 2000MCA).

These instruments, combined with the traditional methods of hand-drawn illustrations of the specimens, allowed us to adeptly identify and analyze ores, crucibles, furnaces, and slag, so as to formulate a probable image of the life and metallurgical methods of the time period (Pleiner, R., 2000).

Diffraction system=XPRT-PRO, Cooper anode material, $\lambda=1.5405980\text{\AA}$, tension 40KV, current 40mA, Nickel filter, detector 7010015 name "PIXcel".

4 RESULTS AND DISCUSSION

4.1 XRF- analysis of slags

The powder samples of slag, placed in cups with Mylar foil at one end, were measured in secondary target mode using a Mo secondary target, which allows the excitation of several elements with X ray lines in the range 3 – 16 keV. The COREX program, which uses fundamental parameters and intensities of scattered peaks, was used for quantitative analysis.

The results of the analyzed samples are presented in table 2. The experimental error of the concentrations, expressed as relative standard deviation, is 6 – 12 % for major elements, while for minor elements it ranges between 10 – 20 %.

4.2 XRD- analysis of slags

Mineralogical characterization of phases was carried out by X-ray diffractometry. The software used is X'Pert HighScore Plus. Reflected light microscopy has shown metallic Fe grain (Fig.5).



Figure 5: Stereomicroscopic view-Iron grain found during polishing in Mërqi sample

Phase compositions from XRD qualitative analysis are:

- Varosh: wüstite fayalite, magnetite and quartz.
- Mërqi: magnetite, wüstite, fayalite and hematite.
- Hajmel: Wustite magnetite, fayalite
- Qukës: wüstite, magnetite quartz, fayalite.

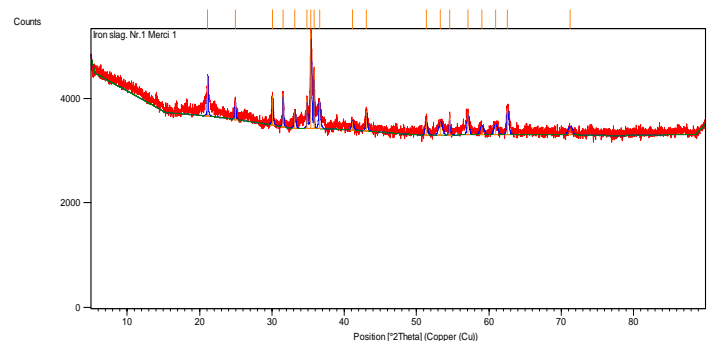


Figure 6: XRD –analysis for slag founded in Mërqi

Table 2: μ - X ray fluorescence results on slags founded in Albania. (Value are expressed in parts per million ppm, except some which are expressed in wt. %; 'bdl' indicate when results are 'below detection limit')

Chemical elements	Sample			
	Mërqi	Hajmel	Varosh	Qukës
K (%)	0.26	0.37	2.4	0.80
Ca (%)	0.51	1.5	2.0	2.35
Ti (%)	0.06	0.11	0.33	0.096
Mn (%)	0.20	0.26	1.3	-
Fe (%)	52	51	18	49
Cr (ppm)	-	-	409	bdl
Ni (ppm)	-	Bdl	126	-
Cu (ppm)	258	192	73.1	78.6
Zn (ppm)	72	15.4	28	45
As (ppm)	254	16.4	11.3	bdl
Rb (ppm)	5.8	10	62	12.1
Sr (ppm)	21	30	135	27.2
Pb (ppm)	bdl	-	6.8	-
Ga (ppm)	-	Bdl	5.9	-

4.3 Microstructure results

After a precise selection and preparation of samples, preliminary stereoscopic tests were carried out under the microscope. In figure below are shown four images taken by reflected light microscope for each sample in which are shown the iron metallic, fayalite, hole and wüstite respectively.

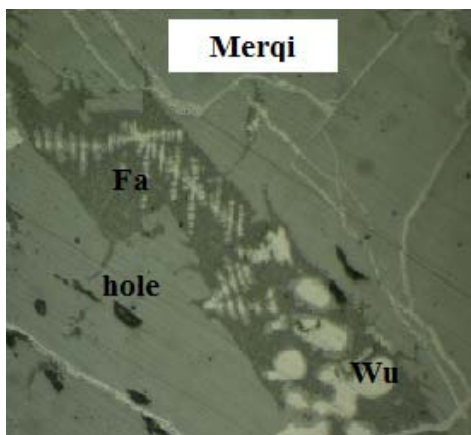


Figure 7: Photomicrographs of slag founded in Mërqi, (x200 magnification). hole; Wu = wüstite; Fa=fayalite

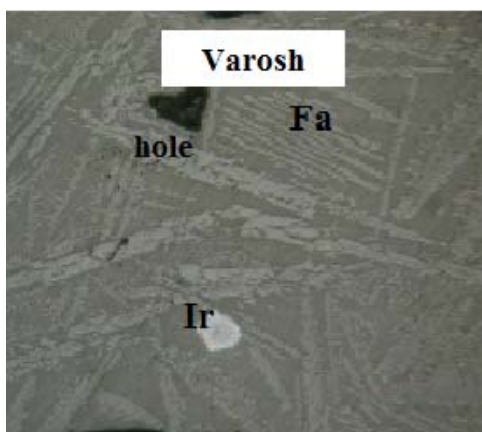


Figure 8: Photomicrographs of slag founded in Varosh, (x200 magnification). hole; Ir =iron; Fa=fayalite

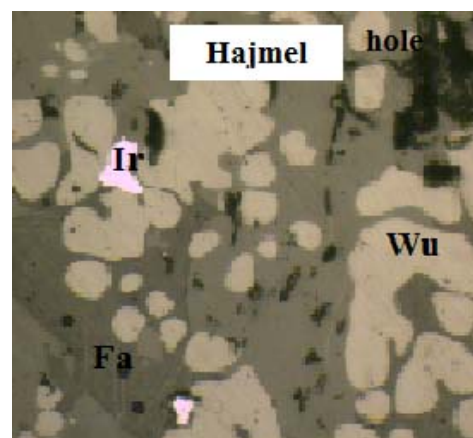


Figure 9: Photomicrographs of slag founded in Hajmel (x200 magnification). Ir=iron hole; Wu = wüstite; Fa=fayalite

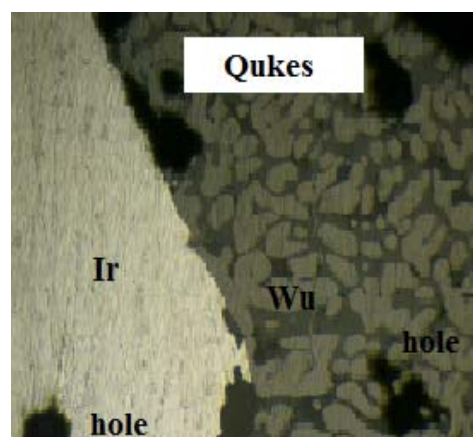


Figure 10: Photomicrographs of slag founded in Qukës, (x200 magnification). Hole; Wu = wüstite; Fa=fayalite; Ir= Iron

4.4 Conclusion

Preliminary analysis of the Albania samples has demonstrated that all four slags derive from the ironworking process. The four types of slag have different compositional and mineralogical composition.

Firstly we saw that all samples are iron slag and some of them are with high percentage of iron. Secondly, from XRF analysis we take all chemical elements present in our sample. Using the chemical composition of the slag inclusions can be determined in future the geological origin of an archaeological iron artefact. Reflected light microscopy and X-ray diffractometry have shown metallic Fe, magnetite, hematite, wüstite, fayalite and quartz. All samples examined in this study are fayalite-type slag, and are considered products of iron metallurgy. Fayalite crystals in elongated aggregates were found in the underlying silicate mass. Investigated samples don't present the similar magnetic properties. Varosh show a weakly magnetic different from sample founded in Hajmel and Merqi that show that are magnetic because they are composed from wustite and magnetite. This characteristic shows that those slags were formed at different stages of the ore processing during the reduction process. They combine features of slags from the higher and lower parts of the bloomer. Qukes sample demonstrate strongly magnetic properties. Those slags would be formed in the upper part of the bloomery, where hematite, as one of the byproducts of the smelting process, is altered to magnetite.

REFERENCE

- Bachmann. H-G, 1982, The identification of slags from archaeological sites. Institut of Archaeology.
- Ceka, Neritan 2000. Ilirët. Tiranë: Shtëpia Botuese e Librit Universitar.
- Ingolia, C. Triscari, M. Sabatino, G Archaeometallurgy in messina: iron slag from a dig at block p, laboratory analyses and interpretation , Mediterranean Archaeology and Archaeometry, Vol. 8, No. 1, pp. 49-60
- JONES R.T, 2004 Economic and environmentally beneficial treatment of slags in DC arc furnaces Pyrometallurgy Division, Mintek, Randburg,2004 ,, South Africa
- Humphris. J et al,2009, Variability in single smelting episodes – a pilot study Nusing iron slag from Uganda, Journal of Archaeological Science 36 (2009) 359–369
- Pleiner, R., 2000. Iron in Archaeology: the European Bloomery Smelters. Archaeologicky U stav Aver.
- Pierre, Cabanes et al 2008. Harta Arkeologjike e Shqipërisë. Tiranë: K&B Klosi&Benzenberg.
- Scott, David 1991. Metallography and microstructure of ancient and historic metals. Singapore: The J. Paul Getty Trust.

Study of vulnerability and characterization of stone columns from Seville (Spain)

R. Ortiz, P. Ortiz, J.M. Martín and T. Cordero

University of Pablo de Olavide, Department of Physical, Chemical and Biological Systems, Seville, Spain

M.A. Gómez-Morón

Andalusian Institute of Cultural Heritage, Seville, Spain

M.A. Vázquez

University of Seville, Department of Crystallography, Mineralogy and Agricultural Chemistry, Seville, Spain

M.P. Mateo, G. Nicolas

University of A Coruña, Laser Applications Laboratory, Ferrol, Spain

Abstract: The aim of this research was the characterization of archeological columns of different periods found in Seville (Spain) by studying their conservation degree and vulnerability situation. This work is part of a project which is being carried out in the Historical City of Seville and consisting on the analysis of the risk and vulnerability in Historical Centers. In the city of Seville, a large number of these columns could be recognized as reused in the cathedral, inside and outside churches, in civil Monuments and as a reinforcement of building corners in the city. Marble, limestone and granite columns have been investigated in order to carry out the mineralogical and petrographical description of the stones and to evaluate their conservation degree and vulnerability to environmental hazards. Several analytical techniques have been employed to determine composition of specimens and their weathering forms.

1 INTRODUCTION

The quality of the stones used in columns made them attractive for subsequent reuse in the same places or in a new location. Only when they are broken or mainly destroyed, they are employed for mortars as lime or aggregates. In the city of Seville, a large number of these columns could be recognized as reused in the cathedral, inside and outside churches, in civil Monuments and as a reinforcement of building corners in the city.

Marble, limestone and granite columns have been investigated in order to carry out the mineralogical and petrographical description of the stones and to evaluate their conservation degree and vulnerability to environmental hazards.

The effects of weathering on stone columns require a multidisciplinary approach to understand the damage mechanisms and the vulnerability conditions.

This work is part of an Andalusian Project titled “Design and validation of a methodology to carry out risk and vulnerability maps in Historical Centers” that has been carried out in the Historical City of Seville and which aim is the analysis of the environmental influence in the weathering of monuments, and the proposal of a new standard methodology to evaluate vulnerability and conservation degree.

With this purpose, more than 150 columns have been studied to evaluate the conservation degree and the mechanism of the main weathering forms.

2 MATERIALS AND METHODOLOGY

The stone columns studied are calcareous and granite stones of different sizes and shapes. Most of them are roman columns reused in different Churches, or monuments. Meanwhile only three of the columns are maintained in their original place (*Fig. 1*).

These natural stones are under exterior conditions, so they are directly exposed to temperature changes, erosion and pollution in the center of the city.

The study of the weathering forms has been carried out on 175 columns by means of visual inspection. These macroscopic pathologies have been described by the terminology of NORMAL regulation 1/88 (1990), Ordaz and Esbert (1988), Martin (1990), Fitzner et al. (1992 & 1995) and the ICOMOS recommendations (2008).

For this work, five samples have been taken from deposits and black crusts on columns following the recommendations of the technical commission CNR-ICR NORMAL 3/80 (1980).

Sampling has been carried out on five columns according to the most common variety found in the city: white and green marble, red and black limestone and grey granite.



Figure 1: Column of granite from roman period in their original location.

For the mineralogical and petrographical study, we have used an optical microscope Kyowa with a digital camera and X-ray diffractometer brand Bruker (model D8 Advance), using $\text{CuK}\alpha$.

The elemental chemical analysis over the stratigraphies of the crusts and deposits has been studied by means of an electron scanning microscope JEOL JSM-5400, with x-ray energy detector, Inca X-sight. The chemical composition has also been analyzed with an X-rays fluorescence spectrometer Panalytical (model AXIOS) with Rh tube.

LIBS measurements were carried out by a set-up consisting of a conventional arrangement

including pulsed Nd:YAG laser, focusing and collecting optics, spectrograph and detector and it was described elsewhere (Ctvrtnickova et al., 2009). The laser operated at its second harmonic 532 nm wavelength with a pulse duration of 5 ns and its maximum energy output was 300 mJ/pulse. The laser beam was directed normally to the sample surface and focused by a planoconvex quartz lens. Microplasma created on the sample surface was collected by a quartz optical fiber and transmitted to an Echelle spectrograph coupled to an ICCD camera. The spectrograph spanned the spectral region of 200–850 nm simultaneously with high resolution, thus it allowed multi-elemental analysis under the same experimental conditions for each element. The detector delay time and integration time were set to 1 μs and 10 μs , respectively. The data acquisition was carried out in two modes, either accumulation of 5 pulses on the sample surface in order to determinate the elemental composition of the deposit layer, or firing 100 pulses to the same position in order to acquire the depth profile of the layered sample. All experiments were performed in air under atmospheric pressure.

The interest of LIBS over other techniques is the fact that the analysis does not require preparation of the specimens and the damages induced are minimal which has become a crucial point for cultural heritage artifacts. Hence, a higher number of measurements can be carried out leading to a more complete study of crusts and contamination species responsible of degradation.

3 RESULTS AND DISCUSSION

3.1 Vulnerability of stone columns

The most dangerous weathering forms found in the granite columns is detachment of different size, whilst marbles has pitting and limestones present loss of material mainly in veins or zones of different porosity.

Chromatic alteration is very usual in the columns due washing of metal structures of reinforcement or ornamental purpose, but also it is caused by the internal oxidation of iron.

Losses of materials are common in most of the column due to the man action. Fissures were

detected in a few columns mainly related to changes of texture and rarely to mechanical effects.

Biocrust are located in granite columns associated to vegetation and humidity, while black crust and deposits were found in any column near traffic (Fig.2).



Figure 2: Granite column affected by crust, deposits and iron spots.

3.2 Mineralogical and Petrographical Description

Thin section microscopy and XRD analysis was carried out on the materials of five columns. The results show that four samples are mainly composed of calcite (marbles and limestones) with micas in green marbles while the granite column is composed of quartz, K-feldspar and biotite.

The main weathering product is gypsum that has been detected by XRD and OM. The epigenetic layer of gypsum is a product of transformation of calcite in surface, what implies a direct relationship with the presence of sulfur oxides in the atmospheric environment of the columns. Deposits on granite samples are mainly composed of terrigenous particles and/or organic compounds that are not detected by XRD.

XRF results show that calcium is the main component in the four calcareous samples; meanwhile silicon is the main component in granite column according to the lithotype descriptions.

Sulfur content is over 2% w/w in limestones and white marble. It corresponds with the gypsum, according to DRX and petrographical characterization that implies a chemical process of weathering.

The profile of crust and deposits allow knowing the origin of the damage and the

vulnerability of each material. For this reason, this study has been completed by LIBS and SEM-EDX.

3.3 Study of crusts and deposits depth by LIBS

LIBS analyses have been performed on black and clean zones of samples to obtain a representative spectrum of each zone with an accumulation of five pulses in order to get a suitable signal.

LIBS spectra of marbles and calcareous stones are dominated by Ca emission lines, according to their composition that is based on calcite. In contrast, Si, Al, and Li emission lines dominate the LIBS spectra on granites in a range of relationships due to their mineralogical composition (quartz, K-feldspars and biotite).

LIBS measurements show also the presence of Al, Si, Mg, K, Sr, Na and Ba lines both in black crusts and clean zones of marbles, while granite present mainly Si, Al and Li over the stone and Ca, Mg and Na on the deposits.

V and Ti lines appear in the layers of black crust on calcareous stones. The presence of both elements could be explained by pollution and, in case of titanium, it could be caused by desert sand storms (Colao et al., 2004).

Depth profiling has been performed in the samples shooting in the same point to evaluate the evolution between the crusts or deposits (upper part) and the stones (inner part). In such profiles, while the intensity of characteristic element of the upper layer diminishes in depth, the base material element intensity increases. The intersection of corresponding curves represents the deposits/stone interface (Mateo et al., 2006).

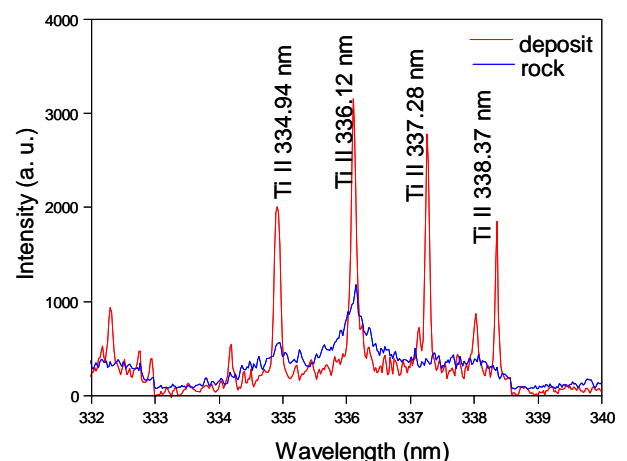


Figure 3: Titanium from the deposits and crust over the white marble column.

The interface is reached after 10-20 pulses in calcareous stones while the interface is reached after 5 pulses in granites, which implies that the encrustation is thinner in calcareous stones, surely due to the presence of gypsum crust though LIBS was not suitable to detect sulfur in the current experimental set-up.

3.4 Study of crusts and deposits depth by SEM-EDX

Line scans of main components have been carried out on the perpendicular sections by SEM-EDX, showing different types of surface alteration:

A) Surface alteration composed by sulfur and calcium (Fig. 4).

The green and white marbles, red and black limestones are in this group (green marble and white marble). This weathering form is caused by the reaction of calcite with the sulfur oxides present in the environment. The porosity and texture of these samples define the extension of the weathering surfaces.

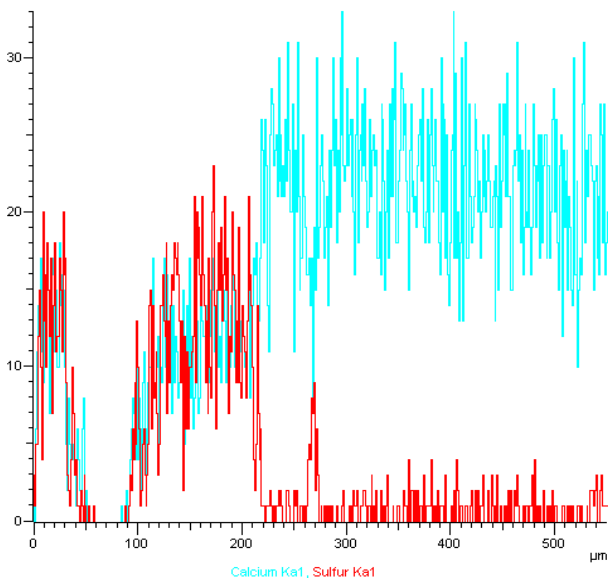


Figure 4: Ca/S Depth profile of marble encrustation by SEM-EDX.

B) Surface alteration composed by deposits, where chemical reaction has not occurred. These deposits are mainly composed by dust from terrigenous and anthropogenic particles or organic remains. These deposits have mainly been found in granite.

Similar weathering layers have been described by Bromblet and Verges-Belmin (1996) in

calcareous stone or Silva *et al.*, (1994) and Schiavon *et al.*, (1994) in granites. The crusts over calcareous stones are mainly caused by the epigenetic formation of gypsum generated by SO₂ from traffic pollution, but the mineralogical composition and texture of granite prevent the gypsum crust and allow deposits or biocrusts.

The Historical Center of Seville has environmental conditions that show a clear influence of the traffic in the presence of black crust on calcareous stones (Ortiz *et al.*, 2010). Similar studies of the influence of sulfur oxides in monuments has been largely analysed by Lefevre *et al.* (2005), Thi Ngoc Lan *et al.*(2005), Camuffo *et al.* (2006) and Grossi *et al* (2006) in different cities.

Parallel surface section has also been analyzed by SEM-EDX to study the atmospheric particles. The results show aggregates of variable habits of gypsum (Fig. 5) and other particles with calcium, silicon, magnesium, iron, chloride, sodium, potassium and aluminium.

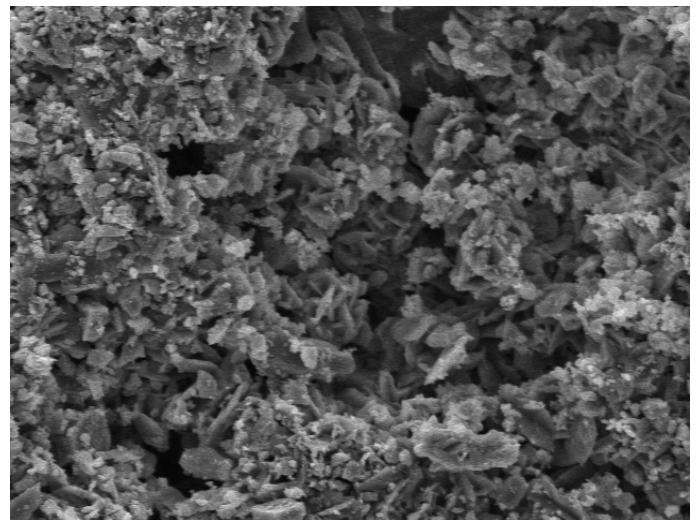


Figure 5: Gypsum on encrustation over marble column.

4 CONCLUSIONS

The main weathering forms in granites are detachments, deposits and biocrusts in contrast to marbles and calcareous stones that present pitting and black crusts with gypsum (CaSO₄.2H₂O). Other damage depend on the location and other anthropogenic factors. In summary, the vulnerability of the column depends on the location, building owners and the mineralogical and petrographical conditions of the stone.

According to LIBS and SEM-EDX results, the

surface weathering forms are composed of Al, Si, Ba, K, Na, Ti, V, Mg and Ca, while XRF technique also detects S, Fe, Mn and P. The atmospheric particles on the superficial alteration can have an anthropogenic or terrigenous origin, including the weathering of the building materials and its restoration products, except the gypsum that is due to the traffic pollution.

ACKNOWLEDGEMENT

This Project has been carried out thanks to the funds of the Junta de Andalucía Project RIVUPH (HUM 6775).

REFERENCES

- Bromblet, P. Verges-Belmin., V. 1996. L'élimination des sulfates sur la statuaire calcaire de plein air: une habitude discutable. Le dessalement des Matériaux Poreux. Journées d'études de la SFIIC. 55-64.
- Camuffo, D. Pagan, E. Del Monte, M. Lerevre R.A. Ausset, P. 2006. Modelling the penetration of SO₂ within the pores of calcareous stones and the concentration of gypsum in the near surface layer. *Heritage, Weathering and Conservation*, London, 435-440.
- CNR-ICR. 1980. Materiali lapidei: Campionamento. Normal 3/80, 1-6.
- CNR-ICR. 1990. Alterazione macroscopiche dei materiali lapidei: Lessico. Normal 1/88, 1-36.
- Colao, F. Fantoni, R. Lazic, V. Morone, A. Santagata, A. Giardini, A. 2004. LIBS used as a diagnostic tool during the laser cleaning of ancient marble from Mediterranean areas. *Applied Physics A Materials Science & Processing*, Volume 79, Issue 2, 213-219.
- Ctvrtnickova, T. Cabalin, L. Laserna, J.J. Kanicky, V. Nicolas. G. 2009. Laser ablation of powdered samples and analysis by means of laser-induced breakdown spectroscopy. *Appl. Surf. Sci.* 255: 5329-5333.
- Fitzner, B. Heinrichs, K. Kownatzki, R. 1992. Classification and mapping of weathering forms. *Proceedings of the 7th International Congress on Deterioration and Conservation of Stone*, Lisboa, II, 957-968.
- Fitzner, B. Heinrichs, K. Kownatzki, R. 1995. Weathering forms - Classification and mapping. *Denkmalpflege und Naturwissenschaft. Natursteinkonservierung I*. Ed. Ernst & Sohn, 41-88.
- Grossi, C.M., Brimblecombe, P. 2006. Sulfate and carbon compounds in black crusts from the Cathedral of Milan and Tower of London. *Heritage, Weathering and Conservation*, London, 441-446.
- ICOMOS-ISCS. 2008. Illustrated glossary on stone deterioration patterns. ICOMOS International Scientific Committee for Stone (ISCS).
- Lefevre, R.A. Jonescu, A. Ausset, P. Chabas, A. Girardet, E. Vince, F. 2005. Modeling the calcareous stone sulphation in polluted atmosphere after exposure in the field. In: R. Priklyl & B. Smith (eds.), *Natural Stone Decay*. London: Geological Society. Submitted.
- Martín, A. 1990. Ensayos y experiencias de alteración en la conservación de obras de piedra de interés Histórico-Artístico. Ed. Fundación Ramón Areces. Madrid, 609.
- Mateo, M.P., Nicolas, G. Piñon, V. Yañez, A. 2006. Improvements in depth-profiling of thick samples by laser-induced breakdown spectroscopy using linear correlation. *Surf. Interface Anal.* 38: 941-948.
- Ordaz, J. Esbert. R.M. 1988. Glosario de términos relacionados con el deterioro de las piedras de construcción. *Materiales de Construcción*, Madrid, 38, 209, 39-45.
- Ortiz, P. Vázquez M.A., Ortiz, R. Martín, J.M. Ctvrtnickova, T. Mateo, M.P., Nicolas, G. 2010. Investigation of Environmental Pollution Effects on Stone Monuments in the Case of Santa Maria La Blanca, SEVILLE (SPAIN). *Applied Physics A: Materials Science & Processing*. Volume 100, Number 3, 965-973.
- Schiavon, N. Chiavari, G. Fabbri, D. Schiavon, G. 1994. Microscopical and chemical analysis of black patinas on granite. III Symposium on the conservation of Monuments in The Mediterranean Basin. Venecia, 93-99.
- Silva, B. Casal, M. Prieto, B. Rivas, T. Guitián, F. 1994. Forms and factors of weathering in the Cathedral of Santiago de Compostela. III Symposium on the conservation of Monuments in The Mediterranean Basin. Venecia, 743-748.
- Thi Ngoc Lan, T. Thi Phuong Thoa, N. Nishimurab, R. Tsujino, Y. Yokoi, M. Maeda, Y. 2004. New model for the sulphation of marble by dry deposition Sheltered marble - the indicator of air pollution by sulfur dioxide. *Atmospheric Environment* 39: 913-920.

Multispectral imaging - a fast and accurate method for artworks documentation

Lucian Ratoiu and Laurențiu Angheluță

National Institute of Research and Development in Optoelectronics - INOE 2000, Centre of Excellence for Restoration by Optoelectronic Techniques, Romania

Abstract. Spectral imaging techniques provide significant information in the documentation process of the artworks. In order to respond to this open process of data collection a variety of methods and techniques for investigation, monitoring and diagnose can be applied. By enabling a compared visual recording of the object, in different spectral ranges, the multispectral camera and, more recently, the hyperspectral camera have proved to be very useful methods in the cultural heritage domain. Since an artwork is a complex object elaborated through a strict and difficult technological process the most suitable documentation should be one that can highlight the intrinsic characteristics of the structure. In accordance with this specific task the multilayer recording technique, provided by the multispectral camera, enhances a better understanding of the object, linking the technological aspects with the degradation factors which are not always distinguishable in the visible spectrum. This paper is focused on different case studies of artworks including technique, period and also cultural provenience.

1 INTRODUCTION

In the difficult and high responsible task of conserving and restoring artworks a key issue is to accurately investigate in order to diagnose and identify the active degradation sources. The open process of documentation is designed not only for precise administration of the data resulted before, during and after a restoration intervention but also to enhance the understanding of the artwork as it was conceived and as it is exhibit in the present days. In order to capture the artist *fingerprnt* key markers of his characteristic technique can be highlighted through different investigation techniques.

Technological analysis of the artwork is an “intimate” approach which can reveal typical features of the artist. Some of this characteristically “markers” may involve even some technical defects or deficiencies that can influence the later behavior of the artwork. We can have a better image regarding this instance by thinking at an oxymoronic style¹. In many cases the degradation process is not only amplified by this peculiar factor but in fact

represents the main cause of decay².

Visible inspection represents our first contact with the artwork and has a double function – one that implies an esthetical view and another one, more critical, concerned on the conservation status of the artwork, or to be more specifically focused on her materiality. The so called *naked eye* investigation is, like in other disciplines³, a general overview based on the experience of the investigator. But even massive experience cannot reveal information that has no correspondence in visual spectrum. As a multidisciplinary domain present conservation relies on scientifically data generated by the use on nondestructive and noninvasive techniques. One of the most used in the preliminary stage of documentation and diagnosis is the multispectral imaging⁴. The information resulted implies not only conservation features but also significant data concerning the art history field.

² A famous example is the “Last Super” painted in an experimental technique by Leonardo da Vinci

³ Medicine - from which conservation and restoration of the artworks as a domain was inspired

⁴ Hyperspectral imaging designates in fact more finely divided spectral channels than multispectral imaging. See the review of Haida Liang - Advances in multispectral and hyperspectral imaging for archaeology and art conservation, Applied Physics A - materials Science & Processing, Springer-Verlag 2011

¹ In some cases contemporary and modern artists ware intentionally using materials characterized by their fast rate of degradation.

Analysis of the underdrawings or *pentimenti*⁵ can generate large areas of research for art historians interested in the technological developments of an artist throughout his career.

Combined with other complementary techniques implied in the documentation and investigation process of artworks this early stage method can generate additional data when is superimposed over an accurate multilayer data package.

2 PRINCIPLES AND INSTRUMENTATION

The basic principle of multispectral camera relies on the interaction between the light and mater - See *Fig 1*. Pigments are inorganic or organic substances that are insoluble or substantially insoluble in water or other organic medium in which they are used as dispersions. The properties of the paint or coating are depending on the properties of the mixture formed by the binder, pigments and other additives.

To describe very shortly the imaging system we can list his essential components: lighting, focusing optics, detector and the key element that makes the difference between multispectral cameras – the means of wavelength selection [4], [10].

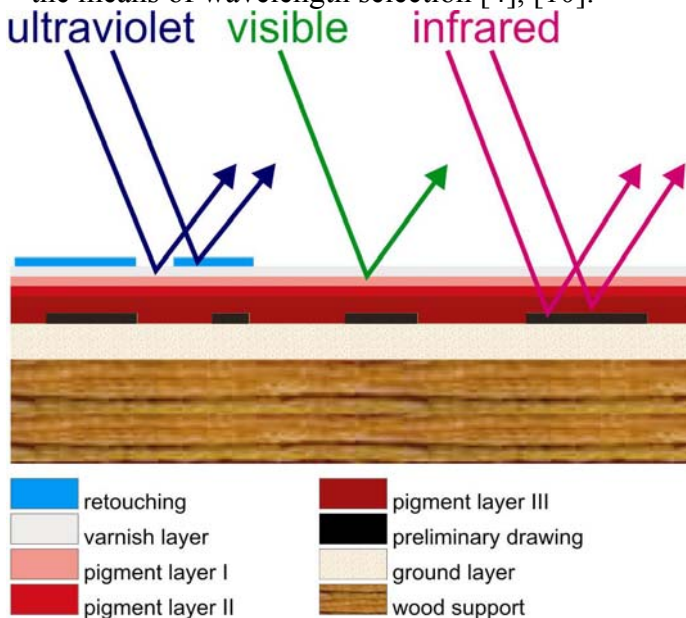


Figure 1: Principle of multispectral imaging data acquisition on a virtual panel painting cross-section

When a photon is incident on the surface of a medium, the energy can be absorbed, transmitted and/or reflected by that surface, with a wavelength

determined by the material characteristic properties. The ratio of the energy reflected or scattered by the surface to the incident energy is termed the reflectance.

From the tradition and history of art we know that artist have expressed in many ways throughout centuries according to their type of message and used a variety of materials. On certain wavelengths of the EM spectrum materials can exhibit different behavior, a fact that can be quantified for distinct tasks in accordance to the area on which the investigation is focused. This nondestructive method allows examination of the underlayers but also of the conservation status from the top layer, giving an important overview for the early stage diagnosis.

The spectral range of the camera used for acquisitions by CERTO⁶ is located between 365 - 1100 nm which means that the recordings could be provided from near UV - VIS - near IR with different spatial resolution. Being a fast and portable method multispectral imaging had become a widely used type of recording for both movable and immovable cultural heritage.

3 DESCRIPTION OF THE IMAGING MODES AND APPLICATIONS

The complexity of an artwork resides not only in the symbolic message but also in intimate designed structure. Many of the artists throughout career experienced specific technique which expresses a certain *fingerprint* of their own.

Multispectral imaging enables a *smooth* characterization of the component layers starting from the first layer located at the top of the surface and following the structure into the depth, a depth that is constrained by the wavelength, illumination and material characteristics.

3.1 Visible examination

The visual inspection is the most common type of analyze in the documentation process and represents our first contact with the work of art. This approach is established unmediated by direct *naked*

⁶ Centre of Excellence for Restoration by Optoelectrical Techniques - INOE 2000; Magurele, Ilfov

⁵ Changes of the original composition during the process of painting

eye observation. The visible examination can produce two types of analyze - one with aesthetically value and another one, more pragmatic, made by a specialized investigator (art historian, conservator, scientist, art investor etc). In this sense experience and a good understanding of the artwork technology can highlight significant data related to the state of conservation. What is important to know is that these two types of regarding an artwork are related one to each other. Any change that occurs in the color or in the shape of the composition affects not only the aesthetical impression over the viewer but also her status as a valuable object.

Multispectral imaging technology offers higher color accuracy than conventional RGB cameras - more color channels being used to sample the visible wavelength range. Combined with colorimetric analyzes this method can be very efficient in monitoring the process of pigments fading.

Typically recorded images in the visible spectrum are used as reference sources for the other imaging modes.

3.2 *UV examination*

UV imaging is a well-known method used in the examination of artworks since the 1920's and basically it was assigned to discriminate varnishes or overpaintings [11], [6].

Fluorescence is a type of luminescence (emission of light exclusive of thermal sources) exhibited by some materials (e.g. pigment) which irradiated by electromagnetic radiation (ultraviolet light) emits light of visible color. Unlike phosphorescence light is emitted by the sample only while the UV stimulation is active. Fluorescent lamps or the active source of radiation exploit the ability of ultraviolet radiation to interact with materials known as phosphors.

The available recording modes for this range of the EM spectrum are the UV fluorescence and the UV reflectance. These two types of imaging are highly recommended to analyze the superficial layers (top layers) since UV radiation has very low power to penetrate the paint layers. Examination can discriminate the nature of materials used in the composition of the artwork and therefore highlight

differences between old and new materials included in the artwork structure (repainting, additions or completions of material). Also this method enables to verify the quality of the varnish layer or the glaze⁷, in the case of ceramics etc. The acquisition implies the use of an active source of radiation characterized by a wavelength ranging in the near UV region (also called black light 315-400 nm).

Old paint or varnish layers exposed to UV radiation emits more fluorescence light comparing to newly applied materials and therefore retouched areas of the picture appear darker in fluorescence image. Also fluorescence imaging is particularly attractive for monitoring purposes since it can be used to document the presence of organic contaminants and compounds on an artwork either prior to, during, or after conservation or restoration process [12].

Other interesting results of UV examination are the distinction of organic binding media and recognition of pigments with well-known fluorescence behavior.

UV reflectance recording mode, which is displayed in grey tones, can characterize and highlight two important aspects concerning the top layer of an artwork - the flatness and the roughness. These two characteristics can provide two type of information: one that concerns technological detail and the other one which is related to the conservation status.

3.3 *NIR reflectography*

Underdrawings are important technological details used by artists in order to preserve the accuracy of the originally designed composition. In general the composition sketches were produced using charcoals or pigments⁸ and usually the background on which the drawing was displayed had a light tone⁹. This particular aspect is significant in

⁷ UV examination can provide data only from the top of a surface.

⁸ There were two possibilities to display the preliminary drawing using pigment: one was to make a fast sketch using a brush (pigment was mixed with a binder), the other one was to convey dry pigment from a small cotton bag through a drawing made on paper (before the display the paper had to present a network of holes who followed the lines of the drawing).

⁹ In the tradition of panel painting but also in the preparation stage of a canvas, in general, the ground was made from a mixture of animal glue and *gesso* (chalk). The white color of the ground plays an

the quest of highlighting the presence of an underdrawing[7]. As preliminary drawings are covered by other layers (pigments, varnish), it is obvious, that a nondestructive method must be used in order to reveal this technological feature without destroying the painting. Being imported in the study of the artworks by Van Asperen [1], [2], [3], in the 60's, IR reflectography is currently a well-known method applied to investigations not only on easel painting but also on paper documents, panel painting or mural painting.

The capability of recording depends on the illumination system but also on the wavelength selection of the camera sensor. Sometimes the resolution of the acquisition is sacrificed in order to obtain data from the underlayers.

4 CASE STUDIES

For a better understanding of the multispectral imaging some case studies will be presented. In this way we will try to focus on different types of techniques and materials.

A. Case study: identifying technical details that prove the authenticity of a porcelain Japanese plate, dated XIX century; private gallery collection.

Imari porcelain is the name for Japanese porcelain that were made in the town of Arita. They were exported to Europe extensively from the port of Imari, Saga between the second half of the 17th century and the first half of the 18th century.

Export of Imari to Europe stopped in mid-18th century when China began export to Europe again, since Imari was not able to compete against China due to high labor cost. But export of Imari porcelain surged back at the end of 19th century (in Meiji era) when Japanese art flourished in Europe. Thus in western world today two types of Imari ceramics can be found, one is those exported in mid Edo period and those exported in Meiji.

So though there are many types, westerner's conception of Imari, in popular sense, represents the Imari produced and exported in large quantities in

mid 17th century. The type is called Kinrande. Kinrande Imari is colored porcelain with under glaze cobalt blue and over glaze red and gold.

Because there were often used copious gilding, sometimes with spare isolated sprigged vignettes and often densely patterned in compartments analyze of technological details are essential for proving the authenticity of this objects.

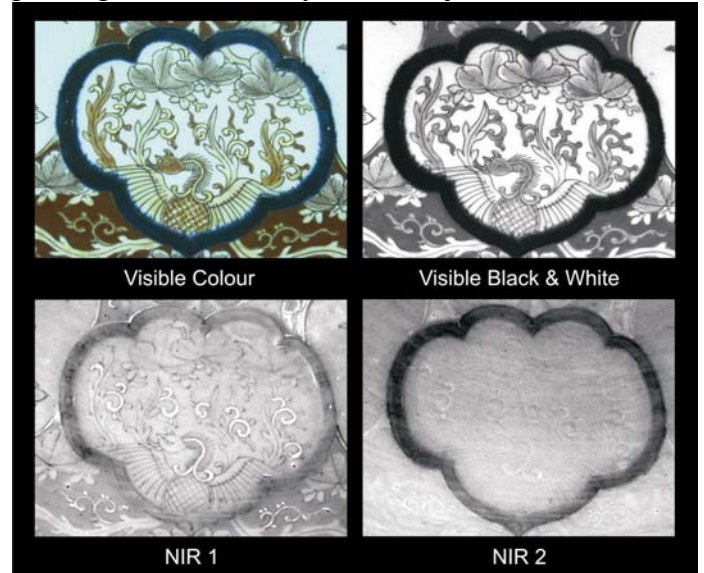


Figure 2: Front side detail - Imari porcelain plate dated approximately XIX century - Japan; Private collection

The four recordings have provided additional data regarding the technological features which are characteristic to this specific type of artwork. Modern industrial tools for contemporary ceramic production enhance the productivity process but fail to approach original handmade quality of the traditional objects. In order to confirm the authenticity of the Imari plate NIR images were recorded to highlight some of the technological features. By comparing the two reflectography images with the visible Black and White we could underline some interesting details. For example in the NIR 1 image are well seen the lines of the drawing but also the areas of the plate where it was used gold leaf. In the NIR 2 image we can distinguish the first stages in realization of the plate - division of the main decoration areas with cobalt blue and elaboration of the preliminary drawing (very smooth and complex draw most probably copied after a previous sketch).

In contrast with the complex front side decoration of the plate this floral motif was a free expressive sketched made with cobalt blue. No

important role in the NIR reflectography acquisition because it reflects almost all the radiation while the black carbon of the drawing is absorbing. In this mode is established the contrast required for discriminating the presence of the underdrawing.

preliminary drawing was used in this case¹⁰. In the NIR recordings are highlighted the spots from where the decoration was started. Because of their thickness the glaze layer could not cover properly. In these conditions those points represent the most exposed areas to the degradation process.

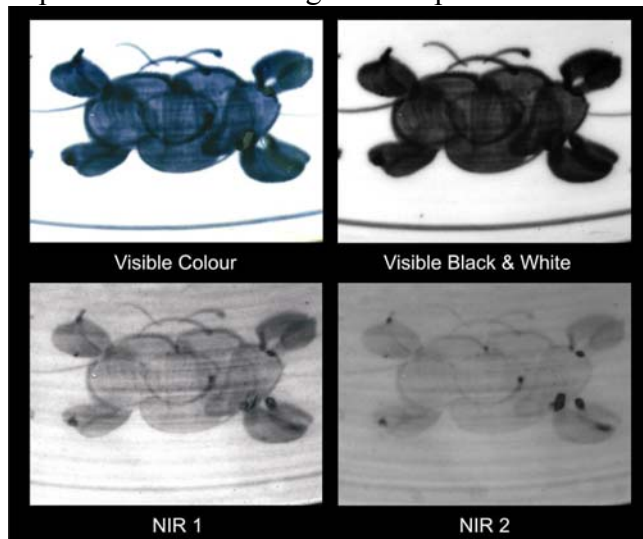


Figure 3: A back side detail of the plate. Floral motif made with cobalt blue

Other interesting detail underlined is the circular stroke direction of the glaze applied after the painting stage which proves that this final phase was made manual with a brush.

These listed technological features enabled by the use of NIR reflectography represent significant evidence in order to confirm the authenticity of the Japanese porcelain plate. To be more precisely regarding the term of *authentic* - we cannot practically demonstrate that this really is an Imari porcelain plate but we can strongly sustain that the artwork was manufactured in accordance with the Imari porcelain tradition.

B. Case study: highlighting characteristic technological features in an impressionist painting Easel painting - first half of XX century, Romanian impressionist school - private collection

This painting displays a rural landscape with a character placed in the foreground. The recorded detail is located in bottom side of the artwork.

By using the NIR and Visible imaging modes we could establish some interesting technological features regarding the manner of painting. As references were used the visible acquisitions. The

¹⁰ See in comparison the NIR 2 recording from Fig 2

shape, size and stroke directions of the brush could be examined in the NIR recordings. Also in the NIR reflectography acquisitions are highlighted the stages of the composition developed by the painter. Small strokes characteristic to the impressionist movement have been used to create the landscape. This kind of stroke is uniformly displayed on the full surface of the painting. From the technological point of view is important to know that the painter was not using *impasto* technique like many of the impressionists¹¹. Instead he preferred to have a thin layer of paint displayed smoothly on the canvas. The typical style of not using frequent superimposed layers is emphasized in the NIR 2 recording. Also from this image we can figure that the painter preferred to make a free sketch using pigment instead of the charcoal drawing. This detail reflects that the painter choused to have a spontaneous and fast manner of work - most probably this painting was made *en plain air*¹².

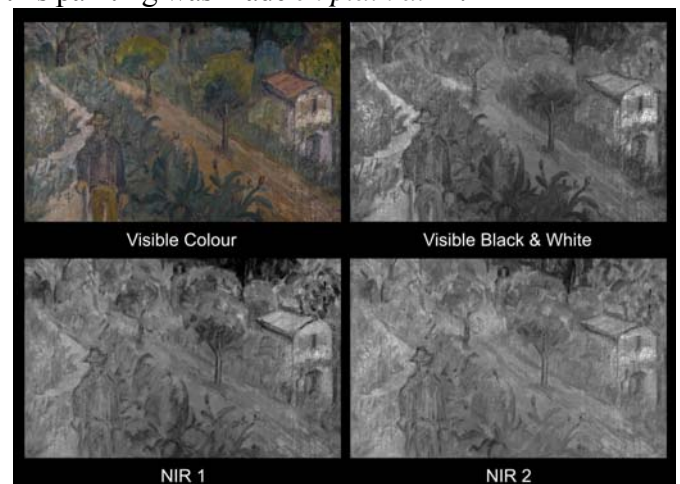


Figure 4: Acquisition modes of the multispectral camera highlighting differences which appear in the depth of the paint layers

C. Case study: multispectral investigation of a mural painting included in a restoration process. Magurele church - Ilfov county, mural painting detail - dated half of the XIX century. Since some previous investigations made in NIR reflectography have demonstrated that there are no under paintings beneath this representation we focused our attention on the surface characterization.

UV recordings usually can generate important

¹¹ To obtain the effect of diaphanous the painter used more oil than pigment.

¹² "In the open air" - is a characteristic fast type of working in natural light - very popular to the impressionist movement, who developed in the same time with the introduction of paints in tubes.

information regarding the top layer features. In fluorescence mode is highlighted the presence of a restoration intervention made at the link between the hand of the left side character and the central representation of the crown. This intervention follows as a trajectory the path described by the fracture that crosses the full detail. These typologies of cracks are generally induced by earthquakes.

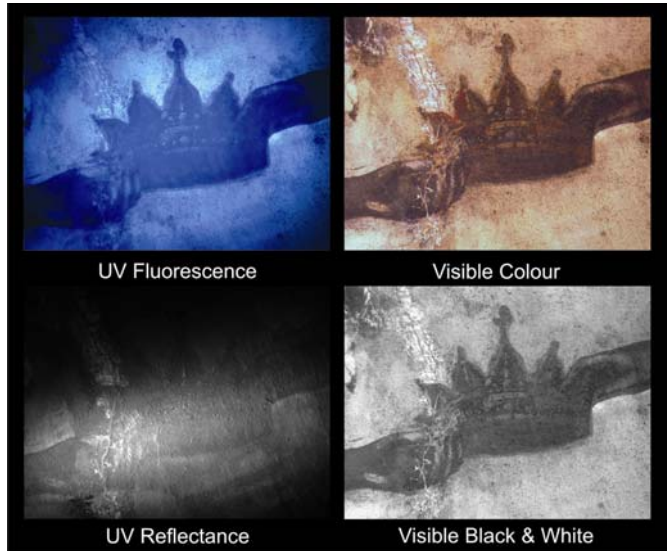


Figure 5: UV and visible recordings of a mural painting - detail located in the narthex vault of Magurele church

In the UV reflectance mode only details from the top of the surface can be exposed such as smoke and dust deposits. Important features are also the marks of the crack that designates the border between original painting and later intervention. From the Visible spectrum recordings we notice the influence of smoke and dust deposits over the chromatic tones of the painting. The resulted documentation can be regarded as an important reference in the elaboration of a methodology for restoration.

D. Case study: comparison of different spectral modes used to investigate a painting made on paper support.

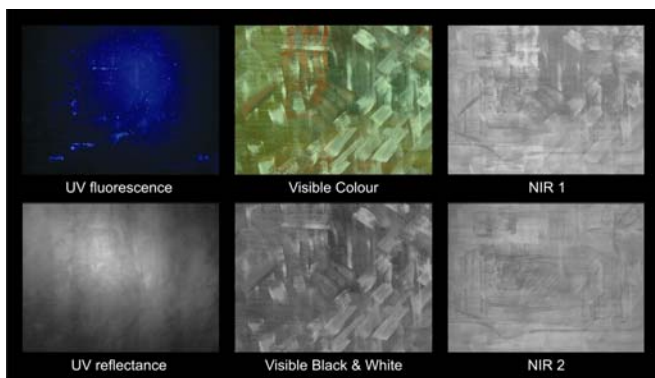


Figure 6: Comparison of recordings from three different regions of the EM spectrum

As an overview on Fig 6 it can be noticed a gradual transition from the left side which is dedicated to the UV region to NIR reflectography images grouped in the right side.

The UV recordings are focused in highlighting features that appear at the top of surface. UV reflectance recording gives a prompt characterization of the surface planarity and roughness while in UV fluorescence mode are highlighted the deposits of dust, the small scratches and the fluorescent materials from the surface. The Visible color mode recorded with high accuracy the specific aspect of the painting. In order to comment the NIR recordings we have made a continuously comparison with the Visible Black & White acquisition, image which represents the reference in this case.

In the NIR 1 is distinguished the charcoal underdrawing only in the left side of the image. The explanation for this aspect is the thickness of the paint layers in that region but also the high reflectance of those pigments. By going further in to the depth, while using a different range of the wavelength for NIR 2 recording, we notice that the underground is display uniformly on the whole image.

5 CONCLUSIONS

For the quality and the control over the restoration process of artworks modern techniques for documentation, investigation, monitoring and diagnosis are essential [12]. In accordance to this strategically methodology multispectral imaging represents an ideal method for an early stage process of data acquisition. Being characterized as a fast, nondestructive and portable technique multispectral imaging can easily be applied to different type of artworks.

Additional information recorded from other spectral ranges can determine key decisions in the perspective of conservation.

Being structured as a multilayer examination this imaging method can be used not only for the evaluation of the conservation status but also for the art history field. In this case significant features are the possibility to highlight traces of lost decoration or to study the presence of underdrawings.

The few presented case studies are validating the capabilities generated by this nondestructive, fast and accurate method in the field of cultural heritage and underlines once again the important role of a scientific approach in art investigation.

REFERENCES

- [1] Van Asperen de Boer, J.R.J - Reflectography of paintings using an infra-red vidicon television system, *Studies in Conservation* 14 (1969) 96–118.
- [2] Van Asperen de Boer, J.R.J - A note on the use of an improved infrared vidicon for reflectography of paintings, *Studies in Conservation* 19 (1974) 97–99
- [3] Van Asperen de Boer, J.R.J - Examination by infrared radiation, *PACT* 13 (1986) 109–130
- [4] Haida Liang - Advances in multispectral and hyperspectral imaging for archaeology and art conservation, *Applied Physics A – Materials Science & Processing*, Springer-Verlag, 2011
- [5] Ashwini K. Bendiganavale and Vinod C. Malshe - Infrared Reflective Inorganic Pigments, *Recent Patents on Chemical Engineering*, 2008, 1, 67-79
- [6] M. Hain, J. Bartl, V. Jacko - Multispectral analysis of cultural heritage artifacts, *MEASUREMENT SCIENCE REVIEW*, Volume 3, Section 3, 2003
- [7] Mauro Bacci et al - A study on a set of drawings by Parmigianino: integration of art-historical analysis with imaging spectroscopy, *Journal of Cultural Heritage* 6 (2005), pp 329–336
- [8] Philippe Colantoni et al - Analysis of multispectral images of paintings, *14th European Signal Processing Conference (EUSIPCO 2006)*, Florence, Italy, September 4-8, 2006
- [9] M. Attas et al - Near-infrared spectroscopic imaging in art conservation: investigation of drawing constituents, *Journal of Cultural Heritage*. 4 (2003) 127–136.
- [10] Christian Fischer and Ioanna Kakoulli - Multispectral and hyperspectral imaging technologies in conservation: current research and potential applications, *REVIEWS IN CONSERVATION NUMBER 7*, 2006
- [11] A. Pelagotti, L. Pezzati, A. Piva and A. Del Mastio - Multispectral UV fluorescence analysis of painted surfaces, *14th European Signal Processing Conference (EUSIPCO 2006)*, Florence, Italy, September 4-8, 2006
- [12] M. Simileanu, W. Maracineanu, J. Striber, C. Deciu, D. Ene, L. Angheluta, R. Radvan, R. Savastru - ADVANCED RESEARCH TECHNOLOGY FOR ART AND ARCHAEOLOGY ART4ART MOBILE LABORATORY, *Journal of Optoelectronics and Advanced Materials*, vol.10, nr.2, ISSN 2-2008, pg. 470-473;

The combined use of archaeometric techniques for non-invasive analysis of paintings: the study of Albanian icons by Onufri

E. Franceschi & D. Nole

Department of Chemistry and Industrial Chemistry, University of Genoa, Genova, Italy

S. Vassallo

Restorer, Genova, Italy

Abstract: The present study is part of a project concerning the characterization of Albanian Byzantine and post-Byzantine icons, through the identification of pigments, of painting technique and the state of conservation of the artworks. The Albanian iconographers produced an incredible number of icons from the 14th and 19th century and about 6000 of them are conserved in the Museum of Medieval Art of Korça (Albania). The study of these artworks is conducted by non-destructive methods, X-ray fluorescence, visible light reflectance spectrophotometry and UV fluorescence analysis, according to an analytical procedure developed in our Laboratory. With this procedure we can recognize the inorganic pigments from their typical features. Moreover, the study of the optical properties of paintings is of fundamental importance for correct restoration. A number of zones for each painting were chosen where carrying out measurements. The present work, concerning the study of four icons of first half 16th century by Onufri, has allowed us to recognize the palette and the painting technique used in these works of art by this famous painter

1 INTRODUCTION AND RESEARCH AIMS

1.1 *The Museum of Korça*

The Museum of Medieval Art of Korça (Albania) houses important artworks of various periods by both anonymous and famous masters. Amongst the artworks are icons of the fourteenth and fifteenth centuries and masterpieces executed by leading painters, such as Onufri, Nicholas, Onufri Qiprioti, Konstantin the Teacher, Konstantin Jeromonaku, Konstantin of Shpati, David of Selenica, and the Çetiri brothers, a family of painters from Grabovë (Korça district). The most important sixteenth century artist in this museum is Onufri, who was a great exponent of the icon and fresco painting of this period. His signature was identified for the first time in the frescoes of St. Nicholas church in Shelcan (Elbasan district). His paintings can also be found in many other churches in Berat, Elbasan, Kastoria (Greece), Zerze (Prilep-Macedonia) and elsewhere.

1.2 *The previous studies of Albanian icons*

A few studies on Albanian icons have been

conducted in these last years (*Civici et al. 2005; Civici 2006; Franceschi et al. 2010; Franceschi et al. 2011*), but this amount of work is very small compared to the large number of unstudied icons in Albania that are in need of conservation.

1.3 *The present work*

This article reports the study of three post-Byzantine icons of the first half of sixteenth century (*Figs 1 a,b,c*), painted with the tempera technique on wooden panels by the Albanian painter Onufri: Resurrection of Lazarus, 54x34.5 cm, Nr. Br 56; Transfiguration of Christ, 54x34.5 cm, Nr. Br 58; Resurrection of Christ, 54x34.5 cm, Nr. Br 59, decorated for the Iconostasis in the church of the Annunciation in Berat; and The Virgin with Child, 79x68 cm, Nr. 3628 (*Fig. 2*) coming from the church of Constantine and Helen in Berat and traditionally attributed to Onufri.

The aim of this research is to identify which pigments are the original pigments used by the painter, which areas of the icons have been restored and which pigments were added during restoration.

Additionally, the painting technique used by this famous artist in order to confirm the correct attribution of The Virgin with Child.

This information will be very useful to art historians and can be used to aid future restorations.



Figure 1: Photos of the Icons from the Iconostasis in the church of the Annunciation in Berat (Albania):

a) Resurrection of Lazarus; b) Transfiguration of Christ; c) Resurrection of Christ.



Figure 2: Photo of the Icon from the church of Constantine and Helen in Berat, attributed to Onufri.

2 METHODOLOGY

The historical, artistic and cultural importance of the studied icons guided us to use non-destructive techniques, with a methodology already employed in previous works, (Franceschi et al. 2010; Franceschi et

al. 2011), including X-ray fluorescence, visible light reflectance spectrophotometry and UV fluorescence. For each icon from 9 to 12 measurement spots have been selected. In the case of Transfiguration of Christ and The Virgin with Child two small samples were also taken from the back of the paintings. In the case of Resurrection of Christ only photographic and visual inspection, besides reflectance spectrophotometry, were used; for the other icons the following archaeometric techniques were applied.

2.1 Optical microscopy and macrophotography

Optical observation and photographic documentation were achieved using a Dino-lite portable digital microscope and a Canon EOS 350D camera equipped with a Canon Zoom Lens EF-S 18–55 mm.

2.2 X-ray fluorescence spectrometry (XRF)

Elemental analysis was performed using a Lithos 3000 portable system and an appropriate Lithos program by Assing to process the data. The apparatus consists of a Mo tube, a Zr filter and a semiconductor silicon detector, cooled by the Peltier

effect. The operating parameters were: 25 kV, 0.3 mA and an acquisition time of 120 s. The elements with the highest intensity detected on the paintings, such as lead, iron or mercury, were used as internal standards for calibration of the data.

2.3 UV fluorescence

This analysis was conducted using a ceiling light with four Sylvania black light blue F18W/BLB-T8 bulbs. The digital camera used for recording images was a Canon EOS 350D, used without a barrier filter. This is a non-destructive superficial analysis that is used to identify the presence of one or more film-forming substances such as varnishes applied on the work (resins, oleoresins, proteins, etc.) and can also generally detect previous restorative interventions.

This technique allows us to assess the condition of the paint, as well as detect and/or enhance the presence of restorations or biological attacks, even when they appear indistinguishable to the naked eye. It can also provide some information about pigments that may have their own particular fluorescence; these included the yellow rose of zinc white, the bright light of lead white and the non-fluorescence of titanium white.

2.4 Reflectance spectrophotometry

Measurements were performed using a Minolta CM-2600 portable spectrophotometer equipped with an integrative sphere inside the apparatus and a Xenon lamp to pulse the light on the sample surface. Light is reflected by the surface with an angle of 8°. It is captured by a silicon photodiode that measures the spectrum between 360 and 740 nm with an interval of 10 nm. Colour coordinates may be used to characterize the pigments too; they are based on the CIEL*a*b* system using an illuminant D65 with an observer angle of 10°. In this system, L* represents colour lightness while a* and b* are the coordinates of chromaticity. Coordinates +a* and -a* indicate red and green values while +b* and -b* indicate the yellow and blue values, respectively.

2.5 SEM – energy dispersive system

Scanning electron microscopy (SEM) was

conducted using a Jeol 5600 LV scanning microscope equipped with an energy dispersive X-ray spectroscopy (EDS) by Oxford. The elemental composition was determined using the prepared cross-sections in low vacuum.

2.6 FTIR spectroscopy

Fourier transform infrared (FTIR) spectra were measured by means of a Fourier transform infrared spectrometer Spectrum One System by Perkin Elmer that operates between 7,800 and 350 cm⁻¹, with Universal ATR equipment.

3 RESULTS AND DISCUSSION

The inorganic pigments used for the paintings were identified based on their principal characteristic elements, their relative abundance and by comparing their reflection spectra with the literature data as well as with those of a pigment database developed in collaboration with the Soprintendenza per i Beni Architettonici e il Paesaggio della Liguria.

The results are discussed separately for each icon.

3.1 Resurrection of Lazarus

Twelve spots were selected, where we performed the XRF measurements. In order to cover most completely the palette of colours. One spot more was selected to carry on the reflectance spectrophotometry.

3.2 X-ray fluorescence spectrometry

The data obtained from the X-ray fluorescence (XRF) measurements were processed as discussed in the literature (*Seccaroni & Moiola 2004*). From these data, we detected the presence of various elements in the different layers of the painting.

The experimental data obtained by X-ray fluorescence, specifically the counts measured for the most sensitive peak of each element for each analysed spot, are collected in Table 1. Note that when arsenic and lead occur simultaneously in a sample, their principal peaks are superimposed and cannot be used for analysis. Consequently, when arsenic and lead occurred in the same area (spot 10), we considered the counts of K β (11.73 keV) and L β (12.61 keV)

respectively. The same peak overlap occurs when sulfur (S $K\alpha$ 2.31 keV) and lead (Pb $M\alpha$ 2.35 keV) are present in the same spot. For this reason it was difficult to ascertain the presence of sulfur in the analysed spots of this icon. From the elements detected it is possible to ascertain the different pigments present and the preparative layer composition. In addition the occurrence of elements as titanium and zinc can suggest the restoration phases occurred in different periods. Titanium was found in three spots (1,2,10)

and zinc in five (1,5,9,10,11), thereby indicating the occurrence of restoration interventions. In fact, these elements have to be attributed to white ZnO (Kühn 1986) and TiO₂ (Laver 1997) pigments. These pigments have been used only since the nineteenth and twentieth centuries, respectively. It is important to note that from the experimental data we can exclude any correlation between titanium and iron (Helvig 2007), suggesting the use of modern titanium white.

Table 1: The counts of the main peaks of the elements detected in the analysed points of Resurrection of Lazarus.

spot	colour	Ca	Ti	Fe	Cu	Zn	Au	Hg	As K β	Pb L α	Sr
1	golden ground	195	7	69	10	37	505	603		tr	170
2	golden ground	250	3	82	12		352			27	160
3	red dress	6		9	60			4170		870	105
4	cave dark shadow	30		292	8					3370	112
5	light brown of mountain	10		64	124	15				5050	15
6	green garments	13		60	8115					1200	57
7	red garments	45		1760	53			975		800	130
8	light red grave	7		14	22					4670	20
9	dark red grave	24		1015	42	6	20	50		3385	74
10	brown of mountain	31	6	180	735	10			70	3260	70
11	red garments	15		155	50	14		57		3970	50
12	red suit	3		19	26					4980	30

Table 2: The counts of the main peak of the chief elements detected in the analysed points of Transfiguration of Christ.

spot	colour	Ca	Fe	Cu	Hg	Pb	Sr
1	background	168	62	4		75	176
2	red	25	28	47	3654	302	155
3	white	17	28			5307	7
4	brown	57	489	114		2456	71
5	light brown	61	880	102		3262	55
6	brown	29	1413	395		4076	33
7	green	84		20743		2425	185
8	light red	33	61	64	623	12397	30
9	dark red	174	4710	110	3417	2227	344
10	red	88	160	964		6060	276

3.2.1 UV fluorescence

In Figure 3 the whole UV picture of Resurrection of Lazarus is shown. Details are shown in the Figures 4 and 5, compared with the visible light photographs.

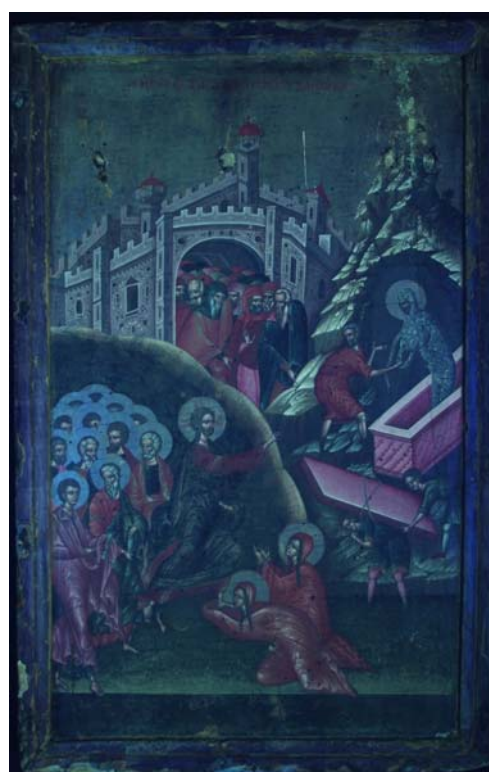


Figure 3: The UV photograph of Resurrection of Lazarus.



Figure 4: Detail of the Resurrection of Lazarus: on the left the UV photograph, showing the presence of lead white (white fluorescence), gold leaf (light blue fluorescence), red ochre and iron oxides (darkening), cinnabar (purple fluorescence). Woodworm holes are visible in the macro-photograph.

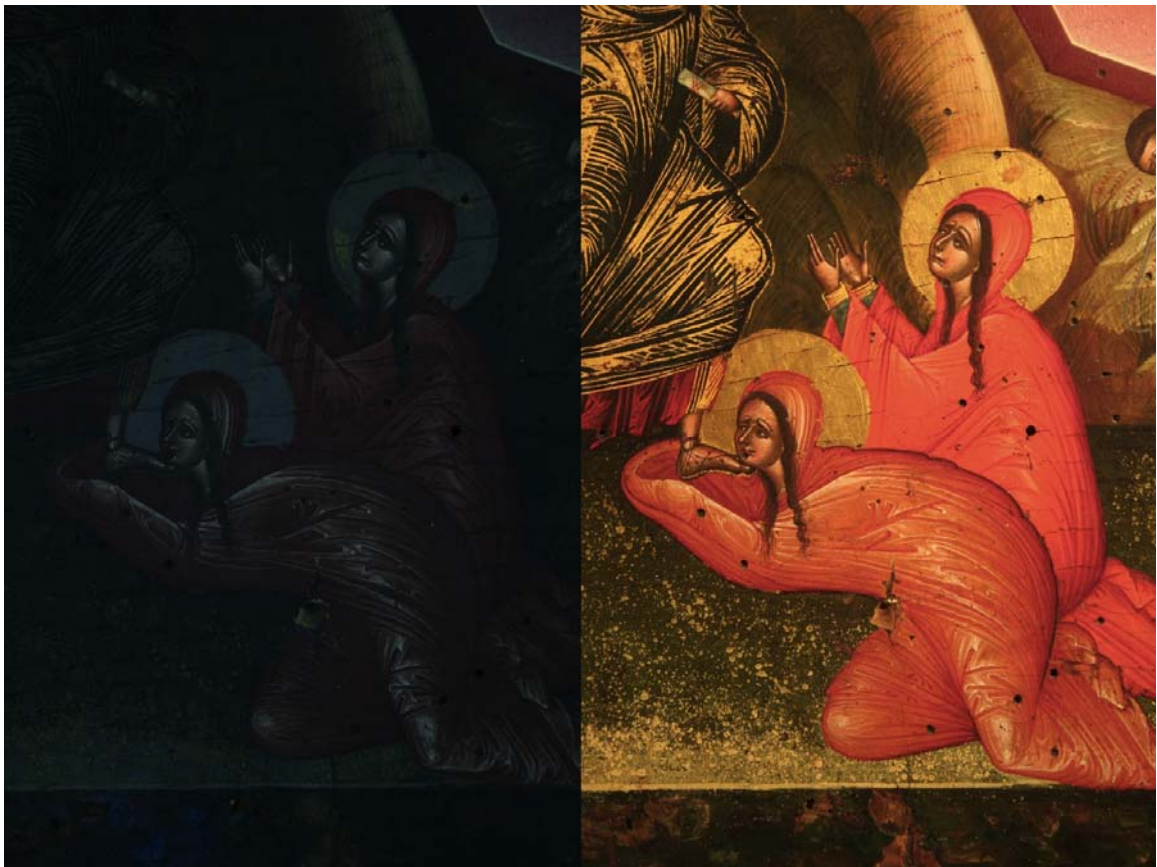


Figure 5: Detail of the Resurrection of Lazarus: on the left the UV photograph, showing the presence of lead white (white fluorescence), gold leaf (light blue fluorescence) and gold in powder, iron oxides (darkening), cinnabar (purple fluorescence), restoration interventions (see for example the aureoles). Woodworm holes are visible in the macro-photograph.

3.2.2 Reflectance spectrophotometry

In Figures 6 and 7 the twelve spectra obtained on measured areas of the icon are reported, with the curve relative to the thirteenth measurement, performed in correspondence of the red dress of Saint Martha. The data can confirm the use of the pigments identified by means of the other measurements.

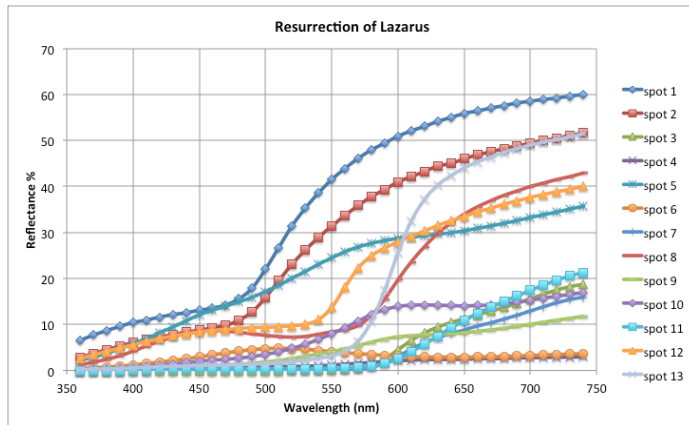


Figure 6: Reflectance spectrophotometric curves for Resurrection of Lazarus: twelve spots correspond to the XRF measurements, the thirteenth to the red dress of Saint Martha.

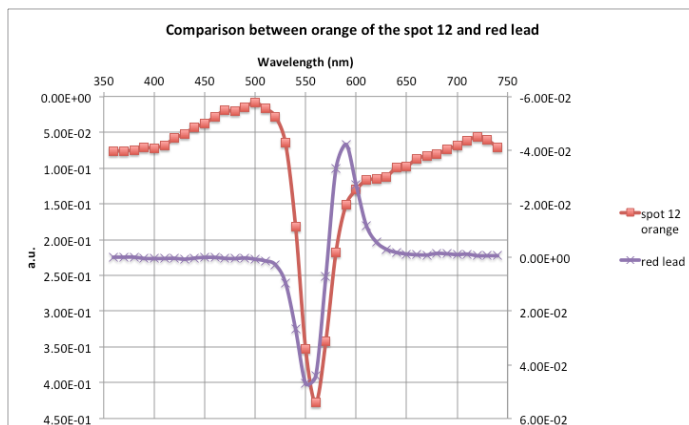


Figure 7: Reflectance spectrophotometric curve for Resurrection of Lazarus, spot 12: the second derivative of the experimental curve is compared with the spectrum of standard red lead. The comparison shows the use of red lead in mixture with other pigments, giving a darker tonality

3.2.3 Cross section

The sample taken from the back of the wooden panel was observed by optical microscope and electron scan microscope, and analysed by means of FTIR spectroscopy.

The stratigraphy is shown in Figure 8. The preparation layer of the backside of the Table has been obtained by mixing gypsum, colored with carbon particles, and a collagen based glue (as

indicated by the FTIR measurement reported in Fig. 9). In part is present lime too and its alteration product, calcium oxalate.

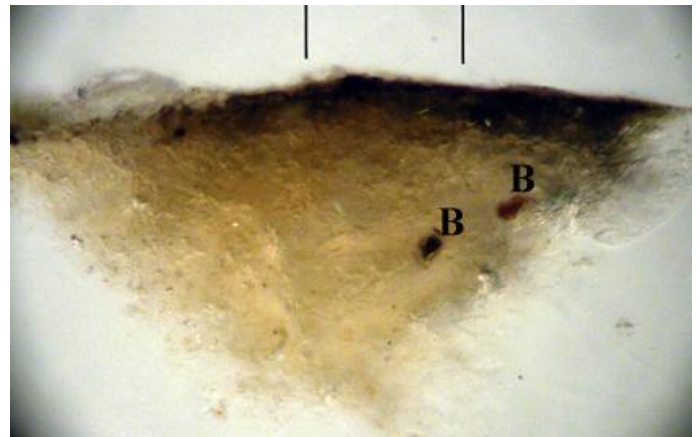


Figure 8: Cross-section of a micro-sample from the back of the Table, showing the preparation with gypsum colored by carbon particles. With B are indicated remains of pigments.

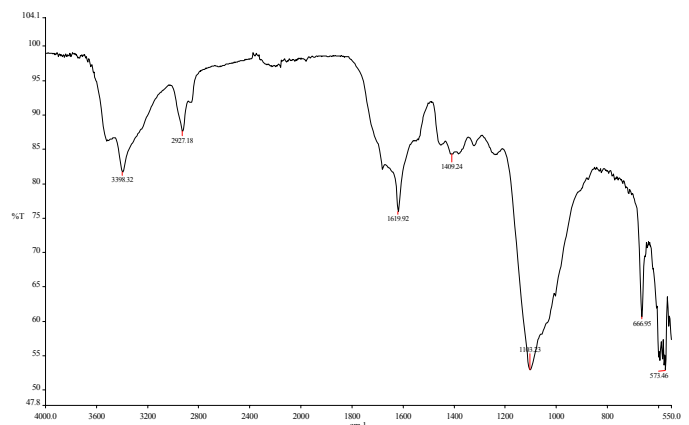


Figure 9: FTIR spectrum obtained on the micro-sample of preparation of Resurrection of Lazarus, showing the preparation formed by the mixture of gypsum and collagen glue, with traces of white egg.

3.3 Transfiguration of Christ

Ten spots were selected in order to carry out the XRF analyses. One more spot, in correspondence of the red inscription, was chosen for the reflectance measurements.

3.3.1 X-ray fluorescence spectrometry

The counts measured for the main peak of the principal elements for each analysed spot, are collected in Table 2. The count for Zn (spot 10), indicating a restoration intervention, is not reported.

3.3.2 UV fluorescence

Figures 10 and 11 display the UV photographs obtained for the Transfiguration of Christ.



Figure 10: The UV photograph of Transfiguration of Christ highlights the areas recently restored and the presence of fungal and bacteriological activity. As it regards the pigments it is noteworthy the use of lead white, cinnabar and ochers.

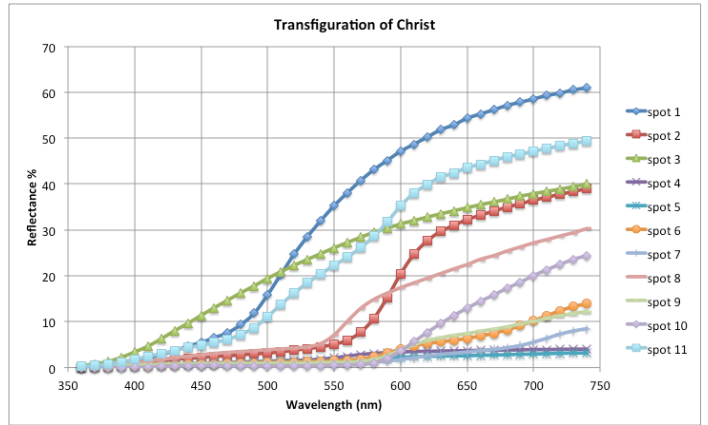


Figure 12: Reflectance spectrophotometric curves for Transfiguration of Christ.

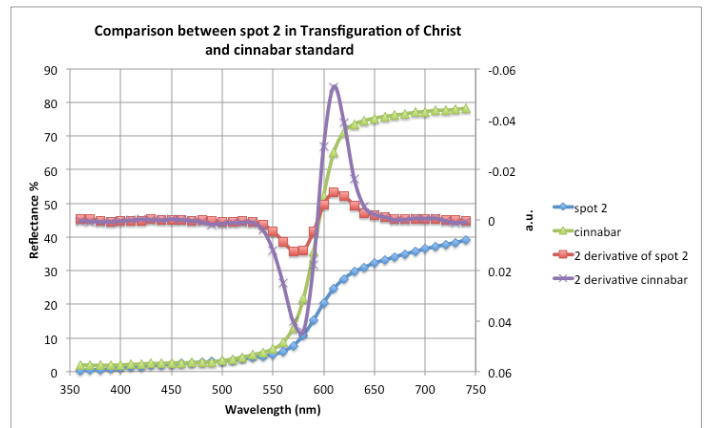


Figure 13: Reflectance spectrophotometric curves for Transfiguration of Christ: the comparison with cinnabar standard of the curves and their second derivative confirm clearly the main composition of the pigment.

3.4 Resurrection of Christ

In the case of this icon we achieved only UV, visible light images and reflectance spectrophotometry. A comparison between some selected images is reported in Figures 14 and 15. Spectrophotometric curves are shown in Figures 16 and 17.



Figure 11: A detailed UV photograph of Transfiguration of Christ compared with the visible light photograph; noteworthy the behavior of malachite in the green areas, the cinnabar given as pure pigment and in mixture with other red pigments, the different ochers containing iron. Woodworm holes are visible in the macro-photograph.

3.3.3 Reflectance spectrophotometry

In Figures 12 and 13 the reflectance spectra and their elaboration in second derivative are compared with the reference spectra for some pure pigments.

Figure 14: The UV photograph of Resurrection of Christ highlights the areas recently restored. As it regards the pigments it is noteworthy the use of lead white, cinnabar and ochers. The fluorescence of indigo mixed with lead white is evident.





Figure 15: Detail of the UV photograph of Resurrection of Christ, compared with the visible light photograph. It is noteworthy the use of lead white in spots that contour the Saints on the left; cinnabar has a strong change of colour under UV radiation; the ochers used in several areas become darker. The fluorescence of indigo mixed with lead white is evident. Woodworm holes are visible in the macro-photograph.

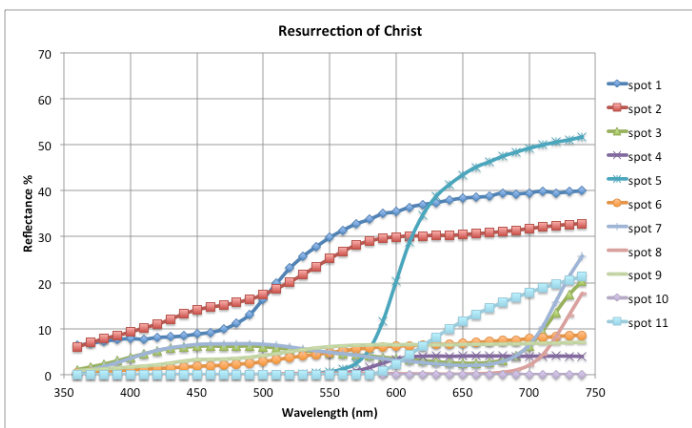


Figure 16: Reflectance spectrophotometric curves for Resurrection of Christ:

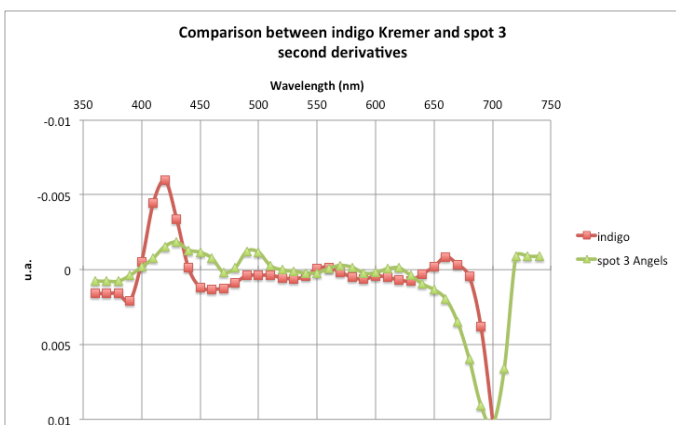


Figure 17: Reflectance spectrophotometric curves for Resurrection of Christ: the comparison with a standard sample of indigo (Kremer) and the measure corresponding to spot 3 suggests the use of indigo as pigment in mixture with other pigment, probably lead white.

3.5 The Virgin with Child

Nine spots were selected to perform XRF and reflectance spectrophotometric measurements.

3.5.1 X-ray fluorescence spectrometry

In Table 3 the results of the measurements are collected. The counts for Zn (spots 1, 4, 5, 6, 9), Ti and Cr (spots 1, 4, 6), Cd and Se (spot 5), indicating areas where restoration interventions occurred, are not reported. This method suggested the use of a number of original pigments (cinnabar, red lead, ochre for flesh, orange and red); a copper based pigment, likely malachite for the green paint on a layer of green earth; the variety of tonalities was obtained from appropriate mixtures of these pigments and white lead.

The pigments used in restoration are very probably zinc oxide (no barium has been found), titanium dioxide, chromium oxide green and cadmium sulfo-selenide red.

Table 3. The counts of the main peak of the chief elements detected in the analysed points of The Virgin with Child.

spot	colour	Ca	Fe	Cu	Au	Hg	Pb	Sr
1	background	28	102	12			22	119
2	gold	9	138	45	1302	3654	333	607
3	red	18	2166	24		8297	404	277
4	green	9	181	4888			7055	149
5	dark red	38	2352	41		23		242
6	green	52	456	395			189	192
7	red	5	38	31		8490	612	254
8	orange	2	60	39		145	10447	41
9	flesh	37	1343	15		745	4271	250

3.5.2 UV fluorescence

Figures 18 and 19 show the UV photographs of the Virgin with Child icon.

3.5.3 Reflectance spectrophotometry

In Figures 20 and 21 the reflectance spectra and their elaboration in second derivative are compared with the reference spectra for some pure pigments.

3.5.4 Cross section

The sample taken from the back of the wooden panel was observed by optical microscope and electron scan microscope. The stratigraphy is shown in Figure 22. The preparation layer of the backside

of the Table has been obtained by mixing gypsum, colored with ochre particles, with a leant that was not identified (see the FTIR spectrum reported in *Figure 23*). In part is present lime too.



Figure 18: The UV photograph of the *Virgin with Child* highlights the areas recently restored. As it regards the pigments it is noteworthy the use of lead white, cinnabar and ochers.



Figure 19: Detail of the UV photograph of *The Virgin with Child*, compared with the visible light photograph. It is easy to observe the extended areas of restoration, the use of lead white to obtain light tonalities or white (see the eyes and flesh of the Virgin), the use of iron based pigments to obtain brown colour and the green of the dress obtained using malachite and lead white. The colour change to purple under UV radiation emphasizes the presence of cinnabar.

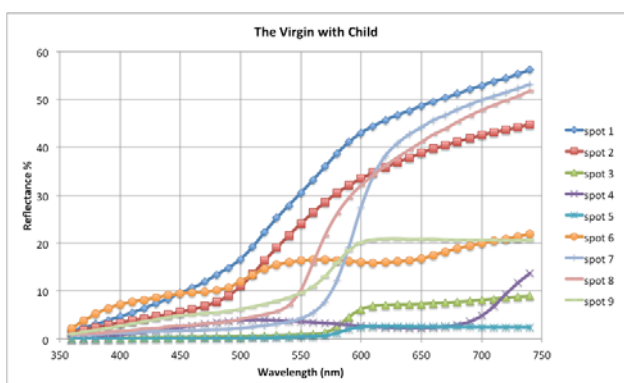


Figure 20: Reflectance spectrophotometric curves for *The Virgin with Child*:

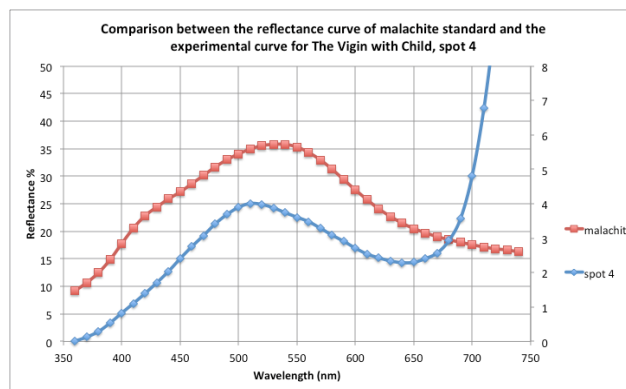


Figure 21: Reflectance spectrophotometric curve for *The Virgin with Child*, spot 4: the comparison with pure malachite shows deep differences, in part due to the presence of green earth under the paint layer and Chromium oxide of the restoration intervention.



Figure 22: Cross-section of a micro-sample from the back of the *Table*, showing the preparation with gypsum colored by few ochre pigment particles on a fragment of the wood of the panel.

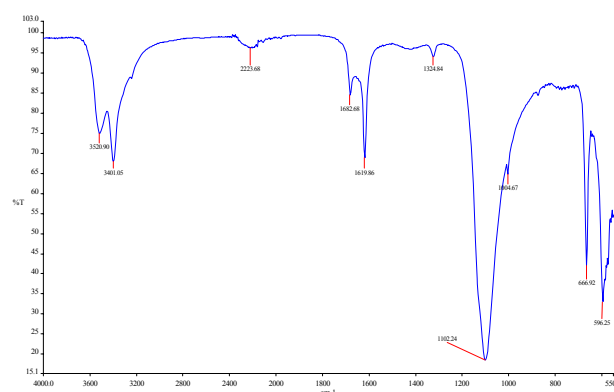


Figure 23: FTIR spectrum obtained on the micro-sample of preparation of *The Virgin with Child*, showing the preparative layer containing gypsum with traces of lime. It was not possible to recognize the organic ligand.

4 CONCLUSIONS

Non-destructive methods that we used can give information to identify inorganic pigments and to characterize the preparation technique of the

icons. In our study of Albanian icons of different periods we could distinguish different palettes and the different techniques used by Byzantine and post-Byzantine artists. For the preparation layer, for instance, in two previously analyzed Byzantine icons (*Franceschi et al. 2011*) the anonymous painters used gypsum or lime, but in a different way one from the other; Onufri used, in the three works from the Iconostasis, gypsum, with various contents in strontium. This aspect will be very important in the studies of painting conservation (*Franceschi & Locardi in prep.*).

The preparative layer in *The Virgin with Child*, appears different from that present in the other artworks, leaving the doubt if this icon should really be made by Onufri himself or more probably by his School. We could also observe that the artistic works of Onufri preserve the Byzantine tradition, innovating it with new mixtures of pigments, mainly in the red colours.

We also identified the zones of previous restoration in the icons and the kind of pigments that the restorers employed.

Besides this, in particular, the reflectance spectral curves of different pigments recorded in this work and elaborated in their second derivative, will be useful for future restoration intervention and for characterization of the conservation state of the artworks studied.

REFERENCES

- Civici, N. 2006. Non-destructive identification of inorganic pigments used in 16–17th century Albanian icons by total reflection X-ray fluorescence analysis. *J Cult Herit* 7:339–343.
- Civici, N. & Demko, O. & Clark, R.J.H. 2005. Identification of pigments used on late 17th century Albanian icons by total reflection X-ray fluorescence and Raman microscopy. *J Cult Herit* 6:157–164.
- Franceschi, E. & Nole, D. & Vassallo, S. 2010. *Icone Albanesi post-Bizantine: un approccio archeometrico*, Paper presented at VI Congresso Nazionale di Archeometria (AIAr), in Pavia, 15–18 February 2010.
- Franceschi, C. M. & Franceschi, E. & Nole, D. & Vassallo, S. & Glozheni L. 2011. Two Byzantine Albanian icons: a non-destructive archaeometric study. *Archaeol Anthropol Sci* 3:343–355. DOI 10.1007/s12520-011-0073-0.
- Helvig, K. 2007. Iron oxide pigments: natural and synthetic. In: Berry BH (ed) *Artists' pigments. A handbook of their history and characteristics, vol 4*. Publishing Office, National Gallery of Art, Washington: 39–109.
- Kühn, H. 1986. Zinc white. In: Feller RL (ed) *Artists' pigments. A handbook of their history and characteristics, vol 1*. Cambridge. University Press, London:169–186.
- Laver, M. 1997. Titanium dioxide whites. In: West FitzHugh E (ed) *Artists' pigments. A handbook of their history and characteristics, vol 3*. Oxford University Press, New York: 295–356.
- Seccaroni, C. & Moioli, P. 2004. *Fluorescenza X. Prontuario per l'analisi XRF portatile applicata a superfici policrome*. Nardini Editore, Firenze.

Non-destructive investigation using Raman spectroscopy of stone archaeological artefacts from Apesokari – Crete (Greece)

G. Flouda

Archaeological Museum of Herakleion, Heraklion, Greece

G. Vavouranakis

University of Athens, Department of Archaeology and History of Art, Athens, Greece

Th. Katsaros and Th. Ganetsos

Byzantine & Christian Museum, Athens, Greece and T.E.I. of Lamia, Material Analysis & Research Lab.

B. Tsikouras

University of Patras, Department of Geology, Section of Earth Materials, GR-265 00 Patras, Greece

Abstract: This paper presents the results of the macroscopic petrographic classification of stone vessels and tools recovered from two Bronze Age burial assemblages excavated at Apesokari/Crete, Greece. Macroscopic investigation of finished stone materials cannot always lead to conclusive results. Therefore, using the non-destructive method of Raman Spectroscopy we were able to confirm a range of various lithologies in the stone vessels and tools. They include serpentinite, ophicalcite, steatite (talc), diabase, gabbro, marble, sandstone and various limestones. All these rock-types are related to the geological formations occurring in Crete such as the ophiolite sequence, the Phyllite-Quartzite Series, the Plattenkalk Series and flysch deposits from the island. These findings are of broader relevance for exploring the production and consumption patterns of stone artifacts at the micro level. Their integration with the archaeological data helps to examine funerary customs and social processes in Prehistoric Crete before and during the establishment of the first Minoan Palaces.

1 INTRODUCTION

This paper examines stone vessels from two prehistoric funerary assemblages at Apesokari, a site situated in the region of Mesara, south central Crete, Greece. The vessels were found in two communal stone-built tombs, Tholos A and Tholos B, named after their circular burial chamber, which may have been vaulted. Both tombs lie southwest of the modern village Apesokari. They were used in the 3rd and 2nd millennium BC by the community of their neighbouring settlement (*Schörgendorfer 1951a*), which has been excavated on a prominent hill further south.

2 THE ARCHAEOLOGICAL BACKGROUND

2.1 *Tholos B* (Fig. 1) is the oldest of the two tombs, spanning most of the Bronze Age, namely from the Early Minoan (henceforth EM) I to the

Middle Minoan (henceforth MM) III in terms of pottery classification (c. 3000-1700 BC). It was excavated in 1963 (Davaras 1964), but its study was started in 2009 (Vavouranakis, in press). A key point to the history of Tholos B is the period between the EM III and MM IA (c. 2300-1900 BC). This is the period that preceded the establishment of the first Minoan palaces of Crete and thus constitutes the threshold from small kin-based communities to the first state societies on the island.

At this time, Tholos B saw a series of important architectural changes. The initial circular vault was extensively repaired and a suite of six rectangular annex rooms were added to its south. The funerary complex was also furnished with two semi-open air areas, probably for ritual activities, as well as with an ossuary space and a refuse pit for old burials. The annex rooms were used for several burials. Some were deposited directly on the ground and others were placed in clay receptacles. Most

importantly, the number of deposited funerary implements boomed. These are mainly clay vessels for drinking (handleless conical cups) and serving (jugs).

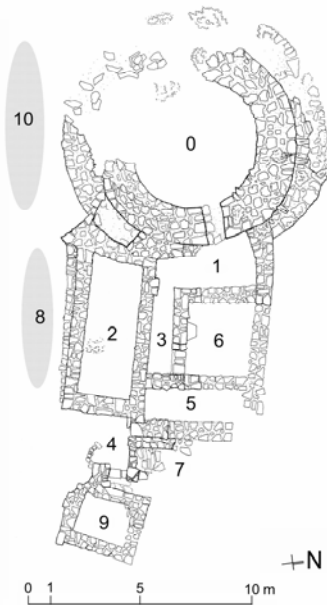


Figure 1: Ground plan of Tholos B at Apesokari.

There is also a marked increase in the deposition of stone vessels. Out of the 38 vessels of the total assemblage, only three may be placed in the early Prepalatial or EM I-II period. The rest are either late Prepalatial (EM III - MM I) or Protopalatial (MM II or c. 1800-1700 BC). As a result, the present study of stone vessels may provide an index of the changes in funerary ritual in Tholos B and by extension to social structure at Apesokari, at a time when politico-economic networks had been widening and social discourse was being intensified. After macroscopic investigation (using stereoscopic observation) and the aid of Raman spectroscopy, these vessels have been petrographically classified as diabase, serpentinite, gabbro and marble.

Peter Warren's (1969) work on Minoan stone vases is of seminal importance for their classification into types. According to his typology scheme, the so-called bird's nest bowl L2940 is of key significance for Apesokari Tholos B, because of its EM II date, which is based upon its prominent drill rings and cylindrical interior. It is made of diabase and has good parallels from other funerary sites in south central Crete, such as Platanos and Odigitria, although stone vessels from the latter are dated in the wider span of EM II - MM I (*Evely*

2012, 172), wherein the Tholos B vessels L2934 (marble), L2951 (diabase), and L2956 (serpentinite) are also dated. Spouted bowl L2934 is of a type common to north Crete, but similar vessels have been found in southern Crete, too. L2947 (*Fig. 2*) is made of diabase, too, and may also be an import from north Crete, as it is almost an exact match to a bowl from Knossos (*Warren 1969, 21-22*). Bowls L2951 (diabase) and L2956 (serpentinite) are very common EM II – MM I types. L2932, a diabase implement (*Fig. 3*), has a spout that forms a bridge with the main vessel body. Despite the EM parallels of its decoration, this spout makes in a duplicate of MM clay vases. The rest of the vessels fall into typical late Prepalatial bowl shapes.

All aforementioned vessel shapes are small sized and thus meant either to provide symbolic offerings to the dead or to implement the consumption of token quantities of food and/or drink by the living. Alternatively, they may have contained pigments for the decoration of the bodies of either the dead or of the living (Bevan 2004 112; Bevan 2007, 98-99). They were all found in the annex rooms of Tholos B, thus allowing the hypothesis that the main tholos area had become at least partly inaccessible, perhaps a kind of a symbolic taboo. The diversity of different shape types from Tholos B suggests that if there were any social hierarchy at Apesokari as a reverberation of the emergence of the nearby palace at Phaistos, it was not expressed through differential access to such artifacts.



Figure 2: Curved bowl L2947 made of diabase from Tholos B.



Figure 3: Bridge-spouted bowl L2932 made of diabase from Tholos B.

2.2 Tholos A

Tholos tomb A (*Fig. 4*) was excavated in 1942, after its partial looting by tomb robbers (*Schörgendorfer 1951b*). It was constructed many generations after Tholos B, most probably in the late Prepalatial period (MM IA, c. 2100-1900 BC) and it was used without interruption at least up to the early Protopalatial period (MM IB, c. 1900-1800 BC; *Flouda, in press*). The minimum number of interred individuals was estimated to 14 (*Flouda, in press*). The burial complex may have also been visited sporadically during the succeeding MM III phase (c. 1700-1600 BC).

The symbolic use of Tholos A as a landmark of the rural landscape was reinforced by its high visibility and the unique architectural plan of its annex complex (*Fig. 4, C-K*), which forms a rectangular compartment. This compartment was perpendicular to the Tholos A entrance and probably designed from the beginning or soon after the completion of the burial chamber as an integral extension of the latter (*Flouda, in press*). The funerary complex was also provided with a paved area featuring an open-air altar (*Schörgendorfer 1951b, 20-22, pl.17*), which was used for collective ceremonies.

The systematic study of the Tholos A funerary assemblage, that was initiated in 2010 (*Flouda, in press*), provided the scope for reassessing the archaeological correlates of the secondary burial practices and of the related drinking events. In this framework, it was suggested that the four annex rooms and the paved area outside Tholos A were used simultaneously with the burial chamber throughout the latter's period of use. The addition of these two features must have aimed from the beginning at spatially defining the conduct of the burial rites.

The 27 stone artefacts from Tholos A (*Schörgendorfer 1951b, pl. 21.1-3, 22.5-6, 23-25*) have been petrographically classified after macroscopic (using stereoscopic observation) investigation and the aid of Raman spectroscopy into the following rock-types: talc (steatite), opicalcite, diabase, serpentinite, black limestone, breccia, gabbro, grey limestone and sandstone. From an archaeological perspective, particularly interesting

are the following unpublished stone miniature vessels: the serpentinite deep bowl L2795 and its lid L2798 (*Schörgendorfer 1951b, 15*), as well as a fragmentary bird's nest bowl of grey limestone, which raises the bird's nest bowl examples from Tholos A to 15.

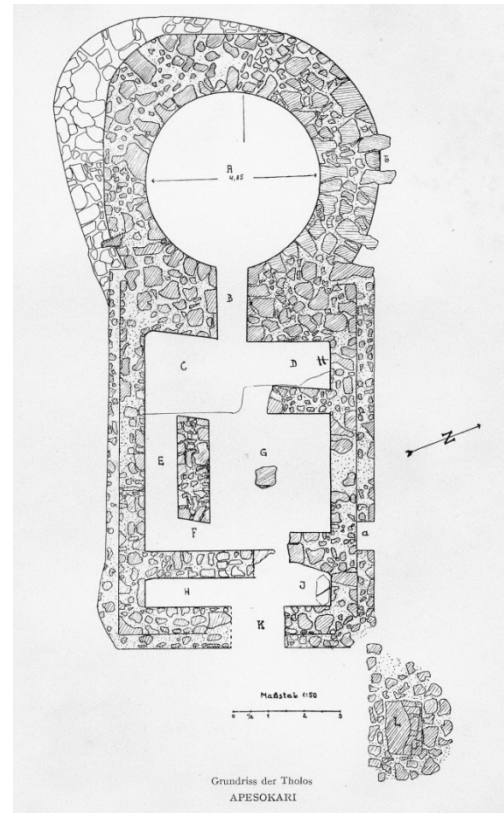


Figure 4: Plan of the Tholos A at Apesokari *Schörgendorfer 1951b, pl. 16*.

Being the only stone objects which were recovered in the main chamber, they indicate that perfumed oil, ointment or some kind of cosmetic pigment were also included in the primary burial (*Bevan 2004, 112; Bevan 2007, 98-99*). Nevertheless, these miniatures cannot be dated solely on typological grounds, because as durable objects they could have been heirlooms from an earlier period (*Bevan 2004, 107, 110, 112*). The lidded bowl (cf. *Warren 1969, 24*, whereby it is identified as chlorite) finds its closest parallel in the early example L1154 from the cemetery at Pseira in east Crete. In any case, the pottery finds from the Tholos A burial chamber suggest that the two vessels possibly belong to the late MM IA-MM IB, namely at the period of the establishment of the first Phaistian palace (*Flouda, in press*).

Serpentinite is also represented by another example, namely the bird's nest bowl L2817 (*Fig. 5*) from the mixed stratigraphic context recovered in the

paved area of Tholos A (*Schörgendorfer 1951b, 20, pl. 24.2*). This vessel and 15 other stone miniatures of various shapes probably span the MM IA - MM IIB, as suggested by the pottery finds. The petrographic classification results of this assemblage are noteworthy, as the vessels represent the remains of activity during and also after the period of use of Tholos A and its annex. However, the aforementioned bird's nest bowl L2817 and the similar example L2816 (*Schörgendorfer 1951b, pl. 23.5*) of diabase (*Fig. 6*) may be the earliest offerings of the paved area, as they belong to Bevan's "hatch-and-inlay group" that probably dates to the late Prepalatial and early Protopalatial period (EM III - MM I; cf. *Bevan 2007, 91*). The new material classification of L2816 is significant, since the early (EM II) low flat examples with circular inlay holes had generally been classified as made of chlorite/chloritite (*Warren 1969, 9-10; Bevan 2007, 91*).



Figure 5: Bird's nest bowl L2817 made of serpentinite from Tholos A.

Last but not least, the assemblage of the largest annex room G that escaped looting comprised among other finds seven stone miniature vessels. Some at least of the stone vessels stored here, as for example the black limestone tumbler L2802 with incurved sides (*Fig. 7*), hint at the practice of drinking toasts or pouring libations, maybe during the post-interment rituals.



Figure 6: Bird's nest bowl L2816 made of diabase from Tholos A.

In order to conclude, the rather limited range of shapes and the use of mainly local stones for the production of the stone artefacts reflect competitive display at the micro level of the social group using

Tholos A. Bird's nest bowls are the most prevalent type within the total assemblage. The fact that the relevant examples from the paved area are miniaturized versions of their larger prototypes specifically implies that their role was symbolic: their content was probably offered to the dead ancestors during the collective ceremonies. Establishing the provenance of their raw material to specific source areas will significantly enhance our understanding of their cultural value. Moreover, their future integration with the archaeological data from the Middle Minoan settlement at Apesokari will help to explore the possibility of the manufacture at a local level (*Palio 2008, 264-265*).



Figure 7: Tumbler L2802 made of black limestone from Tholos A

3 PETROGRAPHIC RESULTS

Non-destructive macroscopic investigation in the lithic vessels found in the two Tombs allowed their classification according to international schemes.

3.1 Diabase

It comprises dark greenish fine-grained, hollocrystalline, igneous rocks mainly with the occurrence of altered green pyroxene and light green plagioclase crystals.

3.2 Serpentinite

It is a dark green lithotype with a homogeneous appearance and typical greasy or waxy luster and a rather soapy feel. They contain mainly serpentine and chlorite.

3.3 Talc (steatite)

Steatite is an empirical term for rocks consisting of talc. Vessels made of talc are rather

soft with a light greenish tinge and a typical soapy feel. Two subtypes have been recognized. The first one is whitish, rather homogeneous with rare disseminated grains of black spinel whereas the second subtype shows additionally laminated, dark green stripes composed of actinolite and serpentine.

3.4 *Ophicalcite*

This rock-type comprises a mixture of serpentine, or other mafic fragments, and calcite. They samples show typically alternating bands of green serpentine and pale reddish calcite while two of them (L2812 and L2813) show brecciation and consist of dark green angular fragments of serpentinites, diabases and basalts in a whitish to reddish calcite matrix.

3.5 *Gabbro*

It comprises a coarse-grained, igneous, plutonic rock with holocrystalline texture. The investigated samples consist of highly weathered gabbroic lithologies with visible grey-greenish pyroxenes and whitish plagioclases. The last minerals are the most weathered constituents and under stereoscopic investigation it can be seen their partial transformation to kaolinite.

3.6 *Black limestone*

It is a sedimentary, fine grained rock composed of micritic calcite with some white veins, few mm wide, filled with sparry (coarse) calcite crystals.

3.7 *Breccia*

Three samples from the Tholos tomb A are made of a rock-type that contains angular fragments of black limestone similar to that above, cemented with variable proportions of a reddish to yellowish calcitic matrix. Few fragments show also white veins filled with sparry calcite. In the calcite cement rare purple fluorite crystals were observed.

3.8 *Grey limestone*

This sedimentary rock-type consists of calcite (mainly micritic) while local fragmentation occurs. Some veins filled with white calcite crystals are visible.

3.9 *Geological implications*

The geological structure of Crete is characterized by a pile of nappes extending along the island that derived from different paleogeographic zones (*Seidel et al. 1981; Seidel & Wachendorf 1986*). They comprise the Arvi Unit (which is an ophiolite suite), the Pindos and Tripolitza Zones, the Phyllite–Quartzite Series, the Talea Ori unit and the Plattenkalk Unit (*Seidel and Theye, 1993; Fassoulas et al., 1994; Kiliass et al., 1994; Jolivet et al., 1996*).

Diabase, serpentinite, talc, ophicalcite and gabbro are all rock-types that are typically found in the ophiolite suite occurring along Crete. Marble is a common rock-type that participates in the Plattenkalk and the Phyllite–Quartzite Series that occur in Crete. Black limestone and breccia of black limestone are rocks very similar to the carbonate rocks found in the Tripolitza Zone of Crete. The breccia may occur in tectonized zones (probably fault) within the black Tripolitza limestone. The grey limestone is common in the island of Crete occurring in the Tripolitza Zone but at different stratigraphic horizons relative to the black ones.

4 RAMAN EXPERIMENTAL RESULTS

Raman spectroscopy can give information on the composition, the stress-strain state, crystal symmetry and orientation, and crystalline defects in a material. Raman is commonly used to determine the molecular structure of organic and inorganic compounds for contamination analysis, material classification, and stress measurements. It requires very little sample preparation and is a non-destructive technique. We used the RockHound 785 Delta Nu with a laser of 785nm excitation wavelength to reduce the fluorescence signature in samples that show strong fluorescence at shorter wavelengths. Spectra can be saved with an automated baseline correction algorithm or in raw form. All spectra are referenced with the laser off to subtract ambient light. The spectral viewer allows users to interpret the most recently acquired spectrum. Spectra may be zoomed or expanded and peak heights and frequencies are reported on the screen. The spectral resolution of

about 5cm^{-1} was determined by measuring the Rayleigh line of the laser.

Figure 8 illustrates the pattern acquired from sample L2947, that indicates the presence of actinolite $\text{Ca}_2(\text{Mg,Fe})_5\text{Si}_8\text{O}_{22}(\text{OH})_2$, a typical product of alteration of pyroxene that occurs in diabases, according to the very sharp peak at 689cm^{-1} , which is the symmetric stretching of Si-O-Si bonds. The presence of a relatively strong 462cm^{-1} Raman peak indicates the possibility of α -quartz crystal inclusions in the sample. In Figures 9 and 10 we present the Raman spectra of the marble samples L2934 and L2950 that verify the presence of calcite in them. The Raman spectrum of calcite displays the main peak at 1086cm^{-1} , corresponding to the symmetric stretching of CO_3^{2-} group. While the approximate position of this peak is characteristic for carbonates in general, the additional peak at 288cm^{-1} (Fig. 9) is specific for calcite, and allows it to be distinguished from aragonite and other carbonates.

The Raman spectrum acquired from sample L2795 suggests the presence of lizardite, after comparison to bibliographic data, a typical polymorph of serpentine, hence confirming that it comprises a serpentinite vessel (Fig. 11). Peaks at $233, 348, 386, 509, 628, 500\text{-}550, 642, 681, 694, 1051, 1101\text{cm}^{-1}$ (Fig. 11) are clearly comparative with the typical Raman peaks of lizardite at $233, 350, 388, 510, 630, 640, 683, 690, 1045, 1096\text{cm}^{-1}$. Especially the bands at $694, 382$ and 233cm^{-1} are produced by Si-O-Si symmetric stretching, SiO₄ tetrahedra modes and O-H-O group variations (Rinaudo et al. 2003).

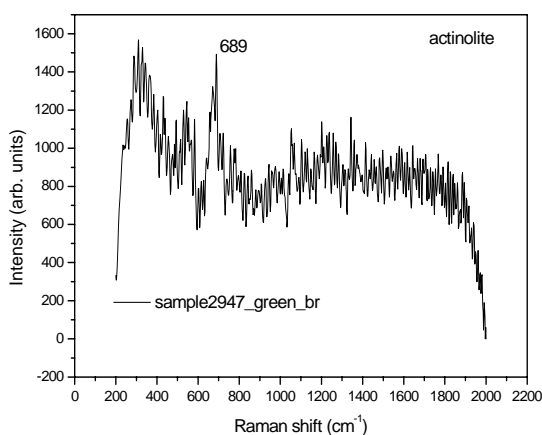


Figure 8: Raman spectrum of the diabase sample 2947 from Tholos B.

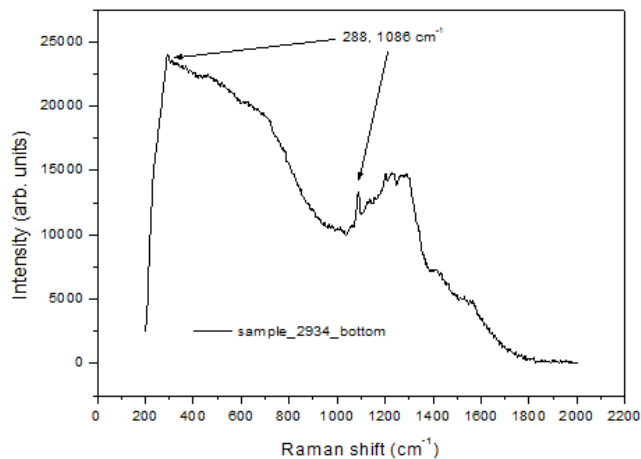


Figure 9: Raman spectrum of the marble sample 2934 from Tholos B.

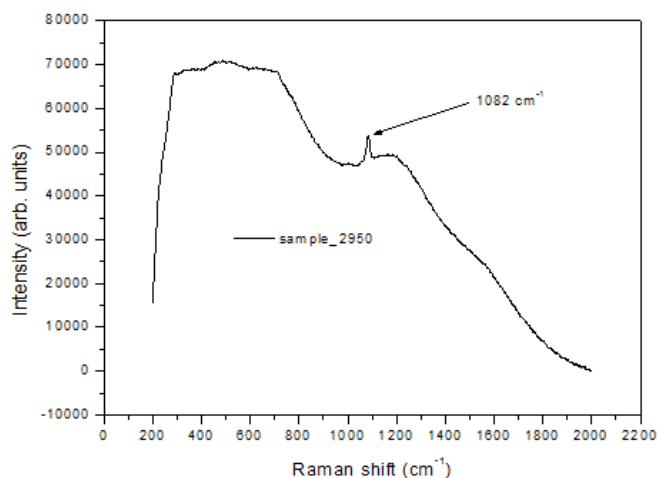


Figure 10: Raman spectrum of the marble sample 2950 from Tholos B.

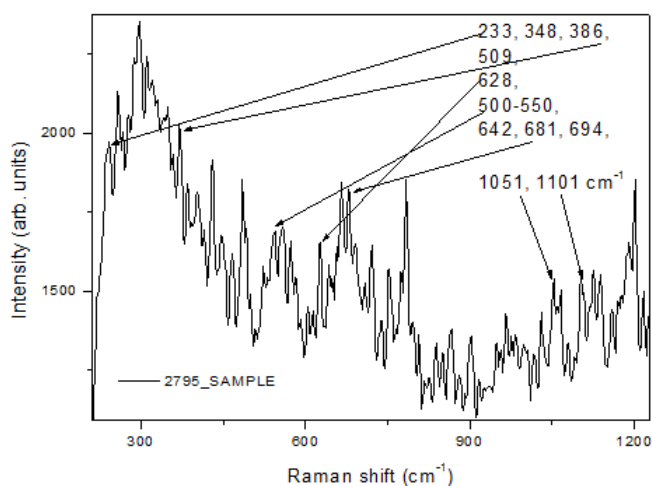


Figure 11: Raman spectrum of the serpentinite sample 2795 from Tholos A.

5 CONCLUSIONS

The stone artefacts from the two tholos tombs at Apesokari that were discussed fall into few specific archaeological types. They are small vessels

probably used for pigments or symbolic offerings in the course of funerary ritual. Their classificatory connections with major nearby sites, such as Lebena, Platanos, Odigitria, the palace of Phaistos or the north part of the island are supported by the Cretan provenance of their raw materials, which has been established by combined macroscopic examination and Raman spectroscopy. This examination indicates that a small-scale society, such as Apesokari, had been able to be part of island-wide networks of communication and emulate related practices, such as the relatively conspicuous consumption of stone implements within funerary ritual.

ACKNOWLEDGEMENTS

The study of the stone artefacts from Apesokari Tholos A was generously supported by the Mediterranean Archaeological Trust and of the ones from Tholos B by the Institute of Mediterranean Prehistory. All inventory numbers refer to the Heraklion Archaeological Museum inventory of stone objects.

REFERENCES

- Bevan, A. 2004. Emerging civilised values? The consumption and imitation of Egyptian stone vessels in EMII-MMI Crete and its wider eastern Mediterranean context. In J.C. Barrett and P. Halstead (eds.), *The emergence of civilisation revisited*: 107-126. Oxford: Oxbow.
- Bevan, A. 2007. Stone vessels and values in the Bronze Age Mediterranean. Cambridge: Cambridge University Press.
- Davaras, C. 1964. Arhaiotites kai mnimeia Kritis. Anaskafai. *Archeologiko Deltio* 19(B3): 441.
- Evely, D. 2012. Stone vases and tools. In A. Vasilakis and K. Branigan (eds.), *Moni Odigitria. A Prepalatial cemetery and its environs in the Asterousia, southern Crete (Prehistory Monographs 30)*: 170-185. Philadelphia: INSTAP Academic Press.
- Fassoulas, C., Kiliias, A. & Mountrakis, D. 1994. Postnappe stacking extension and exhumation of high-pressure/low-temperature rocks in the island of Crete, Greece. *Tectonics* 13: 127-238.
- Flouda, G. In press. Reassessing the Apesokari Tholos A record: preliminary thoughts. *Rivista di Archeologia* 2011, 35.
- Jolivet, L., Goffé, B., Monié, P., Truffert-Luxey, C., Patriat, M. & Bonneau, M. 1996. Miocene detachment in Crete and exhumation P-T-t paths of high-pressure metamorphic rocks. *Tectonics* 15: 1129-1153.
- Kiliias, A., Fassoulas, C. & Mountrakis, D. 1994. Tertiary extension of continental crust and uplift of Psiloritis metamorphic core complex in the central part of the Hellenic Arc (Crete Greece). *Geologische Rundschau* 83: 417-430.
- Palio, O. 2008. I vasi in pietra minoici da Festòs. Padova: Bottega d'Erasmus.
- Rinaudo, C., Gastaldi D. & Belusso E. 2003. Characterization of chrysotile, antigorite and lizardite. *Canadian Mineralogist* 41: 455-465.
- Schörgendorfer, A. 1951a. Die minoische Siedlung von Apesokari. Vorläufiger Grabungsbericht. In F. Matz (ed.), *Forschungen auf Kreta 1942*: 23-26. Berlin: Walter de Gruyter.
- Schörgendorfer, A. 1951b. Ein mittelminoisches Tholosgrab bei Apesokari. In F. Matz (ed.), *Forschungen auf Kreta 1942*: 13-22. Berlin: Walter de Gruyter.
- Seidel, E., Okrusch, M., Kreuzer, H., Raschka, H. & Harre, W. 1981. Eo-alpine metamorphism in the uppermost unit of the Cretan nappe system - Petrology and geochronology - Part 2. Synopsis of high-temperature metamorphics and associated ophiolites. *Contributions to Mineralogy and Petrology* 76: 351-361.
- Seidel, E. & Theye, T. 1993. High-pressure/low-temperature metamorphism in the external Hellenides, Crete, Peloponnese. *Bulletin of the Geological Society of Greece* 28: 49-55.
- Seidel, E. & Wachendorf, H. 1986. Die südägäische Inselbrücke. In: V. Jacobshagen (ed), *Geologie von Griechenland*: 54-80. Gebrüder Bornträger, Berlin.
- Vavouranakis, G. In press. O tholotos tafos B sti thesi Apesokari Mesaras. In M. Andrianakis, I. Tzachili and N. Dimopoulou (eds.), *Proceedings of the 2nd Scientific Meeting for the Archaeological Work in Crete, Rethymno* 26-28 November 2010.
- Warren, P. 1969. Minoan stone vases. Cambridge: Cambridge University Press.

Active Faults and Ancient Roman Greek Settlements in Aegean Region

Musa Tokmak

Archaeometry Middle East Technical University, Ankara Turkey

Vedat Toprak

Geological Engineering Middle East Technical University, Ankara Turkey

Abstract: Turkey is geologically located within an active area (Bozkurt, 2000). Active tectonism in most cases is the primary reason for the natural hazards. Most of the hazards such as earthquakes, landslides, volcanic eruption, tsunami etc are either direct results or triggered by the active tectonism (Ambraseys, 2001). Earthquakes which are the main focus of this study negatively affect the society as they result in loss of human life and commodity. Turkey is a country very rich in archaeological sites (settlements and others) of different periods. Most of these settlements are believed to suffer particularly from the earthquakes. The excavation reports of some ancient settlements have the evidences for this belief (Altunel and Barka, 2001). The purpose of this study is to evaluate the location of settlements in relation to active faults existing in the western Anatolia. The main hypothesis in this study is that there is a genetic relationship between the active faults and the location of the settlement.

1 INTRODUCTION:

West Anatolia (Figure 1) has a lot of Roman and Greek period ancient cities (Figure 2). Some ancient cities are well-known and some are known but not excavated. We have chosen 81 ancient cities (Tubinger Atlas, 1977). From early period to present times the area has been inhabited by different civilizations (Figure 2).

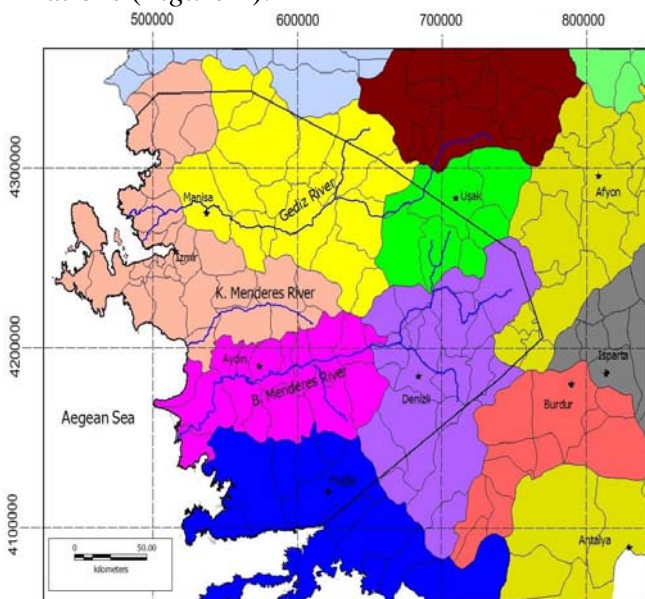


Figure 1: Location map of the study area

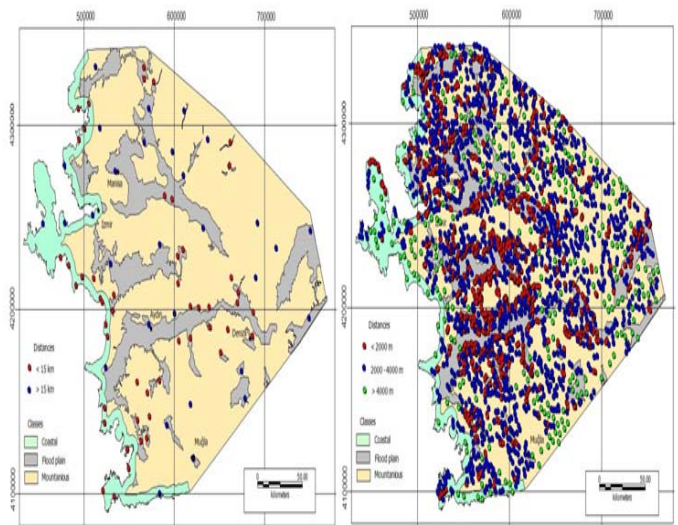


Figure 2: Distributions of Roman and Greek ancient cities (81 ancient settlements, left picture) and distributions of modern settlements in western Anatolia (right Picture)

In the study area the ancient earthquakes' traces in some cities can be seen directly or indirectly (Altunel and Hancock, 1997; Altunel et al, 2003; Altunel, 1998). However, there are many reasons that can cause the damage for ancient cities. For that reason, a special attention must be given in modern archaeological excavations. Collapsed walls, crushed skeletons lying under fallen debris, toppled

columns, lying parallel columns, slipped keystones are the main traces of past earthquakes (Korjenkov and Mazor, 2003).

To investigate of the relationship between settlements and earthquakes in this study: topographic data, morphological classes, ancient settlement data, modern settlement data, rock data, seismic data and active fault map of the area data sets were used. For each data set, first a raw data is obtained from different sources and is processed for the final set to be used in the analysis. All data sets give us the settlements relationship with each data parameters.

1. Morphologic database: This database is composed of three raster maps that contain elevation, slope and aspect values of the region.
2. Ancient settlement database: This database contains coordinates of 81 ancient settlements as well as their morphological and rock type properties.
3. Modern settlement database: It is a similar database as for ancient settlements holding the attribute table for 2569 modern settlements (villages, towns, provinces, etc).
4. Rock type database: This is a vector map that holds the rock type polygons from geological map reclassified for this study.
5. Seismic database: Coordinates of earthquakes reported by Kandilli Observatory (Turkish State Earthquake Investigation Office) for the interval 1900-2011 with magnitude greater than 3.

Figure 3. shows the how the study steps were done.

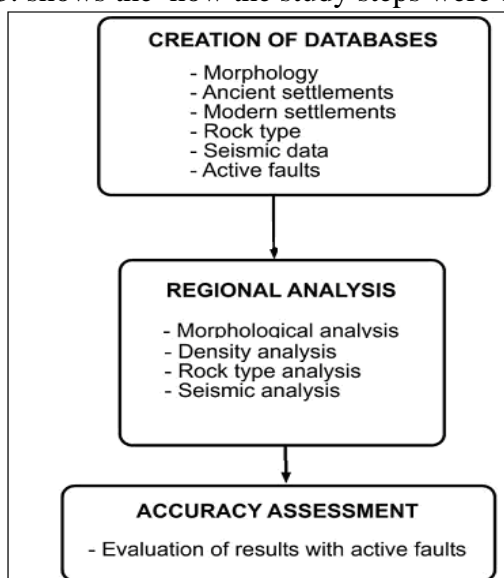


Figure 3: Flowchart showing the major steps of this study

2 MORPHOLOGICAL ANALYSIS:

SRTM data is used in this study to determine three topographic parameters (elevation, slope and aspect) for the whole area, ancient settlements and modern settlements. SRTM data is processed in Mapinfo software to produce initial elevation, slope and aspect maps.

Elevation: Elevation histograms of both ancient and modern settlements are subtracted from the histograms for the whole area (Figure 4). Positive region in the histogram indicates that the percentage of the settlements is greater than the percentage of the region for this interval. Therefore, positive number suggests that this elevation is preferred as a site for settlements. Similarly, the negative areas suggest that these elevations are avoided as settlement site.

This histogram, therefore, can be interpreted as for ancient and modern settlements

For ancient settlements: 1) 0 to 200 meters preferred, 2) 200 to 700 m inconsistent interval, and 3) above 700 m avoided as settlement site.

For modern settlements: 1) 0 to 600 m elevations are preferred. 2) Elevations above 600 m are avoided as indicated by negative values.

Both positive and negative values in the histogram for modern settlements are smoother than the ancient histogram because the number of the modern settlements is much bigger than ancient settlements.

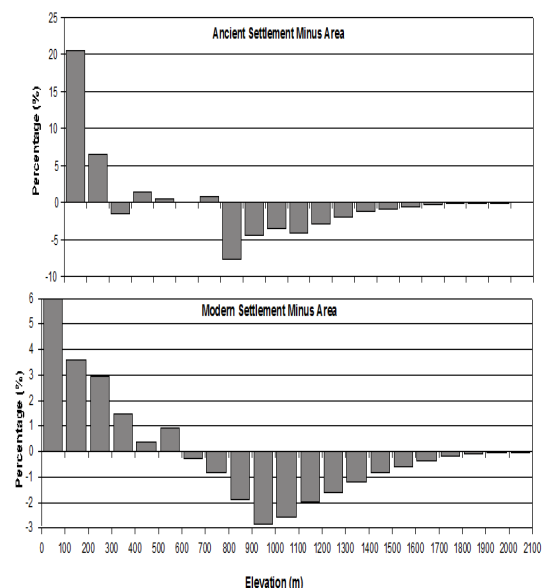


Figure 4: Subtracted histograms of ancient and modern settlements for elevation.

Slope: Similar diagram is prepared for the slope values by subtracting the histogram of settlement slope from the histogram of region slope (Figure 5). These two histograms indicate that:

- For the ancient settlement, the range between 0 and 2 degree obviously indicate the preferred interval. This slope is mostly located in the flood plains and has the highest percentage in the histogram.

- For the modern settlement, the range between 0 and 8 degrees is consistently characterized by positive values.

Comparison of two the histograms suggest that:

- Ancient settlements preferred almost flat areas as indicated by maximum concentration at 0-2 degree slope which is much higher than the modern ones.

- Upper limit of the avoided interval is 8 degrees for the ancient and 10 degrees for the modern settlements which do not suggest a radical change in time.

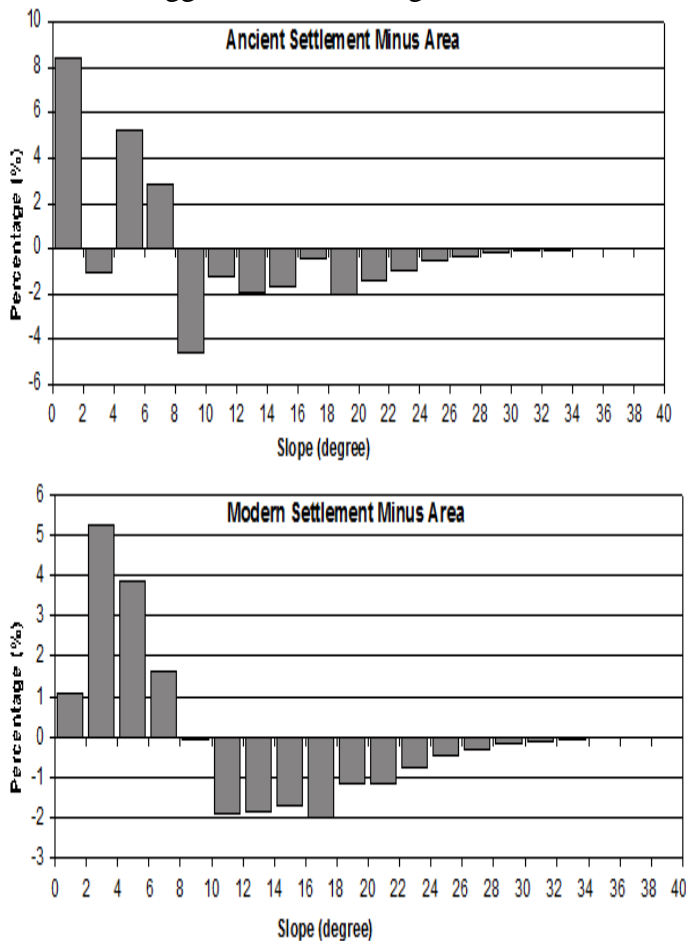


Figure 5: Subtracted histograms of settlements for the slope

Aspect: Aspect values of the settlements are subtracted from that of region to identify positive and negative regions. Results of the process are

given in the histograms in Figure 6. Aspect values are divided into nine intervals including eight principal directions and the flat areas.

According to the information provided by these histograms:

- E, SE and SW slopes are preferred by both ancient and modern settlements
- N and NW facing slopes are avoided by both ancient and modern settlements
- NE and W are avoided by the ancient but preferred by the modern settlements
- Flat, NE and W are preferred by ancient but avoided by the modern ones,
- SE is avoided by the modern settlements; there is no data for ancient settlements.

The most preferred directions for the ancient settlements are Flat, E and S whereas the most avoided directions are N and NE. Modern settlements on the other hand preferred S and SW; avoided Flat, N and NW. The most radical change between two settlement types is observed in “Flat” areas.

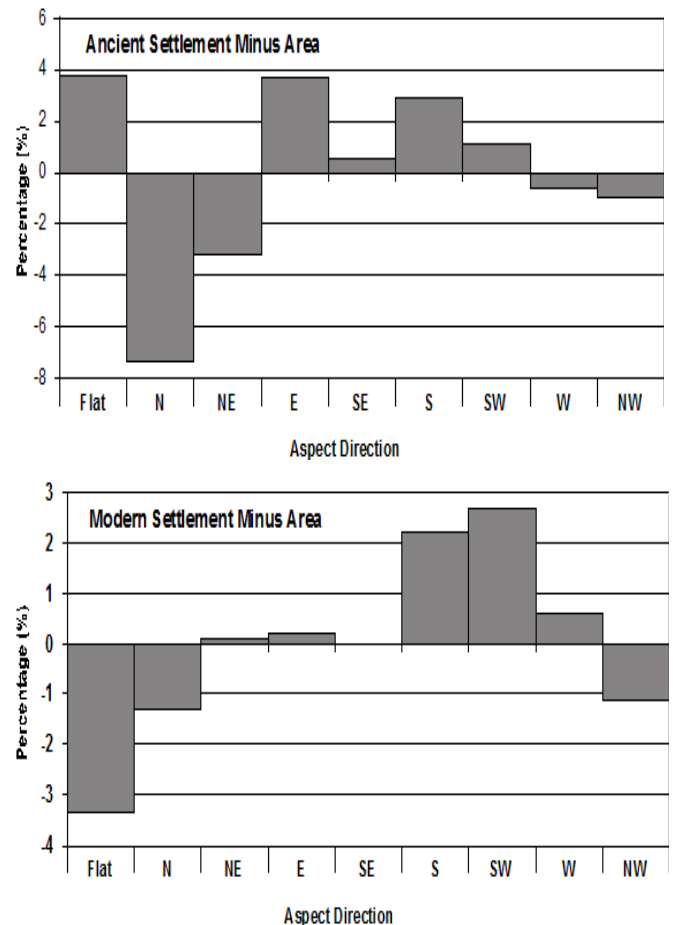


Figure 6: Subtracted histograms of settlements and the region for aspect values

3 DISTANCE ANALYSIS:

Distance analysis aims to investigate how close a settlement is located to an active fault. The studies are has divided into tree morphological classes: flood plains, mountains area and coastal region. The margins of the morphological classes will be used to infer this relationship.

Coastal settlements have a much simpler measurement which is the shortest distance to the shoreline within a buffer zone of 5 km. A total of three distance sets are measured:

- 1) Distance to shoreline for coastal settlements,
- 2) Distance to flood plain for mountainous settlements, and
- 3) Distance to mountainous area for flood plain settlement.

Each measurement set is repeated for both modern and ancient settlements, resulting in a total of six analyses. The results of these analyses are given in the histograms in *Figure 7*. The distances greater than 4.5 km for the ancient, and 7 km for the modern settlements are not shown in the diagrams. The numbers of the settlements in these intervals are very small and can be neglected. *Figure 7* shows that ancient settlements and modern settlements are distributed near the border of flood plain and mountainous area. That means that they are located very near the active fault.

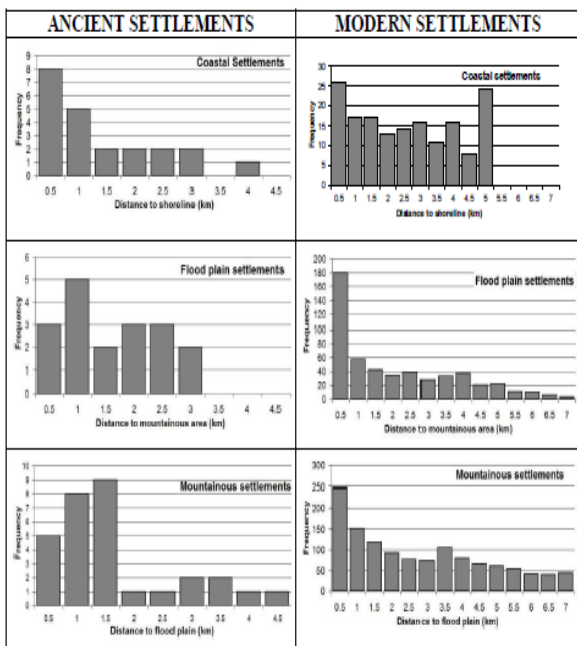


Figure 7: Histograms showing the distances to morphological classes for ancient and modern settlements. The distances given in the histograms are reorganized and plotted in.

Figure 8 on a hypothetical profile across all morphological classes. A buffer zone of 2 km is added to the boundary between flood plain and mountainous area. This zone is defined as “fault zone” because one of the assumptions in this study is that the boundary between these two classes corresponds to an active fault. Since the size of a settlement can be defined in terms of a few km², the width of this zone is assumed as 2 km. Therefore the settlements in this distance are considered to be located within the fault zone. *Figure 8* shows that ancient settlements 44% were located in the fault zone. This value decreased for modern settlements since with technological developments, the people preferred the higher areas to settle.

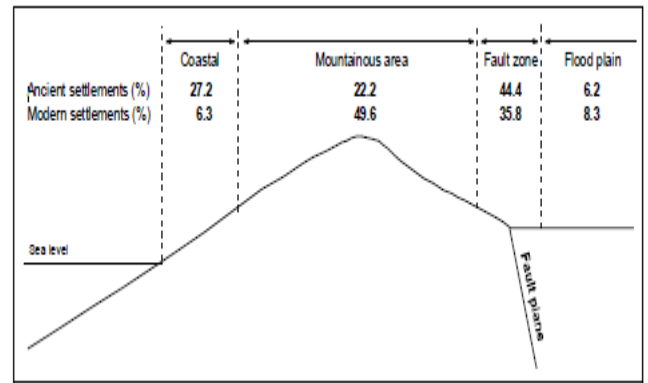


Figure 8: Distribution of the ancient and modern settlements within the morphological classes with a particular emphasis on the “fault zone” assumed between floods plain and mountainous areas.

4 ROCK TYPE DATA ANALYSIS:

Rock type data is provided from MTA and reorganized in this study. The initial map contained more than 100 individual rock types, which were reduced to 7 related classes (*Figure 9*). In fact, the most important rock unit in the database is the Quaternary alluvium, which is deposited within the flood plains. Other units, however, are also tested in relation to their elevation to understand if any rock type is preferred as settlement site (*Figure 9*). Testing the accuracy of this dataset is not practical and possible in this study. *Figure 9* shows that quaternary, continental clastics and igneous rocks were preferred by ancient inhabitants. However, continental clastics rocks were avoided by modern people.

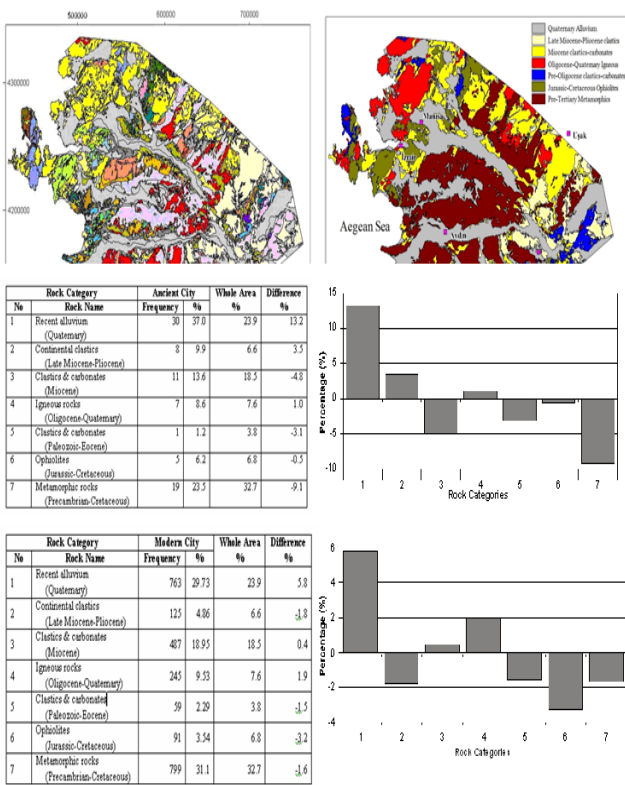


Figure 9: Rock Type and Ancient settlements preference for them
Seismic Data Analysis:

The study area is known for its recent tectonic activity. Earthquakes of different magnitude occur in the area continuously. Since the earthquakes occur along the active faults (Figure 10), the earthquakes of the last century are obtained to have an idea on the distribution of the earthquakes. Particularly the spatial relationship between the earthquakes and the flood plain boundaries is very important for this study (Figure 11). However, it should be kept in the mind that, the earthquakes of such a short period may not accurately reflect the nature of this distribution.

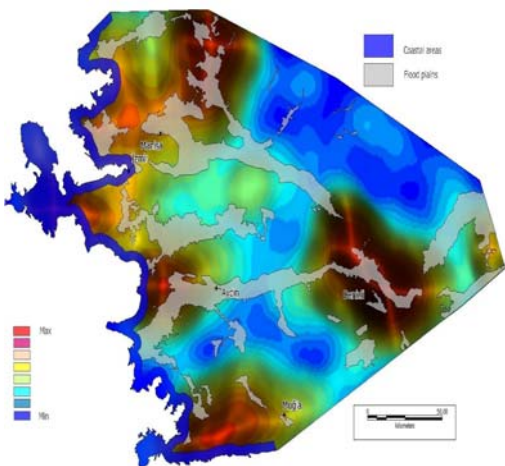


Figure 10: Density map of the earthquakes occurred within the study area in the last century (magnitude 3 and larger)

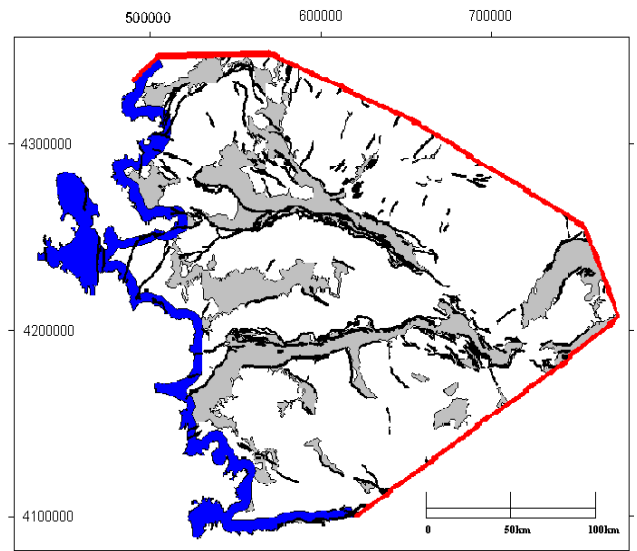


Figure 11: Morphological classes and fault lines in the study area

5 CONCLUSIONS:

This study based on the hypothesis that there is a genetic relationship between the earthquake producing active faults and the location of the settlement.

Three main assumptions used in the study are:

- Active faults can shape the earth and produce a suitable landform to settle.

- Ancient people built their settlements close to the active faults.

- Ancient people did not recognize the “fault line” First these assumptions will be tested and than the main hypothesis will be discussed using the results obtained in the study. The first hypothesis is correct as indicated by the relationship between the morphological classes and the fault lines. The margins of the flood plains coincide with the fault lines. Therefore, the fault lines define the boundary between the flat alluvial plains and steep mountain fronts. This line therefore corresponds to a sudden slope change in the area at the edge of fertile agricultural fields. Another positive factor is that, the groundwater reaches the surface along these fault planes. Therefore, the vicinity of the faultline is an attractive site for the settlement. The second hypothesis is quantified by the percentages of the settlements located close to the fault. The distance analysis indicates that the concentration of the settlements near the fault line is high. The third assumption is justified using the data compiled from

literature on the recognition of the earthquakes. Almost all parts of the world, ancient people attributed the occurrence of earthquake on different beliefs. None of these beliefs considers a “distance” to a physical structure (fault line). Accordingly, earthquake can occur anyway. Although there are some documents for Greek period scholars trying to understand the reason, all theories are far behind the recognition of a fault line. Since the people are not aware of the fault line, they did not change the location of their settlement after earthquakes. This is approved by many ancient settlements insistently built at the same location after it is seriously or totally damaged.

REFERENCES

- Altunel, E. and Hancock, P. L., 1997, Faulted Archaeological Relics at Hieropolis(Pamukkale) Turkey, *J. Geodynamics*, Vol. 24, Nos 14. pp.21-36
- Altunel, E., Stewart,I.,Barka,A., Piccardi,L., 2003, Earthquake Faulting at Ancient Cnidus, SW Turkey, *Turkish Journal of Earth Sciences (Turkish J. Earth Sci.)*, Vol. 12, pp. 137-151
- Altunel,E. and Barka, A., 2001, Impacts of Large Historical Earthquakes on Ancient Cities in the Buyuk Menderes and Gediz Grabens, Western Turkey, AGU Fall Meeting Abstracts
- Altunel,E., 1998, Evidence for Damaging Historical Earthquakes at Priene, Western Turkey, *Tr.J.of Earth Science*
- Ambraseys, N.N., 2001, The Earthquake of 1509 in the Sea of Marmara, Turkey, *Bulletin of the Seismological Society of America*, p.91
- Bozkurt, E., 2000, Timing of Extension on the Büyük Menderes Graben, Western Turkey and its tectonic implications, In: Bozkurt, E., Winchester, J.A., Piper, J.D.A. (eds), *Tectonics and Magmatism in Turkey and the Surrounding Area*, Geological Society, London, Special Publications, Vol.173, pp.385-403
- Korjenkov, A., and Mazor, E.,2003, Traces of Ancient Earthquakes in Medieval Cities Alongthe Silk Road, Northern Tien Shan and Dzhungaria, *Turkish Journal of Earth Sciences (Turkish J. Earth Sci.)*, *Turkish Journal of Earth Sciences (Turkish J. Earth Sci.)*, Vol. 12, 2003, pp. 241-261ol. 12, 2003, pp.241-261
- Tubinger Atlas, 1977, Reichert

Preliminary investigation of some copper alloy medieval objects from the northern Albania

O. Çakaj and E. Duka

Faculty of Engineering Mathematics and Engineering Physics, Polytechnic University of Tirana, Albania

Z. Tafilica

Archeological Department, Historical Museum of Shkodra, Albania

F. Stamati

Centre of Albanological Studies, Tirana, Albania

N. Civici and T. Dilo

Faculty of Natural Sciences, University of Tirana, Tirana, Albania

Abstract. The north territory of Albania is known for its sulphide copper ores. The valley of Përroi i Thatë is located in the north part of Shkodra near the Albanian Alps. During the archaeological excavations in an early Christian basilica in the village of Upper Lohë, Përroi i Thatë valley, some copper alloy objects were found. These objects were located on the traces of a medieval and handicraftsman kiln and according to the archaeological dating they belong to the IV – V century A.D. Based on the basilica structure it is believed that the handicraftsman kiln was not part of the original church which might have served as a shelter or working place for the handicraftsmen long after the church's collapse upon time. The objects were analyzed using optical microscopy (reflected light) for the micro structural investigations; the polarized light microscopy was used to study the corrosion products and X ray fluorescence for the qualitative and quantitative elements content. Also the densities of the objects were measured. Having mostly a copper content of about 99% it is believed that these objects were produced from a handicraft process.

1 INTRODUCTION

1.1 *Middle Age in Albania and copper usage*

After the Roman Empire collapse in 395 A.D. the Illyrian – Albanian territories became part of the Byzantine Empire and two of the most outstanding Emperors were Anastas I from Durrës and Justinian I from Shkupi. They led these territories from antiquity into the medieval times with their reforms, administrative and military measures. During the Middle Age the Albanian territories were included in the main commercial west-east roads and vice versa connecting different Balkan regions and further. Cities like Shkodra (north Albania) and Durrës (centre Albania) were mentioned for working tools, house utensils and belts production while Vlora (south Albania) was famous for the swords

production. The growth of the cities and the creation of the Albanian principalities during the XIV – XV century were reflected in the local coins production. Christianity was introduced in Illyria since the I century A.D. (*Ceka 2000, Cabanes 2008, The Academy of Sciences of Albania 2002*)

At the beginning native copper was used to produce different objects. Then the copper was recovered through processing of malachite and azurite since 5000 B.C. With the passing of time the handicraftsmen learned that impurities or other chemical elements such as tin lowered the copper melting temperature and made the tool production more efficient. According to archaeological excavations during the Bronze Age the objects contained 85% - 95% copper and 15% - 5% of other chemical elements (Pb, Sn, As, etc.).

2 MATERIALS AND METHODS

2.1 Samples description

All the samples were provided from the archaeologist Mr. Tafilica who conducted the excavations in the village of Upper Lohë. (Tafilica 1988, Tafilica 1993)

The samples can be divided into two groups according to their similar structure (see *Figure 1* and 2). The first group is composed of six samples. They have a corroded surface with different sized pores. All the samples have a random shape thus they don't have a well defined one and they are relatively small (see *Table 1*). All the samples have a smooth surface except of the second sample which has a rough one. Another characteristic of these samples are the high number of pores in the structure due to probable dissolved gases during melting.

Having random shape the samples of the first group might have been remnant pieces during objects production processes.

The sample of the second group on the contrary has a flat shape with two lines of oval holes very similar to a grater and is bigger compared to the first six samples. This sample has also a corroded surface. In all the samples' cases no metal is visible; it is completely surrounded by corrosion.

The initial percentage of arsenic in different objects produced during the Bronze Age such as jewelry (arsenic increases the bronze object glitter) is very high (about 17% or less). This happened because it was unknown that arsenic was dangerous for the health. This is the reason why its content decreased in ancient object with the passing of the time.

The presence of zinc in copper increases its strength, hardness and toughness and there are possible evidence of brass objects production since the II – I century B.C. during the expansion of the Roman Empire. (Scott 1991)

1.2 Archaeological excavations in the valley of Upper Lohë, Përroi Thatë

Përroi i Thatë valley is an important region of Shkodra, near the Albanian Alps. The many archaeological monuments found in this area testify that Përroi i Thatë was inhabited since the Bronze Age following all the other historical periods because of its physical and geographical optimal conditions. The population of Përroi i Thatë made their living mainly from farming but also agricultural. There was a decrease of this valley population during the Roman invasion and the opposite happened during the medieval times where the population began to expand on the fields near the Alps.

During the summer of 1988 in the village of Upper Lohë an early Christian basilica (century IV-V A.D.) was excavated. Only its foundations were preserved. During the excavation process, inside the church traces of a handicraftsman kiln were found which had no connection with the stratigraphic or functional structure of the church. In the upper soil but yet not damaged from farming plow about 60cm below the surface of the grass a round area of ash was found (5-7cm thick, 50cm diameter) containing charcoal pieces. Also a small iron trowel, a copper sheet with two lines of long holes similar to a grater and some copper alloy small objects were found. During excavation and analysis of the materials it is believed that this kiln was a temporary establishment of a handicraftsman in the ruins of the church during medieval times. (Tafilica 1988, Tafilica 1993).



Figure 1: Six samples of the first group (I) found on the traces of the handicraftsman kiln. Above the six samples from one side and below the samples from the other side.



Figure 2: The sample of the second group (II). A copper alloy grater found on the traces of the handicraftsman kiln. On the left the grater from one side and on the right the grater from the other side.

2.2 Samples' sizes and densities

The samples sizes (length, width and diameters) were measured using a caliber and also their densities were measured according to Archimedes principle: $\rho_{\text{sample}} = G_{\text{air}} \cdot \rho_{\text{water}} / (G_{\text{air}} - G_{\text{water}})$, where G_{air} and G_{water} are the gravity forces of the sample in air and distilled water.

Table 1: The samples' sizes and densities.

Sample	Length cm	Width cm	Height cm	Density g/cm ³
Sample 1 (I)	3,5	2 0,8*	0,9	7,05
Sample 2 (I)	1,9	1,8	1,3	4,52
Sample 3 (I)	2,3	1,2 0,3	0,5	8,47
Sample 4 (I)	1,4	0,8 0,3	0,7	7,43
Sample 5 (I)	1,2	0,7 0,6	0,6	9,33
Sample 6 (I)		0,6 0,6**		8,73
Sample 1 (II)	4,2	4,1	0,6	7,36

* Two widths were measured because the samples mostly have a non symmetric shape.

** Sample 6 (I) has a nearly spherical shape, this is the reason why its diameters were measured.

Sample 2 of the first group is going to be examined in a future study because of its different surface and small density compared to the other samples.

2.3 Samples' preparation

All the samples were cleaned using water and a brush. Then they were polished in different parts using silicon carbide paper 120, 220, 320, 500, 1000, 1200 and 4000. At the end of the preparation process the samples were polished with cloth, diamante paste 6 μ m, 3 μ m and DP-Lubricant Blue. (MIT 2003)

2.4 Samples' examination

The corrosion products of the polished surface

of the samples were examined using the optical microscope with reflected and polarized light Kozo XJP300. In order to investigate the qualitative and quantitative elements composition of the samples X ray fluorescence was performed. In this study a micro X ray fluorescence portable device was used on random points of each samples' surface (BRUKER μ - X ray fluorescence). To acquire and analyze the different spectra the Spectra ARTAX Version 7.2.5.0. and M-Quant-Calib (BRUKER) softwares were used. For the micro structural investigations the polished surfaces were etched with aqueous ferric chloride (120 ml distilled water H₂O, 30 ml hydrochloric acid HCl, 10g ferric chloride FeCl₃) and examined with optical microscopy (reflected light, Kozo XJP300). For smaller magnification images the XTL6445 stereomicroscope was used. There were taken pictures using Sony TCC-8.1 camera and TS View Version 1.0.0.1 software for all the microscopic observations.

3 RESULTS AND DISCUSSION

3.1 Corrosion products

Before the micro structure examination is performed by etching the surface of the samples the corrosion products should be studied. The penetration of the corrosion deep into the metal is important evidence that the sample is ancient and authentic because it is almost impossible to create it artificially. The corrosion products of copper alloy objects are composed of three main layers. The first one is the primary patina (oxides, sulphides) which is formed since the utilization of the object. The second one is the secondary patina (halogenides, ox hydroxides, carbonates, sulphates, phosphates) that is created around the first patina during the first steps of decomposition in soil or water. And at least the third main layer is the contamination patina which surrounds the first two layers and its chemical content depends from the decomposition environment (Dilo 2009). Figures 3, 4, 5, 6, 7 and 8 represent the samples' surface observations with reflected and polarized light. The images through the microscope with polarized light were taken with the polarizer in a cross position to the analyzer. The photos from sample 1, 5 and 7 (group I) were chosen to be

presented. According to literature the red-brick with brown or orange tones is cuprite Cu_2O which composes the first patina. The second patina is mainly composed by malachite $\text{CuCO}_3 \cdot \text{Cu}(\text{OH})_2$ or $\text{Cu}_2(\text{OH})_2 \cdot 2\text{CO}_3$. Malachite is green with vitreous aspect. (Scott 1991, Sandu 2006, Murphy 2001) Both cuprite and malachite can be seen in samples' 1, 5 and 7 image with polarized light.

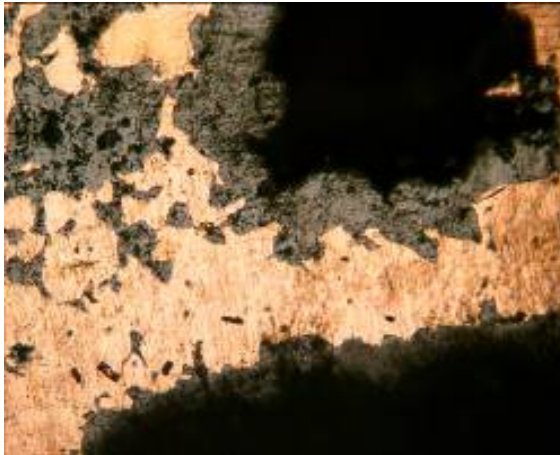


Figure 3: Sample 1 (I), image of the polished surface with reflected light, magnification 100X.

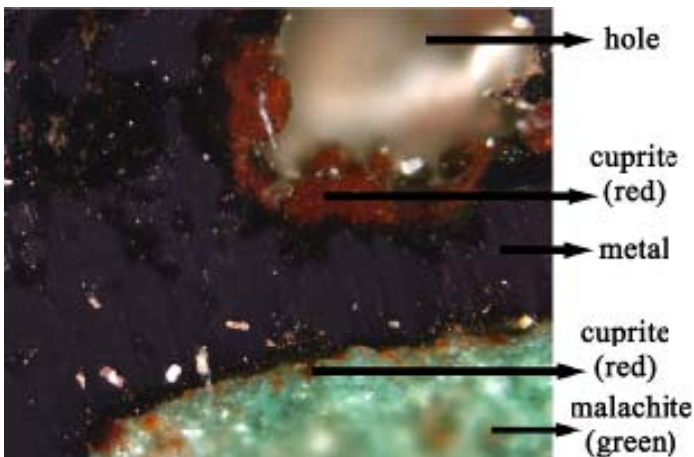


Figure 4: Sample 1 (I), image of the polished surface with polarized light, magnification 100X.

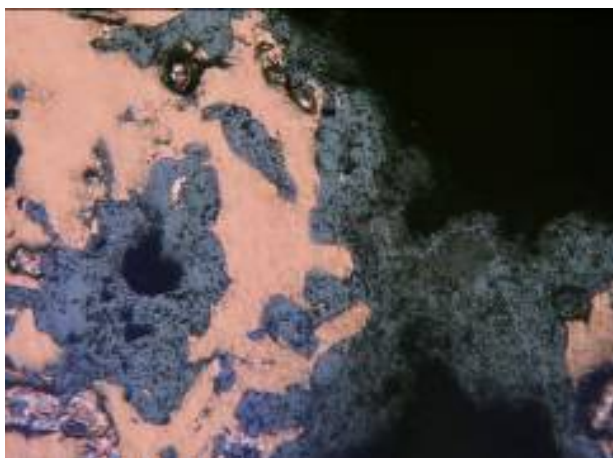


Figure 5: Sample 5 (I), image of the polished surface with reflected light, magnification 100X.

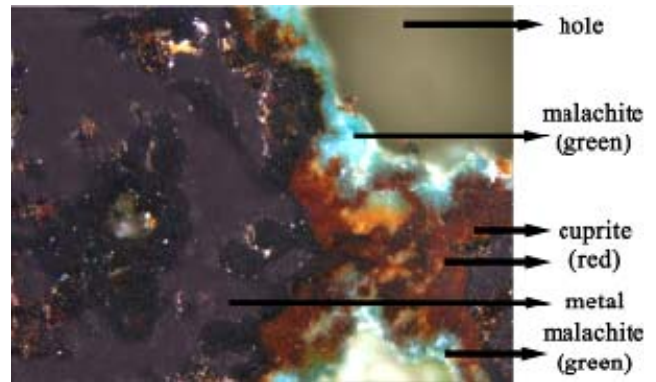


Figure 6: Sample 5 (I), image of the polished surface with polarized light, magnification 100X.



Figure 7: Sample 1 (II), image of the polished surface with reflected light, magnification 200X.

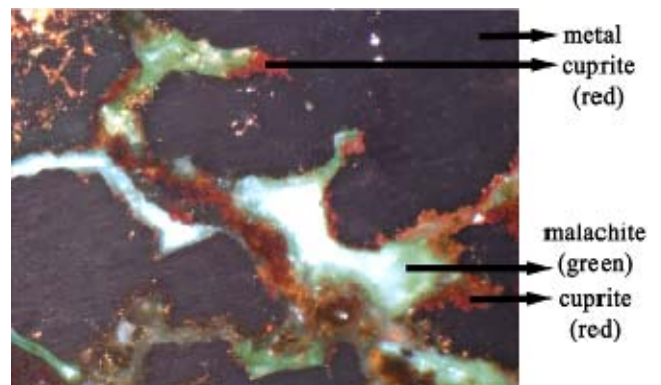


Figure 8: Sample 1 (II), image of the polished surface with polarized light, magnification 200X.

3.2 X ray fluorescence examination

For the qualitative and quantitative characterization of the samples μ - X ray fluorescence was used with a beam spot of $60\mu\text{m}$. The examining points were chosen randomly on the metal surface, on the corrosion near the metal and on the external surface. All the results for sample 1, 3, 4, 5, 6 (I) and 1 (II) are listed in Table 2 as the above order. (Potts 2008)

Table 2: μ - X ray fluorescence results on the metal surface.

Sample	Cu	Pb	Sn	Zn	Fe	Ca	Ni	As
	%	%	%	%	%	%	%	%
Sample 1	99,50	0,25	0,18	-	-	-	-	-
	99,65	0,15	0,15	-	0,05	-	-	-
	99,58	0,25	0,16	-	0,02	-	-	-
	99,30	0,41	0,11	-	0,18	-	-	-
Sample 3	99,17	0,40	0,30	-	-	-	-	-
	99,28	0,32	0,24	-	0,03	-	0,13	-
Sample 4	99,60	0,09	0,26	-	-	-	-	-
	99,59	0,12	0,10	-	0,03	0,01	0,15	-
Sample 5	99,30	0,47	0,16	-	-	-	0,05	-
	99,50	0,29	0,19	-	-	-	-	-
Sample 6	98,90	0,76	0,17	-	0,13	-	-	-
	99,37	0,35	0,13	-	0,04	-	0,12	-
Sample 1	66,92	-	-	33,06	0,02	-	-	-
	67,44	-	-	32,53	0,03	-	-	-
	66,88	-	-	33,01	0,11	-	-	-
	67,12	-	-	32,86	0,02	-	-	-
	67,09	-	-	32,72	0,19	-	-	-
	67,16	-	-	32,82	0,02	-	-	-

The mean values of the μ - X ray fluorescence results on the metal surface are calculated for each sample in *Table 3*.

Table 3: Mean values of the μ - X ray fluorescence results on the metal surface.

Sample	Cu	Pb	Sn	Zn	Fe	Ca	Ni	As
	%	%	%	%	%	%	%	%
Sample 1	99,51	0,27	0,15	-	0,08	-	-	-
Sample 3	99,22	0,36	0,27	-	0,03	-	0,13	-
Sample 4	99,60	0,11	0,18	-	0,03	0,01	0,15	-
Sample 5	99,40	0,38	0,18	-	-	-	0,05	-
Sample 6	99,14	0,55	0,15	-	0,09	-	0,12	-
Sample 1	67,10	-	-	32,83	0,07	-	-	-

In *Table 4* are shown the μ - X ray fluorescence results on the corrosion near the metal and on the external surface of the samples.

Table 4: μ - X ray fluorescence results on the corrosion and external surface.

Sample	Cu	Pb	Sn	Zn	Fe	Ca	Ni	As
	%	%	%	%	%	%	%	%
Sample 1	99,20	0,64	0,16	-	0,03	-	-	-*
	99,60	0,11	0,27	-	0,02	0,01	-	-**
	99,12	0,66	0,09	-	0,13	-	-	-*
	98,38	1,32	0,13	-	0,17	-	-	-**
Sample 3	96,69	1,98	0,19	-	-	0,93	0,08	-**
	99,27	0,14	0,20	-	0,07	0,23	0,09	-**
Sample 4	92,40	5,24	0,18	-	2,01	0,04	0,14	-*
	99,31	0,23	0,14	-	0,22	-	0,09	-*
Sample 5	99,00	0,13	0,27	-	0,08	0,50	-	-**
	97,85	1,22	0,17	-	0,43	0,01	0,33	-*
Sample 6	97,27	1,76	0,05	-	0,80	0,01	0,11	-*
	98,78	0,95	0,07	-	0,10	0,01	0,09	-*

Sample 1	85,00	-	-	9,19	1,43	4,38	-	-*
	79,06	-	-	13,71	0,17	7,06	-	-**
	95,01	-	-	4,95	0,04	-	-	-*

* Examining point on the corrosion near the metal.

** Examining point on the external surface of the sample.

Figure 9 shows all the examining points on metal, corrosion and external surface for sample 1 of the first group. *Figure 10* and *11* are two of the μ - X ray fluorescence spectra of sample 1 of the first group and the second group on corrosion near the metal.

Copper - zinc alloys with up to 35% of zinc are α -brasses, between 35% and 46,6% of zinc these alloys are two phases $\alpha + \beta$ brasses and β brasses when the alloys contain from 46,6% to 50,6% of zinc. (*Scott 1991*)

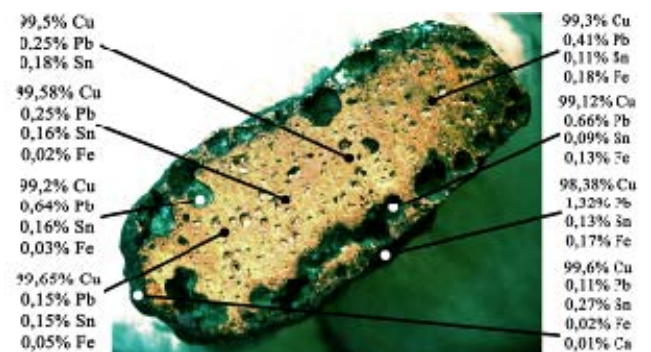


Figure 9: Sample 1 (I), image with stereomicroscope, magnification 8X, different examining points with μ - XRF.

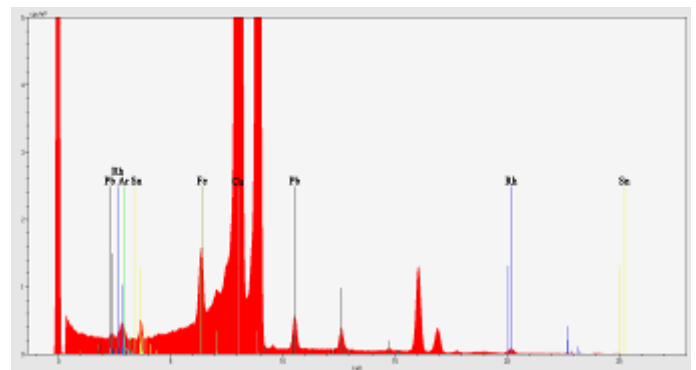


Figure 10: μ - XRF spectra of sample 1 (I) on corrosion near the metal.

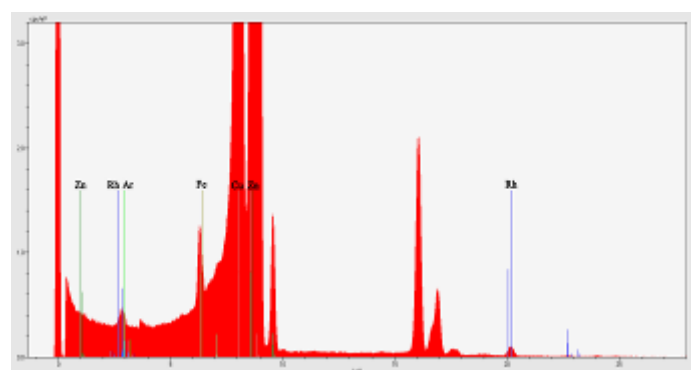


Figure 11: μ - XRF spectra of sample 1 (II) on corrosion near the metal.

3.3 Microstructure results

The polished surfaces of the samples 1, 3, 4, 5, 6 (I) and 1 (II) were etched with aqueous ferric chloride (120 ml distilled water H_2O , 30 ml hydrochloric acid HCl , 10g ferric chloride $FeCl_3$). Different etching times were tested from 3 to 15 seconds in order to obtain the best images of the samples' microstructure. Images of samples 1, 4, 5 (I) and 1 (II) (Figure 13, 14, 15 and 16) were chosen to be presented for the microstructure examination. The initial shape of the grains for the one phase face centered cubic structure (for example copper) is equiaxial hexagonal.

The microstructure of the cast ancient metal is mainly composed by dendrites which are formed because the metal and its impurities have different melting temperatures. Impurities are very common in ancient objects because the production techniques at that time could not allow their removal. Dendrites are easily spotted with a microscope because they have a characteristic tree branch shape. If the microstructure is annealed or low speed cooled the dendrites can be removed and hexagonal grains can be obtained. This is the microstructure observed for samples 1, 3, 4, 5 and 6 of the first group after being etched with aqueous ferric chloride.



Figure 12: Sample 1 (I), image of the microstructure with polarized light, etched for 12 seconds, magnification 40X.

A twin is another important microstructure element which can also be observed with a microscope. The twin is a grain boundary with crystalline mirror symmetry. This means that the atoms on one side of this boundary are positioned as the objects and the atoms on the other side as their reflections. On the sample's microstructure twins look like parallel lines. If these parallel lines are

straight it means that the sample was not cold worked and the opposite if they are curved. Straight twins were observed on the microstructure of sample 1 of the second group.

There are two possible ways to obtain a twin microstructure from the casted metal. The first one is to cold work the sample and then to anneal it. The second way is to anneal the sample and to hot work it. (ASM International 2004, Wayman 2000)



Figure 13: Sample 4 (I), image of the microstructure with polarized light, etched for 8 seconds, magnification 100X.



Figure 14: Sample 5 (I), image of the microstructure with polarized light, etched for 8 seconds, magnification 100X.

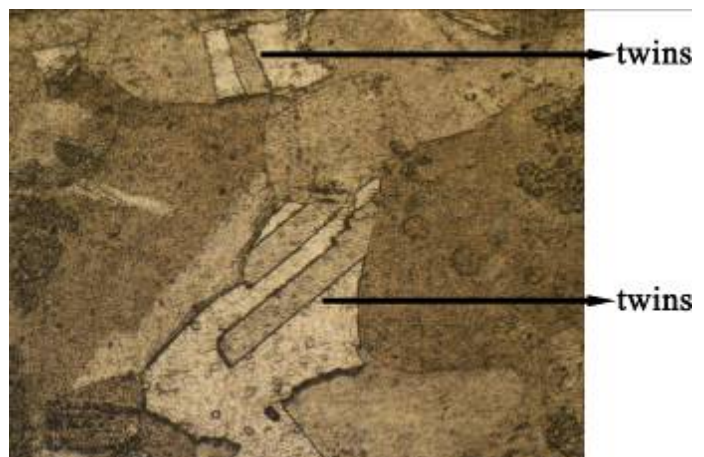


Figure 15: Sample 1 (II), image of the microstructure with polarized light, etched for 15 seconds, magnification 200X.

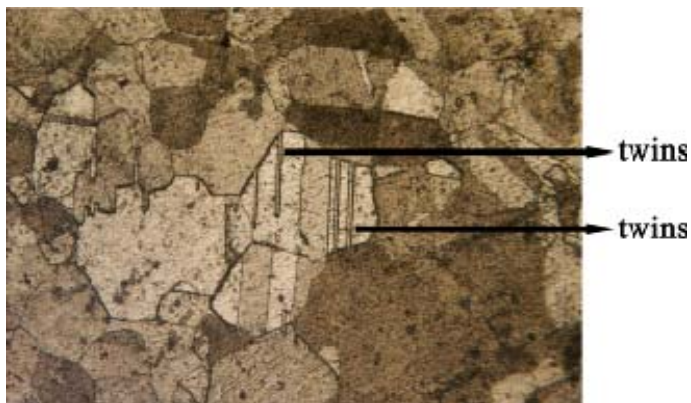


Figure 16: Sample 1 (II), image of the microstructure with polarized light, etched for 15 seconds, magnification 100X.

4 CONCLUSIONS

For all the samples in this study the corrosion products (cuprite, malachite) were observed deep into the metal. From this can be deduced that the samples are authentic ancient objects and not fake replicas.

From the μ - X ray fluorescence results can be concluded that all the samples from the first group are copper objects with over 99% content. The sample (grater) from the second group is a brass object with an average of 67,1% copper, 32,83% zinc and it is a one phase alpha copper-zinc alloy. All the samples in this study contain Pb, Sn, Fe, Ca and Ni on the metallic area with a concentration lower than 0,8%. For the samples of the first group on the corroded areas near the metal and on the external surface the percentage of copper is slightly decreasing while the percentage of the other elements (Pb, Sn, Fe, Ca and Ni) is increasing up to 5,24% for lead. For the sample of the second group the copper content is increasing up to 95,01% and the zinc percentage is decreasing. There is also a high quantity of calcium (up to 7,06%).

On the samples of the first group equiaxial hexagonal grains were observed and from this can be concluded that the metal might have been annealed or cooled with a low speed after being casted.

The presence of straight twins on the microstructure of sample 1 (II) can be explained in two possible production processes of this object: the cast alloy might have been cold worked and then annealed or it might have been annealed and hot worked.

All the samples will be subjected to further investigations.

REFERENCES

- Ceka, Neritan 2000. *Ilirët*. Tiranë: Shtëpia Botuese e Librit Universitar.
- Pierre, Cabanes et al 2008. *Harta Arkeologjike e Shqipërisë*. Tiranë: K&B Klosi&Benzenberg.
- Scott, David 1991. *Metallography and microstructure of ancient and historic metals*. Singapore: The J. Paul Getty Trust.
- Biswas, Arun 1993. The primacy of India in ancient brass and zinc metallurgy. *India Journal of History* 28(4): 309-330.
- Tafilica, Zamir 1988. Gjurmime arkeologjike në Luginën e Përroit të Thatë. *Iliria* 1: 255-268.
- Tafilica, Zamir 1993. Bazilika paleokristiane e Lohës së Sipërme. *Kumtari* 6.
- MIT 2003. The Metallographic Examination of Archeological Artifacts, Laboratory Manual. *Summer Institute in Materials Science and Material Culture*.
- Dilo, Teuta et al 2009. Archaeometallurgical Characterization of Some Ancient Copper and Bronze Artifacts from Albania. *American Institute of Physics*: 985-990.
- Sandu, I. et al 2006. Authentication of Old Bronze Coins. Study on Archaeological Patina. *Acta Universitatis Cibiniensis Seria F Chemia* 9: 39-53.
- Murphy, Douglas 2001. *Fundamentals of light microscopy and electronic imaging*. United States of America: Wiley-Liss, Inc.
- Potts, P., West, M. 2008. *Portable X-ray Fluorescence Spectrometry Capabilities for In Situ Analysis*. United Kingdom: The Royal Society of Chemistry.
- ASM International, The Materials Information Company 2004. *ASM Metals Handbook Volume 9*. United States of America: ASM International.
- Wayman, M. 2000. Archaeometallurgical Contribution to a Better Understanding of the Past. *Materials Characterization* 45: 259-267.

Chemical and mineralogical study of a Yamur from the Thirteen Century

M.A. Gómez-Morón

Andalusian Institute of Cultural Heritage, Seville, Spain

R. Ortiz, P. Ortiz, J.M. Martin

University of Pablo de Olavide, Department of Physical, Chemical and Biological Systems, Seville, Spain

R. Baglioni¹, A. Bouzas

Andalusian Institute of Cultural Heritage, Avda de los Descubrimientos S/N, Seville, Spain

Abstract: The aims of this research were the chemical and mineralogical study of a Yamur from the thirteen Century and the study of their conservation degree in order to facilitate the restoration. The Yamur was located in the upper part of the dome of the Conceptionists Convent in Los Pedroches (Cordoba, Spain). The restoration project was carrying out in the Andalusian Institute of Cultural Heritage (IAPH), according to the silver restoration protocol under the commission of the Andalusian Culture Ministry. The Characterization was carry out by Optical Microscopy (OM), X-ray Diffraction (XRD), Inductively Coupled Plasma (ICP) and Scanning Electron Microscopy coupled to energy dispersive X-ray spectroscopy (SEM-EDX). The spheres are made of brass (copper and zinc alloy) with minor proportion of lead. This composition decreases the melting point and allows the work of the piece. The sphere brass corrosion is due to the presence of cuprite and paramelaconite while the illite found in the deposits could have a soil origin.

1 INTRODUCTION

A yamur is a metal piece that is located on the minarets of Islamic mosques. It consists of three or more spheres, assembled from the highest on the bottom to the lowest on the upper part.

These spheres symbolize the three worlds where God is made known according to the Islamic culture, (mulk, material world, malakut, imaginary world, and yabarut, world of power), representing the perfection of God and the universe (related to circular or spherical shape), and identify the place of prayer in Islamic Culture.

The aim of this work is to study the chemical and mineralogical composition of the Yamur (Figure 1) that is over the Dome of the Convent of Conception, Los Pedroches (Córdoba, Spain).

The three spheres were made of brass, their sizes from the highest to the lowest are: 1.32 m., 0.90 m. and 0.65 m, they are assembled by an iron stem with a flag and a cross on the upper part.

2 MATERIALS AND METHODOLOGY

The first study was the description of the corrosion and the conservation degree of the pieces (spheres, stem, flag and cross).

For this research, 20 samples have been taken from different alloys and corrosion products following the recommendations of the technical commission CNR-ICR NORMAL 3/80 [8].

Metallographic sections have been prepared with FeCl₃ in ethanol according (Scott, 1991).

The mineralogical characterization was carried out by an X-ray diffractometer brand Bruker (model D8 Advance), using CuK α and an Optical Microscope Leica DM4000M.

The elemental chemical analysis over the stratigraphies of the crusts and deposits have been studied by means of electron scanning microscope JEOL JSM-5400, with x-ray energy detector, Inca X-sight. The chemical composition has also been analyzed by inductively coupled plasma (ICP) with a Horiba Jobin Yvon 2.



Figure 1: Yamur before restoration. Image: Eugenio Fernández Ruiz (IAPH)

3 RESULTS AND DISCUSSION

3.1 Damages of the Spheres

The spheres presented a high level of weathering with deposits, even bird droppings, iron stains, deformation, losses, fissures and oxidation products of copper among other pathologies (Fig. 2-3).



Figure 2: Bird droppings, deposits and green corrosion product on a Sphere of the Yamur before restoration. Image: Eugenio Fernández Ruiz (IAPH)



Figure 3: Holes, fissures and green corrosion product on the Spheres of the Yamur before restoration. Image: Eugenio Fernández Ruiz (IAPH)

3.2 Damages of the Iron pieces

The iron pieces that support the sphere contain in the upper part a flag and a cross.

These iron pieces were very rusty and deformed. The flag cross and structural support presented a high level of corrosion and deposits of different origin (Fig. 4).



Figure 4: Deformation and iron corrosion products on the iron structure of the Yamur before restoration. Image: Eugenio Fernández Ruiz (IAPH)

3.3 Chemical and Mineralogical Study of the Spheres

The spheres are made of brass, copper and zinc alloy (65:30), with a 2% w/w of lead according to ICP analysis. The addition of lead in the alloy decreases the melting point and facilitates its work.

The cross section of the brass structure treated with FeCl_3 in ethanol is alpha-phase with equiaxed grains with bands caused by cold working (Fig. 5).

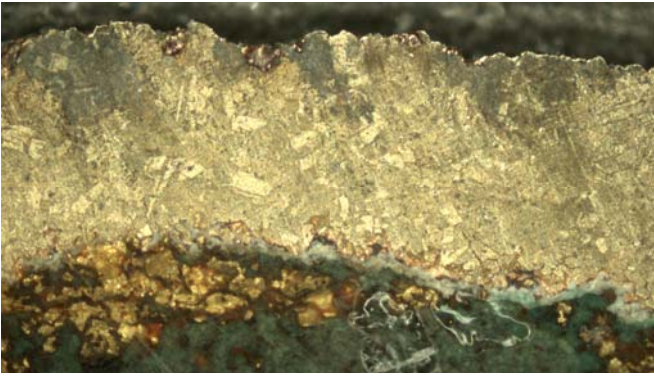


Figure 5: Optical microscopy photograph of the cross section of a brass sample treated with FeCl_3 in ethanol (X5).

The XRD study of the patinas discovered the presence of cuprite (Cu_2O), paramelaconite (Cu_4O_3), and Illite ($\text{K}(\text{AlFe})_2\text{AlSi}_3\text{O} \cdot 10(\text{OH})2\text{H}_2\text{O}$).

Cuprite and paramelaconite (Fig. 6) are generated by sphere brass surface corrosion due to the atmospheric conditions while the Illite found in the deposits could have a soil origin.

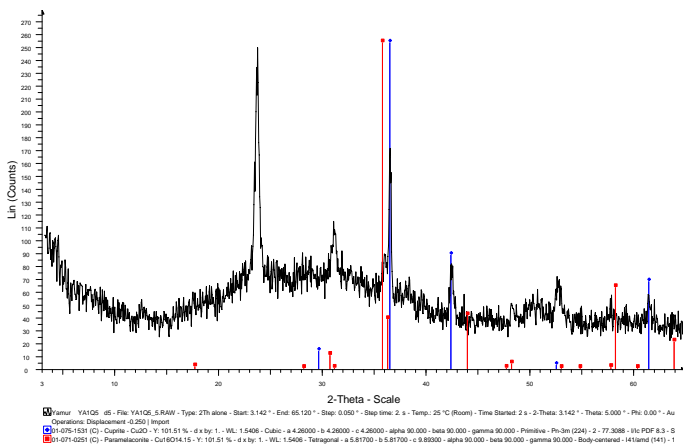


Figure 6: Cuprite (Cu_2O) and paramelaconite (Cu_4O_3) detected by XRD on the spheres.

These brass corrosion products are mixed with calcite (CaCO_3), anortite ($\text{CaAl}_2\text{Si}_2\text{O}_8$), quartz (SiO_2) and gypsum ($\text{CaSO}_4 \cdot 2\text{H}_2\text{O}$) that could have an atmospheric origin and whewellite ($\text{Ca}(\text{C}_2\text{O}_4) \cdot (\text{H}_2\text{O})$) likelihood due to biological microorganism.

3.4 Chemical and mineralogical study of the iron pieces

The flag, cross and stem are covered with a patina mainly of iron oxyhydroxides goethite ($\text{FeO}(\text{OH})$, Figure 7) and lepidocrite ($\text{FeO}(\text{OH})/\text{Fe}_2\text{O}_3 \cdot \text{H}_2\text{O}$) with punctual corrosion of lead: cerussite ($\text{Pb}(\text{CO}_3)$) and hydrocerussite ($\text{Pb}_3(\text{CO}_3)_2(\text{OH})_2$).

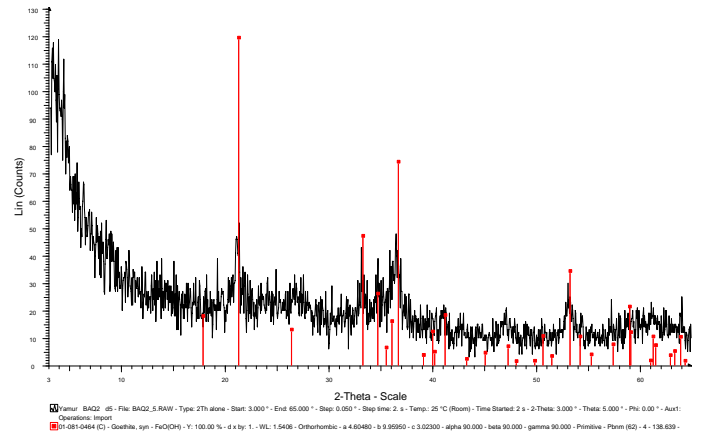


Figure 7: Goethite ($\text{FeO}(\text{OH})$) detected by XRD on the iron structure.

The stem has the worst conservation degree with a lot of corrosion products and deformation that could be induced by a galvanic process by the contact between the iron and brass.

3.5 The restoration

The restoration consists on the following steps:

- Removing the components (spheres and iron pieces)
- Mechanical and hand-made cleaning of the elements of iron and brass.
- Chemical cleaning and neutralizing of chemical products
- Stabilization of metals by corrosion inhibitors (Figure 8).
- Volumetric reintegration with reversible neutral supports to stabilize the pieces.



Figure 8: Stabilization of metals by corrosion inhibitors on a Sphere of the Yamur during restoration. Image: Eugenio Fernández Ruiz (IAPH)

The restoration results are shown in *Figure 9*. The stability of the restored structure allows having again their function on the Dome of the Convent of Conception at Los Pedroches (Córdoba, Spain).



Figure 9: Yamur before and after restoration. Image: Eugenio Fernández Ruiz (IAPH)

4 CONCLUSION

The Yamur is made of brass, copper and zinc alloy (65:30), with a 2% w/w of lead according to ICP analysis. The addition of lead in the alloy decreases the melting point and facilitates its worked. The brass structure is alpha-phase with equiaxed grains with bands caused by cold working.

The corrosion products depend on the composition of the alloys and the environmental conditions.

Sphere brass surface corrosion generates cuprite and paramelaconite due to the atmospheric conditions while the Illite found in the deposits could have a soil origin.

The flag, cross and stem are covered with a patina mainly of iron oxyhydroxides goethite and lepidocrite with punctual corrosion of lead: cerussite and hydrocerussite. These brass corrosion products are mixed with calcite, anortite, quartz and gypsum that could have an atmospheric origin and whewellite likelihood due to biological microorganism.

The stem has the worst conservation degree with a lot of corrosion products and deformation that could be induced by a galvanic process between the iron and the brass.

This research evidences the need to use corrosion inhibitors in the restoration to slow down the corrosion when the Yamur return to their location in the Dome.

REFERENCES

- CNR-ICR. 1980. Materiali lapidei: Campionamento. Normal 3/80, 1-6.
- Scott, D. 1991. Metallography and microstructure of ancient and historic metals . The Getty Conservation Institute, Marina del Rey, California, 185 p.

Document paper treated with nanoparticles investigated by Atomic Force Microscopy

S.M.Doncea, R.M.Ion

Valahia University, Targoviste, Romania; ICECHIM, Bucharest, Romania

J. F. van Staden

PATLAB, Electrochemistry and Condensed Material Institute, Timișoara, Romania

Abstract: Non-aqueous dispersions of some nanoparticles were used in this study for preserving cellulose based materials. The paper aging is the effect of shortening the overall average length of cellulose chain, resulting in catastrophic loss of paper strength. This process can be stopped or slowed considerably through the deacidification treatment. Up to now, $Mg(OH)_2$ and $Ca(OH)_2$ show very good deacidification activity, they providing physical and chemical compatibility with the full support and after conversion into carbonates, keeping the alkaline reservoirs of the paper. But for some inks and papers the degraded risk of rupture is high. To remove this inconvenience, nanoparticles of hydroxyapatite, HA, have been recently used with spectacular results, because its structure is identical to the phosphates found in paper as filling agent, a perfect compatibility between the material support and stationer, being observed, this compatibility being offered by the size distribution, topology and morphology, observed by AFM technique.

1 INTRODUCTION

The preservation of artifacts plays an important role in the degradation of Cultural Heritage materials and delay (Dumitriu *et al.* 2011). Protective treatments, after cleaning and consolidation, confer longer life for the paper artifacts. Restoration fights the opacity of the paper by minimizing the light scattering effects and surface protection from pollutants and water condensation (Feller *et al.* 1985). Currently, most restorers are not correctly trained in restoring works of art. They remove chemicals such as fat, salts, varnishes and pollutants from the surfaces of the works of art by using mostly chemical and mechanical methods. These also affect the substrates of the works.

Nanomaterials have a relevant importance for industrial applications since they have unique mechanical, optic, and magnetic properties (Baglioni&Giorgi 2006).

Alkaline nano-sized particles, used as non-

aqueous dispersions, have been proposed particularly, in this study, for their efficiency in the preservation of cellulose-based materials that degrade through an acid-catalyzed process, which leads to chemical disruption of the cellulose polymer. It has been shown that acid-catalyzed hydrolysis is the main chemical route for cellulose de-polymerization (Ion 2011). The overall effect is the shortening of the average chain length of cellulose that leads to a catastrophic loss of paper strength (Havermann 1995).

$Mg(OH)_2$ and $Ca(OH)_2$ are excellent de-acidifying agents, since they ensure a fair physicochemical compatibility with the support, and after their transformation into the corresponding carbonate, they work very well as alkaline reservoir without originating any undesirable side-products.

$Mg(OH)_2$ and $Ca(OH)_2$ nanoparticles dispersions in alcohols may be applied on paper by spraying or by impregnation. This method produces hydroxide *in situ* and requires dispersants to stabilize the system. The used solvents are volatile, environmentally friendly and with low surface tension so that they

properly work as carrier for solid particles, ensuring a homogeneous and penetration depth within the paper fibers.

Hydroxyapatite, [HA, $\text{Ca}_{10}(\text{PO}_4)_6(\text{OH})_2$], nano-particles dispersions in alcohols may be applied on paper by spraying or by impregnation (*Ion&Doncea 2011*). This method produces hydroxide *in situ* and requires dispersants to stabilize the system. The used solvents are volatile, environmentally friendly and with low surface tension so that they properly work as carrier for solid particles, ensuring a homogeneous and penetration depth within the paper fibers.

For all these nanoparticles, the distribution, topology and morphology, observed by AFM technique, are discussed in this paper.

2 MATERIALS AND METHODS

The nanoparticles of $\text{Ca}(\text{OH})_2$, $\text{Mg}(\text{OH})_2$ and HA have been synthesized as previously reported (*Ion 2003, Doncea 2009*).

The particles size and their size distribution have been measured by Dynamic Light Scattering (DLS) technique, by using a Zetasizer Nano series performs size measurements using a process called DLS – Dynamic Light Scattering (also known as PCS – Photon Correlation Spectroscopy).

The experimental size for $\text{Ca}(\text{OH})_2$ nanoparticles dispersed in 2-propanol was 408,9 nm.

The experimental size for $\text{Mg}(\text{OH})_2$ nanoparticles dispersed in 2-propanol was 188,2 nm.

For HA, the experimental size was 30 nm, in 2-propanol, too. These nanoparticles have been applied on an old book paper, dated from 1935.

Atomic force microscopy (AFM) investigations were carried out with an Agilent 5500 SPM system, described by PicoSPM controlled by a MAC Mode module and interfaced with a PicoScan controller from Agilent Technologies, Tempe, AZ, USA (formally Molecular Imaging). A multipurpose large scanner and Point Probe Plus Silicon SPM Sensor cantilevers (PPP-FM cantilevers), n^+ -silicon material and none coating, of about 227 μm length, 1.8 N m^{-1} spring constants, with the tips oscillated near their resonant frequencies (NANOSENSORS)

in air, of about 64 kHz were used for all measurements. All AFM measurements (256 samples/line \times 256 lines) were done by scanning the surface at a rate of 0.8-1.2 lines per second and were done at room temperature in tapping mode. The original images for the samples, the 3D topographical images and section analysis over the magnetite particles were performed using the PicoView SPM Software, version 1.6.2, Molecular Imaging. Height image data obtained by the AFM is three-dimensional. The usual method for displaying the data is by using a color mapping for height, for example black for low features and white for high features. The images were processed by first order flattening in order to remove the background slope and the contrast and brightness were adjusted.

3 RESULTS AND DISCUSSION

The AFM can profile surfaces at resolutions from micrometers to nanometer scale. The AFM has several advantages over SEM and TEM such as true 3D imaging, working under atmospheric pressure and the possibilities to scan in controlled environmental and under liquids. Also, no special preparation of the samples is required. Besides detail structural features AFM can provide important information on surface forces (adhesion, friction, electrostatic, van der Waals, etc). Also, the measurements can be done *in situ*, i.e., in real time to see the reaction developing during scanning. This makes AFM indispensable tool that can shed light on the nanostructures comprising paper and cellulose (*Paiva et al.2007*).

Up to now, the micro-architecture of cellulose pellicles was investigated by SEM (*Doncea et al.2010*) and others techniques (*Doncea 2009; Doncea 2010*). Micrographs obtained for this sample revealed a densely packed network of cellulose fibers which, within the sheet of paper, appeared to be random in orientation at the micron length scale, with no indication of microfiber directionality. The fibers are homogeneous and seem to originate from rags, probably cotton or linen. The fiber sizes are different and some seem to be broken. Some fibers exhibit encrustations which could be salt crystals. The presence of minerals in paper can often be the

consequence of the way it was produced. The light part of the image can be the consequence of the presence of a thick part of sizing material or of a rupture in the paper.

Analyzing a typical image with a higher amplification was possible to identify not only the cellulose fibers but also the micro- and nanofibrils (Fig. 1). The basic paper morphology features can be seen: cellulose fibers are long (characteristic libriform cells in gymnosperms), with a rounded section (diameters between 15 and 22 μm) and are organized in a random way in the paper; partially degraded primary cell wall during the refining produces debris and separated macro fibrils that bind neighboring fibers thus increasing the paper strength (Zugenmeier 2008).

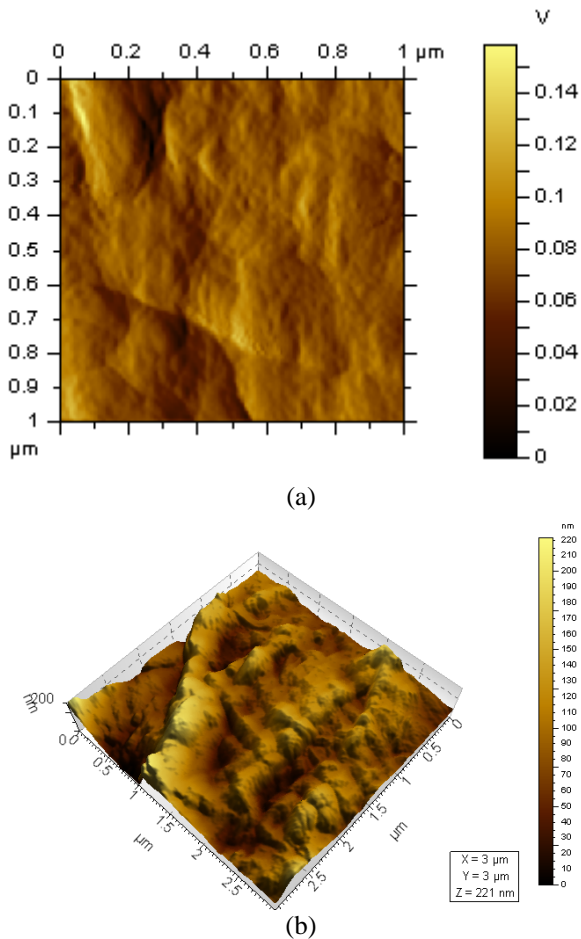


Figure 1: AFM images of macrofibrils (a) by tapping mode and (b) 3D AFM image of macrofibrils

For microfibrils, by AFM was possible to see the small aggregates (Fig. 2).

By spraying on a sheet of paper, less white deposits of $\text{Mg}(\text{OH})_2$ were formed than in the case of $\text{Ca}(\text{OH})_2$, although the same concentration and the same volume of suspension has been applied on the same type of paper. The possible explanation of this

fact is that $\text{Mg}(\text{OH})_2$ has a stronger basic character than $\text{Ca}(\text{OH})_2$, so it neutralizes greater the acidity from the paper. It is also known that magnesium is less visible on the scanning microscopy because it has a smaller contrast, and it seems to cover the most part of the cellulosic fibers. Not the entire quantity of sprayed $\text{Mg}(\text{OH})_2$ nanoparticles reacted to neutralized the acidity of the paper and it will be carbonated, in time in the presence of atmospheric CO_2 .

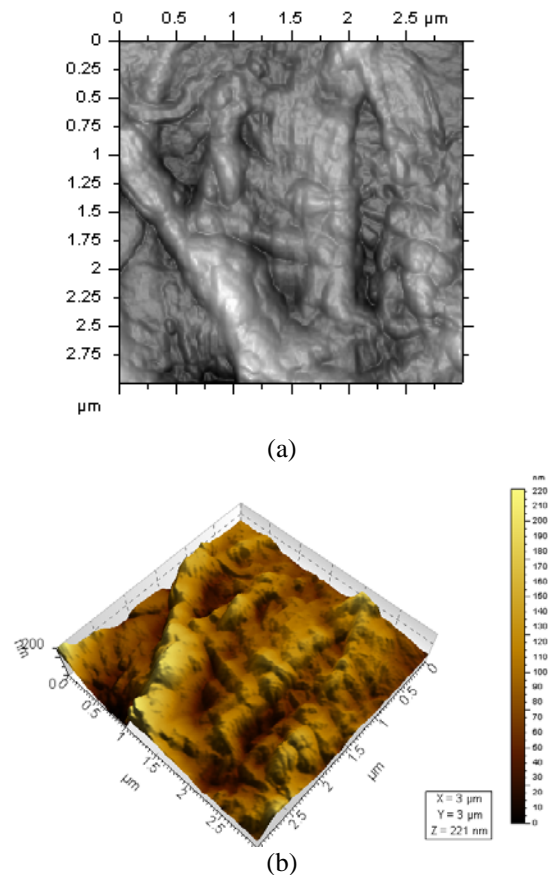
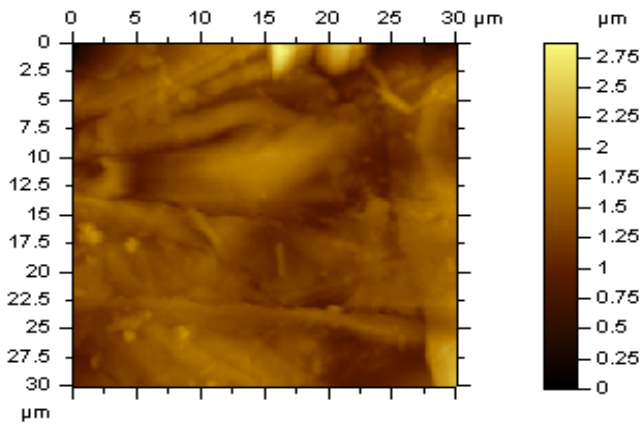
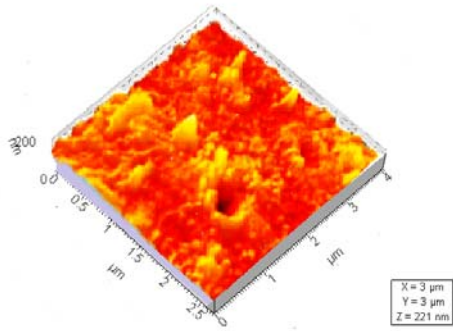


Figure 2: AFM image of microfibrils obtained in contact mode (a), 3D AFM image of microfibrils (b)

From AFM images (Figure 3), by spraying $\text{Ca}(\text{OH})_2$, $\text{Mg}(\text{OH})_2$ and HA, a densely packed network of cellulose fibers within the sheet of paper, appeared to be randomly oriented at the micron length scale, with no indication of microfibril directionality, more pronounced for $\text{Mg}(\text{OH})_2$ and HA. The fiber sizes are different and some seem to be broken. Some fibers exhibit encrustations which could be salt crystals, in contact with $\text{Ca}(\text{OH})_2$, especially. By AFM, 3-D surface topography has been recorded on a 0.5-0.5 mm^2 surface area. AFM revealed a rough surface architecture for HA, the predominant size of grains being in the range of 90-100 nm. The light part of the image can be the consequence of the presence of a thick part of sizing material or of a rupture in the paper (Doncea 2009, 2010).

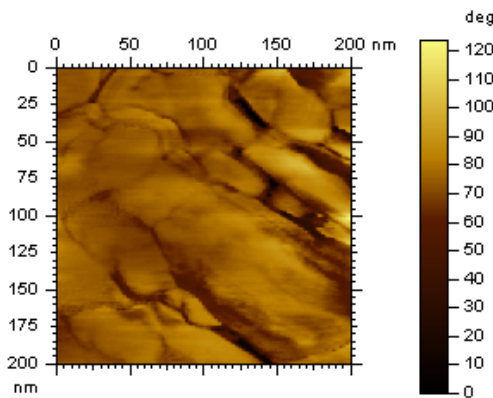


(a)

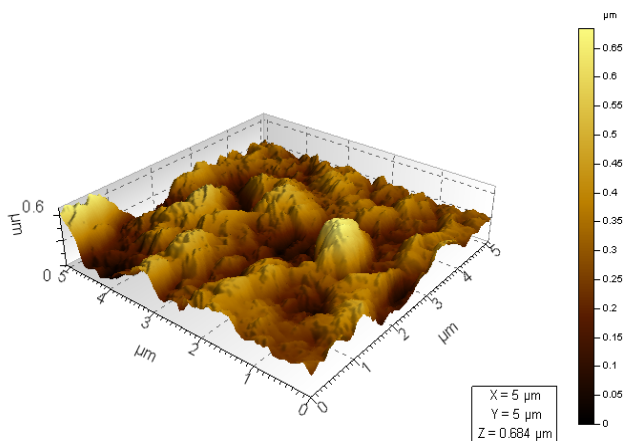


(b)

Figure 3: AFM image of Ca(OH)_2 on paper obtained in contact mode (a), 3D AFM image of Ca(OH)_2 on paper (b)



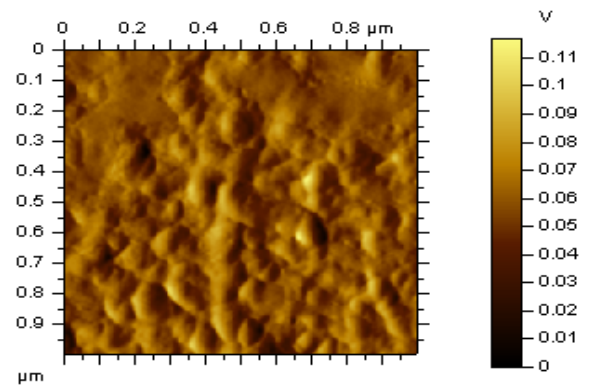
(a)



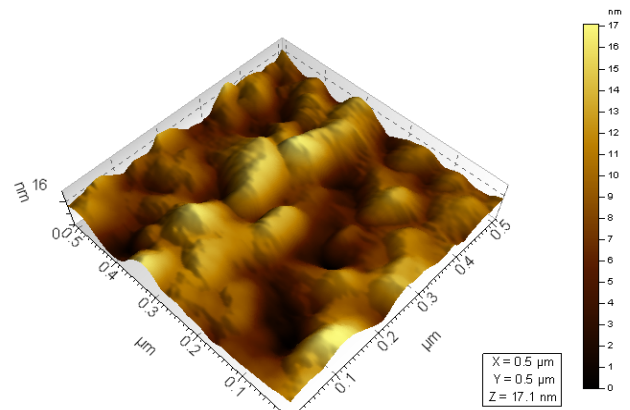
(b)

Figure 4: AFM image of Mg(OH)_2 on paper obtained in contact mode (a), 3D AFM image of Mg(OH)_2 on paper (b)

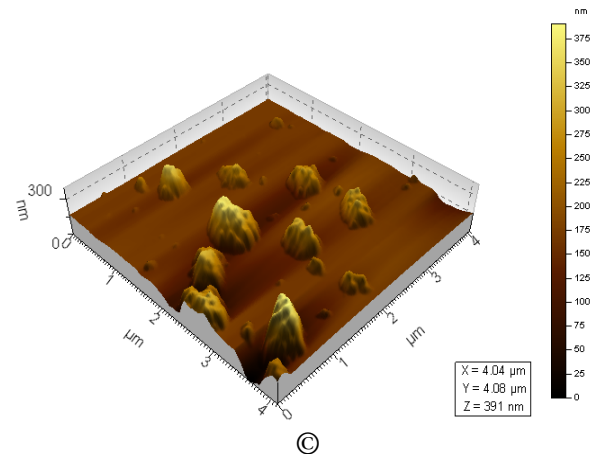
AFM can be used to study cellulose fibers degradation directly on a paper's surface and could provide information on their deterioration and ageing. This technique can produce topographical maps of paper consisting of 3-dimensional images of the surface ultrastructure at molecular level without the necessity to fix samples. For a better observation of the surfaces of the paper, of the fillers and binders, for Mg(OH)_2 and HA, a higher magnified of 5000x has been used to provide a great depth field and to aid to morphological and topographical analysis of the sample, as in Figs. 4,5.



(a)



(b)



(c)

Figure 5: HA sprayed on the paper (tapping mode) (a), 3D AFM morphology for HA nanocrystals on paper (b), and 3D AFM morphology for HA nanocrystals (c)

4 CONCLUSIONS

Mg(OH)₂, and HA are excellent de-acidifying agents, better than Ca(OH)₂ ensuring a good compatibility with the support, working very well as alkaline reservoir without originating any undesirable side-products. AFM can be used to study cellulose fibers degradation directly on a paper's surface and could provide information on their deterioration, ageing and restoring with inorganic nanoparticles.

REFERENCES

- Baglioni P. and Giorgi R., 2006. Soft and hard nanomaterials for restoration and conservation of cultural heritage, *Soft Matter*, 2: 293-303
- Doncea, S. M., Ion, R. M., Fierascu, R. C., Bacalum, E., Bunaciu, A. A., Aboul-Enein, H. Y. 2009. Spectral methods for historical paper analysis: composition and age approximation. *Instrum Sci Technol.* 38(1): 96-106
- Doncea SM, Ion RM, Nuta A, Somoghi R, Ghiurea M. 2010. Optical methods of investigation for book papers conservation with nanoparticles. *Proc. SPIE*, 7821:78211F
- Dumitriu I, Fierascu RC, Ion RM, Bunghez RI, Corobea MC, 2010. Nanotechnology applied in archaeometry: restoration and conservation, *Proc. SPIE* 7821:78211I
- Feller R, Lee S, Curran M. 1985. Three fundamental aspects of cellulose deterioration, *Art Archaeol Techn Abstr, Suppl.* 22(1): 329-54
- Havermans JBGA, The impact of European Related to paper ageing on preventive conservation strategies, *Restaurator* 16(1995) 209-222
- Ion, RM. 2003 *Nanocrystalline materials*, FMR Ed., Bucharest
- Ion, R.M. Doncea, S. M. Ion M.L. (2011) *New Approaches to Book and Paper Conservation & Restoration*: 389– 410, Wien/Horn: Verlag Berger (Ed.)
- Paiva AT, Sequiera SM, Evtuguin DV, Kholkin AL, Portugal I (2007) *Nanoscale structure of cellulosic materials: Challenges and opportunity for AFM. Mod.Res.Educ.Topics Microscopy.* 726-733. A.Mendez Vilas and J.Diaz (Eds.)
- Zugenmaier P. 2008. Cellulose. *Crystalline Cellulose and Cellulose Derivatives: Characterization and structures. Springer Series in Wood Science* 101-174 Berlin, Heidelberg: Springer-Verlag.

Copper bromide laser in cultural heritage monuments restoration

V. Atanassova, K. Dimitrov & M. Grozeva

Institute of Solid State Physics, Bulgarian Academy of Sciences, Sofia, Bulgaria

M. Simileanu & R. Radvan

National Institute of Research and Development for Optoelectronics INOE 2000, Bucharest, Romania

Abstract: Laser cleaning is a modern technique, appropriate to apply in many cases of artworks restoration, since it has certain advantages over conventional cleaning methods. Different types of laser sources are used for cleaning purposes. Some of the most commonly used are Nd:YAG, Er:YAG, CO₂, excimers. We propose the use of another type of laser – the copper bromide laser, oscillating in the visible range nanosecond pulses with 20 kHz repetition rate. The potential of this laser is demonstrated by cleaning of marble slabs contaminated with various popular impurities. Cleaning tests of an authentic archaeological marble sample were also done. Comparison with a Q-switched Nd:YAG laser, oscillating at the fundamental wavelength 1.06 μm and the second harmonic 532 nm, was performed. The results showed that the copper bromide laser is appropriate for laser cleaning and in some cases it can lead to more satisfactory results than obtained with other more commonly used lasers.

1 INTRODUCTION

Conservation of artworks of historical value aims to restore and protect them from further decay. An essential part of the conservation process is the cleaning of the artifacts surface. It consists in removing potential sources of degradation and giving more aesthetic appearance of the object. The most common pollutants and reasons for decay of monuments are results of human activity. These are air pollution, acid rains, soot, oil, paint, etc. There are also some environmental factors that contribute to the artifacts degradation, as salts from the soil and sea, biological growths, etc. (Doehne & Price 2010).

There are different cleaning techniques depending on the type of contamination and the substrate material. The traditional methods include some mechanical or chemical intervention, but these techniques are not selective and controllable, which means that they can be very dangerous for the precious substrates and there are many cases in which it is inappropriate applying them.

Nowadays the laser cleaning is a very popular technique in many restoration laboratories, since the lasers offer certain advantages over conventional

cleaning methods, namely no mechanical or chemical contact with the surface, hence no disruption of historic surfaces (Rode et al. 2008), selectivity of the interaction with matter, localized action, preservation of surface relief, fully controlled removal, environmental safety etc. (Koh 2005).

Depending on the type of contamination and substrate material different laser sources are used at each particular case study. For example, the fundamental wavelength of Nd:YAG laser ($\lambda = 1064$ nm) is the most established laser wavelength for cleaning of stone surfaces (Marakis et al. 2003); CO₂ lasers are used for cleaning of metals; excimers are used for bio-degradents removal like fungi, etc. Of course, there are many others laser sources with which satisfactory cleaning results are achieved.

Recently, a copper vapor laser was successfully applied as a source for cleaning paper and marble artifacts from contaminants (Mokrushin & Parfenov 2008). As it is demonstrated in the paper, the copper vapor laser possesses unique combination of characteristics that favor achieving of good results: generation of visible light (511 nm and 578 nm), with high peak and mean output power, high repetition frequency, excellent beam quality and small divergence.

An advanced version of the high-temperature copper vapor laser is the copper bromide vapor laser (CuBrVL) which has the same power and beam quality characteristics but it has very simplified and compact low-cost construction, it is faster to operate and easy to control the laser beam (Sabotinov 2007, Dimitrov & Sabotinov 1996). Portable versions of the CuBrVL are already produced and could be successfully used for outdoor cleaning (www.pulslight.net).

We report an investigation of the CuBrVL potential for cleaning of stone artifacts. A comparison of the cleaning results achieved by the CuBrVL green line (510.6 nm) and the fundamental (1064 nm) and the second harmonic (532 nm) wavelengths of a Q-switched Nd:YAG laser is done.

2 EXPERIMENTAL

2.1 Laser systems

In our experiments we have used three laser systems:

a. A laboratory CuBrVL system, generating at two visible wavelengths – 510.6 nm and 578.6 nm, with total mean power 25 W and peak power of 42 kW, at beam diameter of 22 mm, was employed. The pulse length was 30 ns and the pulse repetition frequency - 20 kHz. For cleaning experiments we have used only the green line with mean power of 18 W. To direct the laser beam and control the power a scanning system TS8720A was applied. After the scanner, the beam diameter was 16 mm and the laser power ~ 6 W. A scheme of the experimental set-up is shown in *Figure 1*.

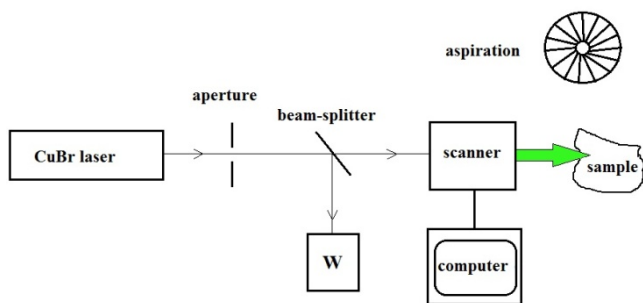


Figure 1: A scheme of the laboratory set-up.

b. An industrial CuBrVL system (Pulslight Ltd.), built for laser machining of metal, with total mean output power of 80 W, pulse peak power of 150 kW, pulse length of 30 ns and repetition frequency of 20 kHz,

was also used (Fig. 2). It was equipped with a scanning head, moving the beam, and XYZ table, moving the sample. In our experiments we have worked at a lower output power: the power of the green line (511 nm) after the scanner was 4 W and the beam diameter 16 mm. By a lense with $f=256$ mm the beam was focused to a spot 30 μ m in diameter.

c. A Q-switched pulsed Nd:YAG laser system (Quanta Ray GCR3), generating on the fundamental wavelength with maximum energy around 500 mJ, pulse length 8 ns and variable repetition frequency up to 10 Hz was used for comparison. The beam diameter was 8 mm.



Figure 2: The commercial CuBr laser system (Pulslight Ltd.).

2.2 Test samples

Sample 1



Sample 2



Sample 3

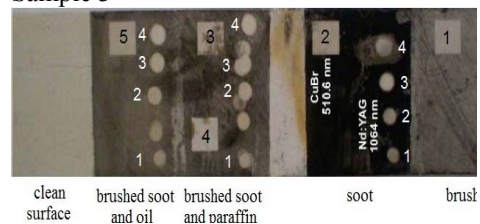


Figure 3: Test samples: 1 - soot contamination; 2 - soot and oil contamination; 3 - different types of contamination.

As test samples different marble slabs that were artificially contaminated with various popular impurities, like soot, soot mixed with oil, paraffin were used (Fig. 3). Cleaning tests on an authentic archaeological marble sample from the ancient town of Serdica (2nd century AD) were also done.

To evaluate the results of the cleaning by the three lasers applied, optical microscopy was used.

3 RESULTS AND DISCUSSION

Small areas of 1 cm² of sample 1 were cleaned by the laboratory CuBrVL. The ablation was performed almost at the focus of the laser beam (diameter of the focal spot 270 μm) at laser fluence 0.52 J/cm², kept the same for all tests. To achieve optimal results the scanning rate was changed from 1000 mm/s to 5000 mm/s. To improve cleaning quality for some of the areas two scans were done. Some of the results are presented in Figure 4.

As it is seen in the photographs better results are obtained at lower scanning rate. Running two scans improves the cleaning quality.

The cleaning experiments with the commercial CuBrVL system were performed at constant scanning rate of 175 mm/s. The laser fluence is changed by changing the sample position – the distance to the focal plane. 1 cm² square of sample 2 and sample 3 were cleaned by changing the fluence and the number of scans.

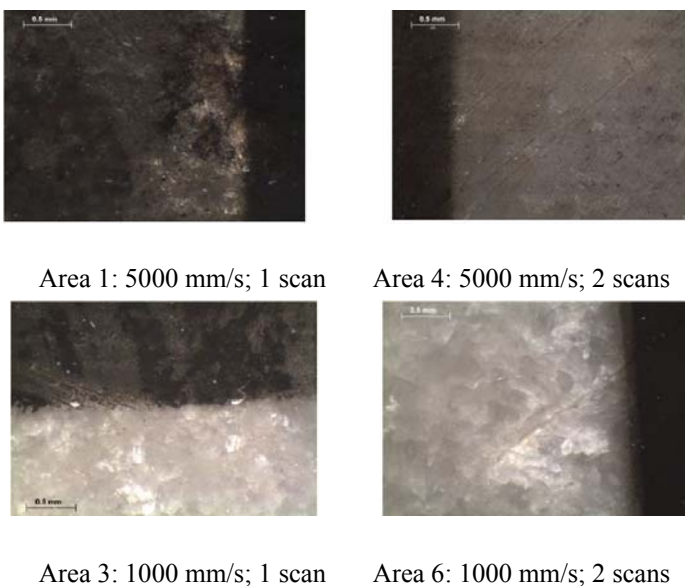


Figure 4: Sample 1: images of the cleaned areas at $F = 0.52$ J/cm² by the laboratory CuBrVL ($\times 35$).

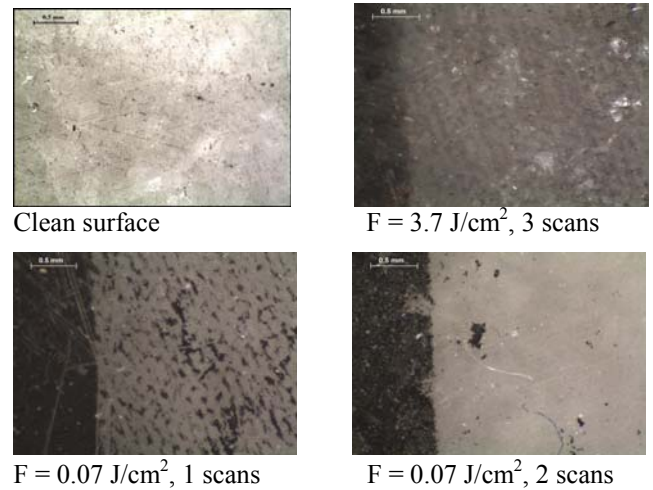


Figure 5: Sample 2: images of not contaminated area and cleaned surface by the commercial CuBrVL system ($\times 35$) at scanning rate 175 mm/s.

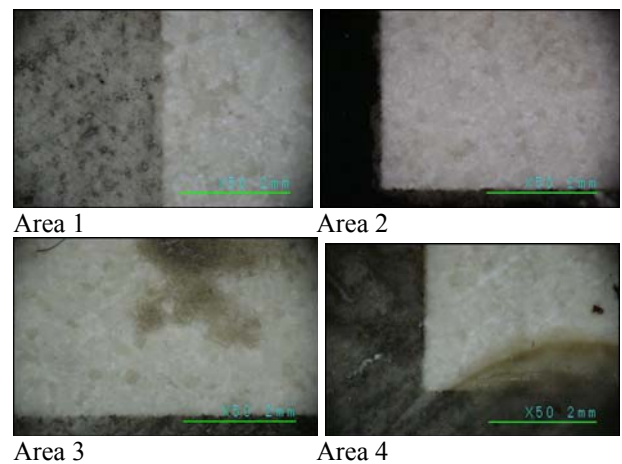


Figure 6: Sample 3: images of cleaned areas by the commercial CuBrVL system ($\times 35$) at scanning rate 175 mm/s and $F = 3.7$ J/cm².

For sample 2, obviously, the optimal cleaning conditions were not achieved. At the higher fluence (3.7 J/cm²), even at 3 scans of the surface the cleaning was not good but some demolition of the surface was observed (Fig. 5).

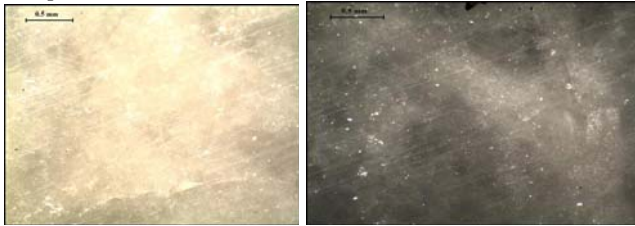
The results for sample 3 were better. At the higher fluence the surface was visually clean and not demolished (Fig. 6). There are problems only for area 3, with the paraffin contamination, where in spite of the soot cleaning, yellow spots remain on the surface.

Figure 7 presents results of cleaning tests with the Q-switched Nd:YAG laser. Sample 2 (soot and oil contamination) was cleaned with $\lambda = 1064$ nm (circular areas) and $\lambda = 532$ nm (rectangular areas). Sample 3 (various contaminations) was cleaned only with $\lambda = 1064$ nm.

Cleaning of soot and oil contamination with the infrared line 1064 nm seems to be efficient but

there is yellowing of the surface of the marble slab. On the other hand the cleaning by the second harmonic – the green line (532 nm), which is close to the wavelength, generated by CuBrVL, was not successful, obviously because of the very low fluence. Cleaning only soot contamination with low fluences ($< 0.7 \text{ J/cm}^2$) at 1064 nm was also not satisfactory, while at higher fluence ($> 1.3 \text{ J/cm}^2$) a surface demolition is observed.

Sample 2: soot and oil (x 35)



$\lambda = 1064 \text{ nm};$ $\lambda = 532 \text{ nm};$
 $F = 0.31 \text{ J/cm}^2$ $F = 0.071 \text{ J/cm}^2$

Sample 3: soot (x 100)



$\lambda = 1064 \text{ nm};$ $\lambda = 1064 \text{ nm};$
 $F = 0.7 \text{ J/cm}^2$ $F = 1.3 \text{ J/cm}^2$

Figure 7: *Cleaning results with Nd:YAG laser*

The cleaning threshold for the different types of contaminations on marble with the fundamental frequency of Nd:YAG laser was found in the range of $0.1 - 0.5 \text{ J/cm}^2$. The best results were observed in the range of $0.3 - 1.3 \text{ J/cm}^2$. The demolition threshold depended on the type of marble and was in the range of $1.7 - 2.2 \text{ J/cm}^2$.

On the other hand, in spite of the low pulse energy ($\sim 0.3 \text{ mJ}$), the results of CuBrVL cleaning were satisfactory due to the possibility to focus the beam in a very small spot ($30 \mu\text{m}$) and also due to the high repetition frequency. The cleaning threshold is similar to that of the Nd:YAG laser, but the demolition threshold is much higher ($> 3.5 \text{ J/cm}^2$). Best results were obtained with fluences in the range of $0.5 - 3.7 \text{ J/cm}^2$, depending on the scanning rate and the number of scans too.

Tests of laser cleaning of a marble slab, found during recent excavations of the old town of Serdica were done by the Nd:YAG laser at $\lambda = 1064 \text{ nm}$ and by the commercial CuBrVL laser at 511 nm (Fig. 8).

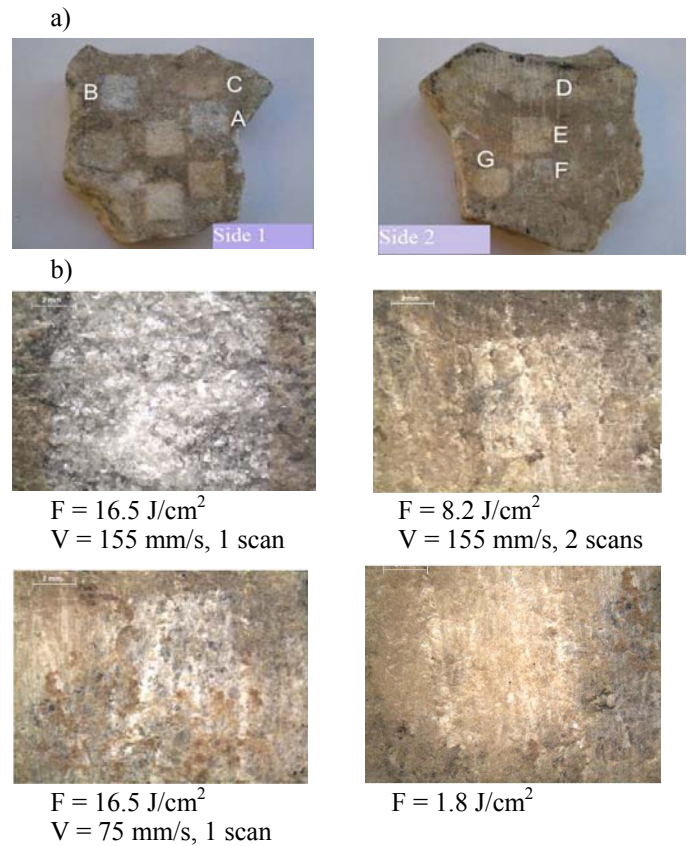


Figure 8: *Marble slab (2nd century AD): cleaning by CuBrVL at different fluence and scanning rate (B, E, F) and by Nd:YAG laser (G).*

The best cleaning was achieved for areas E and F, while area B (and A) was apparently over cleaned and destroyed. In the area cleaned by Nd:YAG laser, demolition of the stone patina was observed.

4 CONCLUSIONS

The first experiments of applying a CuBrVL for cleaning contaminated marble surface are reported. The results showed that this laser is appropriate for laser cleaning in the process of restoration of monuments and other objects of cultural heritage and in some cases it can give even more satisfactory results than other more commonly used lasers.

Ongoing are test for applying the CuBrVL in cleaning of metal, paper and leather artifacts.

ACKNOWLEDGEMENTS

The investigations are part of a Bulgaria-Romania bilateral project *Standardization of laser techniques for investigation and restoration of cultural heritage / Investigation and Restoration*

Protocols for Cultural Heritage Rescue based on Remote laser techniques. The partial support by BG NSF, project TK 02-274/2008 is also acknowledged.

REFERENCES

- Doehne, E. & Price, C. 2010. *Stone conservation – an overview of current research*, Getty Conservation Institute, Second edition.
- Rode, A.; Baldwin, K.; Wain, A.; Madsen, N.; Freeman, D.; Delaporte, Ph. & Luther-Davis, B. 2008. Ultrafast laser ablation for restoration of heritage objects, *Applied Surface Science* 254: 3137–3146.
- Koh, Yang Sook 2005. *Laser cleaning as a conservation technique for corroded metal artifacts*, doctoral thesis, Lulea university of technology, Lulea, Sweden.
- Marakis, G.; Pouli, P.; Zafirooulos, V. & Maravelaki-Kalaitzaki, P. 2003. Comparative study on the application of the 1st and the 3rd harmonic of a Q-switched Nd: YAG laser system to clean black encrustation on marble, *Journal of cultural heritage* 4: 83–91.
- Mokrushin, Yu. & Parfenov, V. 2008. Using the copper-vapor laser to restore works of art, *J. Opt. Technol.* 75: 476-477.
- Sabotinov, N. 2007. Metal Vapor Lasers, *CRC Press, Series: Optical Science and Engineering Series* 121: 449-495
- Dimitrov, K. & Sabotinov N 1996. High-power and high-efficiency copper bromide vapor laser, *Proc. SPIE* 3052: 126.

Micro-Raman spectroscopy for pigments identification in a 19th century manuscript from Bukovina

Cristina Marta Ursescu

'Al. I. Cuza' University Iasi, 'Moldova' National Complex of Museums Iasi, Romania

Elena Ardelean

'Al. I. Cuza' University Iasi, Romania

Laura Ursu

'Petru Poni' Institute of Macromolecular Chemistry Iasi, Romania

Abstract: This study was performed using a method meeting the required attributes of being non-destructive, reliable and sensitive: micro-Raman spectroscopy. The investigated object is a 19th century paper-based illuminated manuscript from Bukovina, historical region in the Austro-Hungarian Empire. The examination by means of this analytical method aimed at making an investigation into the artist's illuminating technique and lead to the identification of carbon black ink along with various shades of red, blue, yellow or green pigments. The main limitation in applying the Raman technique was the fluorescence of certain organic pigments and binders. Appropriate for identifying pigments even from mixtures, with a high spatial resolution, Raman microscopy demonstrated its suitability for the scientific investigation of pictorial layers in fragile historic manuscripts.

1 INTRODUCTION

The progress of conservation science as a multidisciplinary field of research is strongly connected to the wide variety of analytical techniques available. This analytical study was performed using a methods meeting the required attributes of being non-destructive, reliable and sensitive: micro-Raman spectroscopy. Advances in Raman microscopy enables non-destructive technical studies of paper-based historical manuscripts to be carried out for the purpose of identifying pigments and inks from texts and decorations.

A particular benefit of micro-Raman spectroscopy is the ability to focus on individual particles, thus improving the specificity of analysis. The discrimination between the paper and the writing and drawing media proves to be less difficult when the data are provided with minimum interference from either binders or neighbouring pigments, due to the high spatial and spectral resolution of the instrumentation (*Vandenabeele et al. 2007, Cariati et al. 2000, Bersani et al. 2006*).

2 EXPERIMENTAL

2.1 Apparatus

The Raman spectra were recorded with the help of a Renishaw InVia spectrometer, equipped with a 632.8 nm HeNe laser as excitation source. A 50x objective lens with NA= 0.75 of a Leica DM 2500M microscope was used to focus the laser beam on the pigment sample and collect the backscattered Raman signal. The investigated spectral region was 100-1300 cm^{-1} , at low incident laser power selected in order to avoid sample degradation (less than 0.4 mW). For a high signal to noise ratio, the exposure time and accumulation number were optimized.

2.2 Manuscript

The investigated object is a 19th century paper-based illuminated manuscript belonging to Camarzani Monastery in Vadu Moldovei, from the former Bukovina, historical region in the Austro-Hungarian Empire.

The manuscript is an Akathist Hymn dedicated

to the Nativity of Virgin Mary (“Acatistul Nașterii Maicii Domnului” in Romanian). A rather rare book for the Orthodox Christian religious services, the manuscript follows the traditional pattern in post-Byzantine arts. The handwriting makes it datable in the second half of the nineteenth century. The text is written on hand-made paper with Cyrillic letters, in the Romanian language. It contains several areas and types of decoration: frontispieces depicting Virgin Mary's life, along with capital letters and graphic border patterns. Raman investigations were made on two decorated pages: Page 1, on whose verso there is a half page illumination, decorated with frames and polychrome initials and Page 2, containing another miniature in a frame and polychrome initials beginning a passage of text.



Figure 1: Page 1 (left) and Page 2 (right) from the decorated manuscript were the investigated sites were chosen for micro-Raman analysis

2.3 Results and Discussions

Raman microscopy was employed as a common technical investigation involved in identification of carbon black ink along with various shades of red, blue, yellow or green pigments. The results of the micro-Raman investigations are summarized in *Table 1* and *Table 2* for the two illuminated pages.

Table 1: Identified pigments from investigated sites in Page 1

Page 1	Investigated sites	Pigment / compound	Raman bands*, 632,8 nm excitation
Red	letter я, letter O-left	vermilion HgS	255vs; 284w(sh); 344m
Dark	curtain	vermilion,	253vs; 283w(sh);

red		fluorescent background	343m
Yellow	aura	synthetic chrome yellow PbCrO ₄	338w; 360s; 372m; 403w; 841vs
Blue	clothing	synthetic ultramarine	264w; 547vs; 814w; 1096w 585w
Reddish blue	mantle	vermilion + ultramarine	255vs; 284 w(sh); 344 m
Green	letter Д, letter I, table	chrome yellow + ultramarine	254vs, 342sh, 361s, 379m(sh), 552m; 842vs, 988m

*s = strong, m = medium, w = weak, v = very, sh = shoulder

Since the advances in colour chemistry took place in the 19th century, the pigments formulae in the manuscript decoration reflect both local and temporal influences that allowed for a combination between traditional and modern pigments in the colour palette.

Table 2: Identified pigments from investigated sites in Page 2

Page 2	Investigated sites	Pigment / compound	Raman bands*, 632,8 nm excitation
Red	K letter, earth in the background, floral decoration	vermilion	252 vs; 282 w(sh); 343m
Black	Φ letter, leaf decoration	carbon ink (lamp black)	~ 1325 vs(br); ~ 1580 vs(br)
Bluish green	clothing	synthetic ultramarine	258w; 548vs; 822w
Yellow	aura	chrome yellow PbCrO ₄	338w; 360s; 372m; 403w; 841vs
Violet	floral decoration	cochineal lake [4]	1033w; 1106w; 1219w(sh) 1310 vs; 1401w(sh) 1480 w
Dark red	mantle	vermilion, fluorescent background	253vs; 283(w)sh; 343m
Green	floral decoration, sky, triangle	mixture of chrome yellow and ultramarine	253vs; 343m; 555m; 1095m; 1295s; 1405m; 1506m

*s = strong, m = medium, w = weak, v = very, sh = shoulder, br = broad

Although the identification of the inorganic pigments was possible based both on reference materials in Raman data-bases and previous articles on similar materials, the main limitation in applying the technique was the fluorescence of certain organic pigments and binder.

Red and orange pigments

The sites in the manuscript investigated for the

red colour exhibited the characteristic spectral peaks for vermilion, HgS, with the very sharp peak at 255cm^{-1} , the shoulder at 284 cm^{-1} and a medium peak at 344 cm^{-1} (Figure 2).

Most probably, the pigment is the synthesized form of mercury (II) sulphide, since under the microscope it tends to have a finer appearance, with more uniform particles. A darker shade of a red colour was obtained from a mixture with a red pigment that was impossible to be identified due to the fluorescence (Figure 3). Points nearby in the same region of pigment yielded spectra indicative of vermilion at 253, 283 and 343 cm^{-1} .

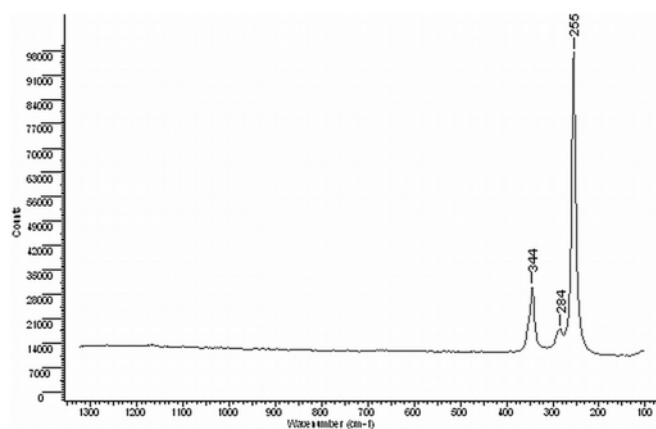


Figure 2: Micro-Raman spectra of the bright red colour

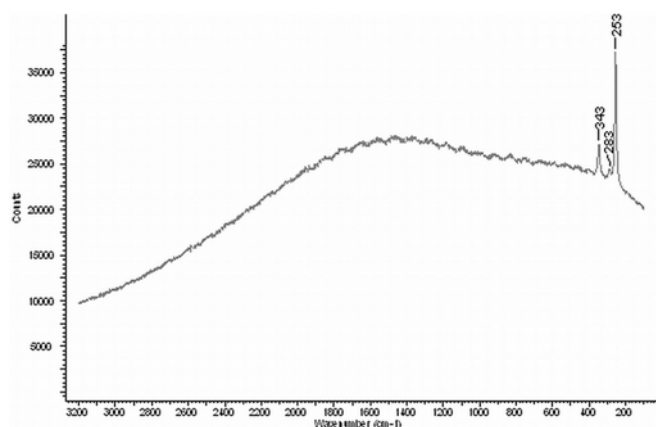


Figure 3: Vermilion spectrum in a mixture for the dark red curtain from Page 1.

For the violet colour in the floral decoration surrounding the religious scene in Page 2, we presumed that Raman vibrations were indications for the identification of the aged pigment cochineal.

Although the Raman published spectra are dominated by fluorescence, our hypothesis is based on similarities with a SERS spectra recorded with a 632.8 nm excitation wavelength for a historical cochineal lake and on the presence of the band proposed by the authors to be used for cochineal

identification at 454 cm^{-1} -specific for carminic acid and purpurin- (Whitney et al. 2006).

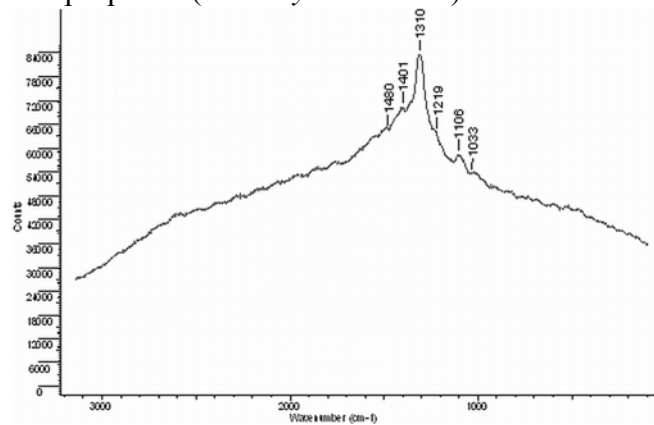


Figure 4: The micro-Raman spectrum for a violet colour in the floral decoration, presumed to be an aged cochineal pigment.

Blue pigments

The micro-Raman spectra for the pigment in the blue sites have been identified as synthetic ultramarine $\text{Na}_8[\text{Al}_6\text{Si}_6\text{O}_{24}]\text{S}_n$, a sodium aluminosilicate. The Raman features are the very strong peak at 547 cm^{-1} , wide bands at 264 cm^{-1} and 803 cm^{-1} , along with an overtone mode at 1096 cm^{-1} . The pigment was used in the pure form to obtain the blue (in Figure 5a) and combined with red vermilion for a reddish blue shade (in Figure 5b).

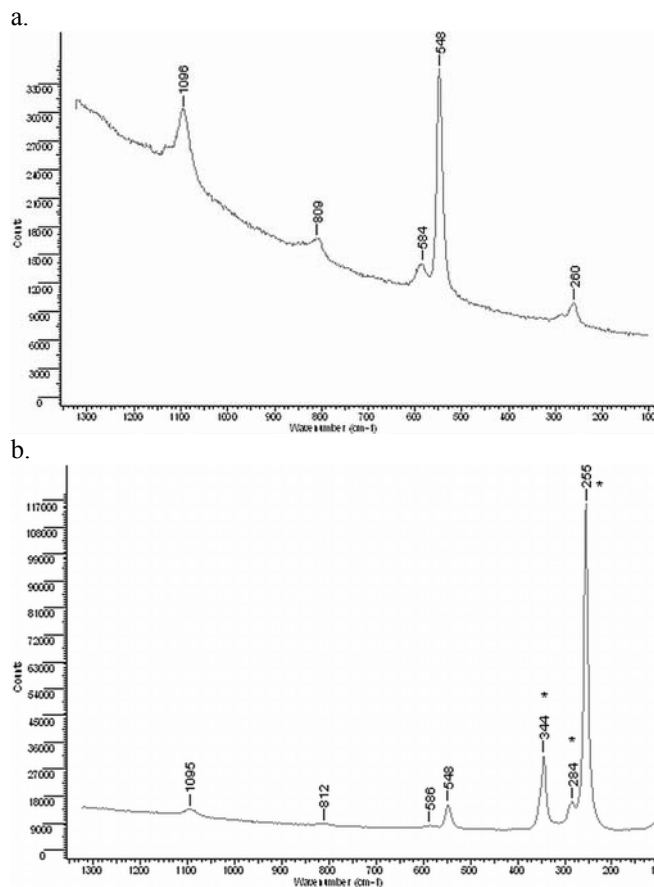


Figure 5: Raman spectrum of (a) synthetic ultramarine in clothes site and (b) reddish blue in the mantle site from Page 1 (the features of vermilion are marked with an asterisk)

Yellow pigments

Raman spectrum (Figure 6) taken from the yellow sites (the aura, in both the illuminations) showed the use of a synthetic pigment, namely lead (II)-chromate PbCrO_4 , with clear peaks at 338, 361, 378 and 839 cm^{-1} (Castro *et al.* 2004).

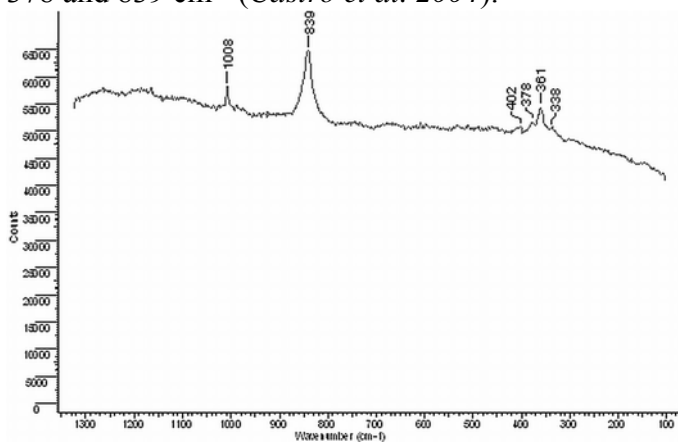


Figure 6: Chrome yellow features in the yellow layer from the aura in the religious scene

Green pigments

Malachite $[\text{CuCO}_3 \cdot \text{Cu}(\text{OH})_2]$ and verdigris $[\text{Cu}(\text{CH}_3\text{COO})_2 \cdot [\text{Cu}(\text{OH})_2]_3 \cdot 2\text{H}_2\text{O}]$ are the two copper green pigments mainly cited as materials used on manuscript illumination (San Andres *et al.* 2010). Although Raman spectroscopy allows for a differentiation between copper sulphate, carbonate or acetate, or between different sulfates based on the wavenumber region 2800–4000 cm^{-1} $-\text{H}_2\text{O}$ vibration-, the Raman features corresponding to those green colours could not be confirmed.

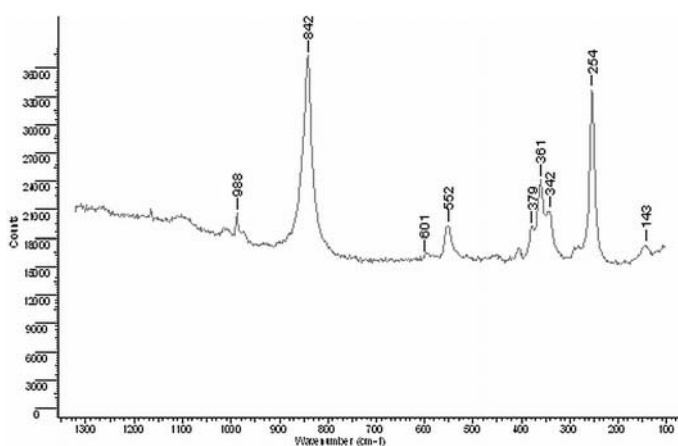


Figure 7: Green colour in the illumination from Page 1, mixture of chrome yellow and ultramarine

The areas with green pigments were examined and seven of them (see Table 1 and Table 2) were giving spectra that showed evidence of both chrome yellow and ultramarine. On the basis of Raman shifts in the spectra, one may assume that the colour

is rather obtained by intimately mixing yellow and blue pigments. A quite strong contribution of vermilion vibrations at 254, 342 and 553 cm^{-1} could be spotted as belonging to impurities during the application of the pigments.

Black pigment

The text and the decoration analysis revealed that carbon ink was used for the black colour. The raw material in the pigment is lamp black, with two strong broad bands at 1346 and 1592 cm^{-1} representative for amorphous carbon (Bioletti *et al.* 2009) and no evidence of supplemental peaks due to calcium phosphate.

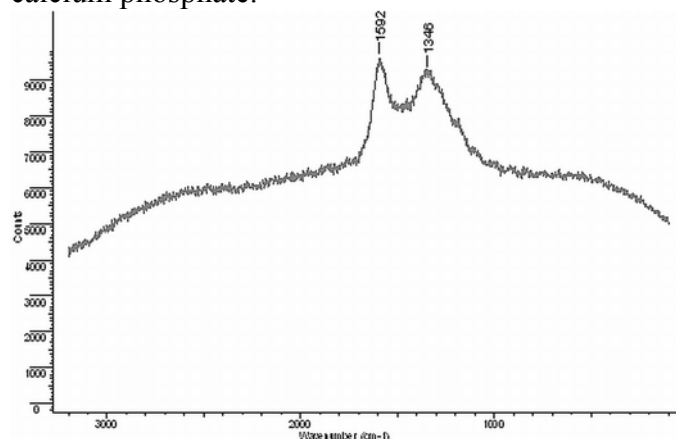


Figure 8: The black area in the leaf decoration, lamp black

3 CONCLUSIONS

The aim of this study was to characterise the illuminator's palette in the 19th century in a Bukovina monastery scriptorium, their work reflecting the tendency of the period when this historical region belonged to the Austro-Hungarian Empire. Appropriate for identifying pigments even from mixtures, with a high spatial resolution, Raman microscopy demonstrated its suitability for the scientific investigation of pictorial layers in the fragile historical manuscripts. For a complete characterisation of the decoration, further research is planned to be undertaken with complementary characterisation techniques such as FTIR and XRF spectroscopy (Burgio *et al.* 2010).

As a contribution to the study of the Romanian art as part of European trends, these results led to a new look at the technique and the pigments in the region. The results indicate a simple palette that could be created from local raw materials sources but also included the use of modern materials. The

use of common materials (e.g. vermilion, carbon inks, cochineal) together with pigments synthesised beginning with the nineteenth century (e.g. ultramarine blue) reflects the access to the changes in the chemical industry during that period in Bukovina.

ACKNOWLEDGEMENTS

One of the authors (Laura Ursu) acknowledges the financial support of Postdoctoral Fellowship Programme of the European Social Fund „Cristofor I. Simionescu” (ID POSDRU/89/1.5/S/55216), Sectoral Operational Programme Human Resources Development 2007 –2013

REFERENCES

- Bersani, D., Lottici, P. P., Vignali, F., Zanichelli, G., 2006. A study of medieval illuminated manuscripts by means of portable Raman equipments, *Journal of Raman Spectroscopy* 37: 1012–1018.
- Bioletti, S., Leahy, R., Fields, J., Meehana, B., Blau, W., 2009. Examination of the Book of Kells using micro-Raman spectroscopy, *Journal of Raman Spectroscopy* 40: 1043–1049.
- Burgio, L., Clark, R. J. H., Hark, R. R., 2010. Raman microscopy and X-ray fluorescence analysis of pigments on medieval and Renaissance Italian manuscript cuttings, *Proc Natl Acad Sci U S A*. 2010 March 30; 107(13): 5726–5731. Published online 2010 March 16.
- Cariati, F., Bruni, S., 2000. Raman Spectroscopy. In Enrico Ciliberto, Giuseppe Spoto (eds.), *Modern Analytical Methods in Art and Archeology, Chemical Analysis: A Series of Monographs on Analytical Chemistry and Its Applications* (Volume 155): 255-278. John Wiley & Sons.
- Castro, K., Vandenabeele, P., Rodriguez-Laso, M. D., Moens, L., Madariaga, J. M., 2004. Micro-Raman analysis of coloured lithographs, *Analytical Bioanalytical Chemistry* 379: 674–683.
- San Andrés, M, de la Roja, J. M, Baonza, V. G, Sancho, N., 2010. Verdigris pigment: a mixture of compounds. Input from Raman spectroscopy. *Journal of Raman Spectroscopy* 41(11): 1468 – 1476.
- Vandenabeele, P., Edwards, H.G.M., Moens, L., 2007. A decade of Raman spectroscopy in art and archaeology. *Chemical Review* 107(3): 675-686
- Whitney, V., Van Duyne, R. P., Casadio, F., 2006. An innovative surface-enhanced Raman spectroscopy (SERS) method for the identification of six historical red lakes and dyestuffs, *Journal of Raman Spectroscopy* 37: 993–1002

Databases:

<http://www.fis.unipr.it/phevix/ramandb.html>

<http://rruff.info/>

<http://www.chem.ucl.ac.uk/resources/raman/pigfiles>

<http://www.irug.org/ed2k/search.asp>

Conserving and investigating a historic textile with a previous adhesive treatment

E. P. Tsvetkova

National Gallery of Foreign Art, Sofia, Bulgaria

Abstract: Conservation-restoration treatment and investigation of historic textiles sometimes hide real challenge for the specialists involved, especially if in the past the objects have undergone previous adhesive treatment. Many of the adhesives that have already come out of practice are known for their adverse effects on textiles. Some of the objects treated with them still exist, need further care and/or more detailed investigation, and could be classified as one of the most delicate to work on. This paper presents the flag of the Stara Zagora rising, 1875, which has been restored in the 60s of the last century. It has been consolidated and lined with flour paste according to the wide-spread practice in the Bulgarian museum conservation laboratories at the time. At present the object is in an extremely poor condition: fragmented, desiccated, very fragile and much stiffened by the adhesive, which in its turn have by now lost its reversibility.

Conservation-restoration treatment and investigation of historic textiles sometimes hide real challenge for the specialists involved, especially if in the past the objects in question have undergone previous treatment employing adhesives. The history of textile conservation and especially the history of its branch, which deals with painted textiles, have documented the use of many adhesive products with the aim to consolidate the degraded textile materials and to delay or prevent their deterioration. In view of achieving these goals almost all types of adhesive products that appeared on the market have been introduced to the field of textile conservation-restoration through the years. Unfortunately, most of them have proved to have many adverse effects together with the good ones, and to alter irreversibly the specific characteristics of the treated objects. These adhesives have already come out of practice but some of the textiles treated with them still exist. A major among these objects is the group of flags and banners. In most of the cases the previously treated artifacts need further care and/or more detailed investigation, and could be classified as one of the most delicate to work on.

This paper will present an eloquent example belonging to the group of textiles described above. The object concerned is a flag, property of the Regional Museum of History in Stara Zagora, Bulgaria. It was the symbol of the *Stara Zagora*

rising, organized in 1875 as a riot against the Ottoman presence in Bulgaria. Later the flag participated in the Russo-Turkish war as well. It is single-ply, sewn up from three horizontal strips of silk fabric dyed in different colours (according to the initial description: white, green and red). Over time, the strips have discolored to similar tobacco nuances. An ellipse of cotton fabric is machine-sewn in the center, to the front of the flag; it bears a pencil drawing of a crowned lion standing on its hind legs.



The front side of the flag before the treatment in 2012

Letters cut out of the same cotton fabric are applied above the ellipse and these form the inscription "FREEDOM OR DEATH". Since the

right end of the object is lost, presently the composition of the decorative elements is disrupted and the elliptical piece with the lion image is shifted to the right; the inscription is preserved up to the second letter of "DEATH" and two of the appliquéd letters in this preserved part are missing as well. The composition center on the reverse side of the flag is formed by a machine-sewn cross of the same cotton fabric; this cross duplicates the location of the lion image from the front side. A rainbow-shaped piece of paper is glued onto the silk fabric above the cross; the paper element has read "FREEDOM OR DEATH" written in ink but only part of the whole piece is preserved.

In 1963 the flag was restored in the laboratory of the National Museum of Military History in Sofia according to the methodology of the Russian specialist Semyonovich - consolidation and lining of historic fabrics with flour paste (flour glue). This methodology was developed in the 30s of the past century in the conservation-restoration laboratory at the Soviet Institute of Archaeological Technology and was approved in 1937. In 1955 Semyonovich published information about the results of the research work (*Semyonovich 1955*), and in 1961 issued a technical and technological handbook of restoration of museum textiles, which describes in details the method and its variations (*Semyonovich 1961*). The Russian methodology was implemented in the Bulgarian museums by the Russian specialists M.Ryabova, L.Osmolnikova and L.Sinelnikova. They were invited to Bulgaria in 1960 and demonstrated the particularities of the flour paste lining by restoring flags of the National Museum of Military History (NMMH). This method became known in our country as *the method of Semyonovich* and in the period 1960-1970 it was systematically applied in the treatments of flags from the Bulgarian museum funds (*Krasteva 1991*). It is a variation of the traditional Eastern starch paste technique. The new support was usually made of silk tulle (gauze), while the adhesive paste used was a mixture of flour glue (30%), gelatin solution, ethanol, and glycerin as a plasticizer and as an antiseptic additive - benzoic acid, thymol or sodium pentachlorophenol. Depending on the condition of the treated object, the paste could be applied only on the new support, only

on the original fabric or on both of them, preferably in concentrations of the adhesive 3-6%; after that the adhesion was achieved by pressing and ironing. After the 70s the execution of flour paste lining of historic textiles continued to be practiced mainly in the former Soviet Union, but after the end of the 80s even there it started to die out.

Although the flour paste lining has been presented as a reversible treatment, which arrests the destruction of textile materials, over time it apparently causes a number of negative effects. Already in the 80s of the last century the problems with the lined objects had already occurred and were calling for new restoration treatment. This situation is reported by Elisaveta Krasteva, an experienced restorer in the laboratory of NMMH, who describes the complications she has encountered when re-treating some flags from the museum's funds (*Krasteva 1991*). 20 years after the initial treatment the textile materials were disagreeably stiffened and dehydrated and were beginning to show inclination to separate from their new supports. Krasteva assesses that the drying up of the original fabrics was caused by the high concentration of the flour glue in the mixture (6-9%) and by the loss of the plasticizer. While executing the re-restoration, she found out that the lining was not entirely reversible, since the success of the attempts to remove the dry flour paste was achieved with difficulty and was not always satisfactory. Krasteva points out that the Bulgarian specialists have resorted to the use of enzymes to extract the adhesive.

Presently, 30 years after the first reports of problems with artifacts lined with flour paste, the flag of Stara Zagora rising of 1875 is even more challenging. As the restoration documentation from 1963 reads, in the period 1962-63 it has been lined with flour paste on gauze dyed in a neutral color. A paste of 3% adhesive solution has been used and it has been applied on both sides of the flag; only the areas under the textile letters have been coated with a paste of 6% solution. In 1966 a second treatment of the reverse side has been executed; its aim was to consolidate areas of detachment from the new support and this has been achieved by applying flour paste consisting of: 2% polyvinyl alcohol, 0.25% gelatin, 3% flour, 5.5% glycerin, and 0.033%

sodium pentachlorophenol.

In the beginning of 2012, after the Museum of History in Stara Zagora had organized a donative campaign to pay for the conservation-restoration of the flag, the object was taken for treatment. It was in an extremely poor condition: heavily discolored, fragmented, desiccated, very fragile and much stiffened by the consolidating and lining adhesives; with areas, where the silk fragments were lost together with the lining support. The flag joins other authentic cultural heritage items to form a selection of different artifacts, which are planned for analysis within the framework of the research project *Laser-induced fluorescence analysis for investigation and conservation of cultural heritage*.



Areas with lost fragments and deformation in the left upper corner of the object

The project is being realized at the Institute of Solid State Physics at the Bulgarian Academy of Sciences and its funding is provided within the program “Young Researchers – 2011” by the “Scientific Research” Fund at the Bulgarian Ministry of Education, Youth and Science. The flag attracted the attention of the project team members with its strongly discoloured appearance, whose interpretation in the old restoration documentation strangely differs from the initial description of the

flag. The 1963 documentation reports that the upper strip of the object is blue and not white as it appears in the documents of the Stara Zagora Museum. The research team hopes that despite the present adhesive products, the analyses would help to identify the dye-substances used and to find the truth about the original colour of the upper strip of the artifact.

The standard approach to investigating the flag has to be modified, since the present adhesive products will affect the procedures and their results. Unfortunately, the attempts to remove the adhesives were unsuccessful. The object being highly fragile and heavily fragmented, the attempts to extract the adhesive substances need to be kept within the most delicate approach, which avoids any drastic manipulations. Moreover, the full extraction of the adhesive products, which have thoroughly impregnated the thin fabric, could lead to total destruction of the highly degraded silk material. The tests made with different solvents, applied by different methods both individually and in mixtures, gave no positive result. It was however found out that the bouquet of aged adhesive products swells in water and that the wet textile materials show a distinctly increased flexibility. This empirical finding allowed the much-needed entire wet cleaning of the flag to be undertaken. The cleaning removed a considerable part of the dust and dirt as well as the yellow products of the fibers’ destruction; it also gave the opportunity to flatten the deformation of the silk and cotton fabrics by gradually drying the flag under press. Another positive finding of the tests is that the non-affected by solvents old adhesive lining can however be removed mechanically; when the stiff and fragile threads of the tulle are detached the flexibility of the silk fabric increases. Assistance to the increased flexibility gave also the new lining with BEVA 371 solution, whose film is very supple. Despite the reluctance to add new adhesive products to the original, the adhesive treatment (lining) turned out to be inevitable, because any stitching through the fragile silk fabric would definitely perforate and additionally damage it. The choice of lining adhesive fell on BEVA 371 solution also in connection to its ability to form non-shiny transparent film, which was

a strictly required property because of the fact that the object is a single-ply flag of two faces. The film of BEVA 371 solution, formed on an appropriately dyed support of silk crepeline, is very thin; the sealing temperature was kept well under the melt-temperature level (95°C) so that the adhesive would only superficially stick to hold the flag's fragments and not melt to impregnate the original fabric. This variant of "cautious" lining provides a possibility to continue on trying to remove the old lining adhesive in the future.



The reverse side of the flag after the new adhesive lining with BEVA 371 solution has been executed

The investigation and conservation-restoration treatment of the flag are not yet completed. The present and further procedures are aimed at preserving the survived tangible evidence and at reducing the risks of its damaging. The conservation-investigation process will try to contribute to the list of the analyses applied so far and to enrich the information for the artifact and its long history.

REFERENCES

- Krasteva, E. 1991. Problems during the second restoration of flags. Bulletin of the National Museum of Military History vol.IX: 83-87 (in Bulgarian).
- Semyonovich, N. N. 1955. Restoration and investigation of works of art. Moscow: 52-79 (in Russian).
- Semyonovich, N. N. 1961. Restoration of museum textiles. Theory and technology. Leningrad (in Russian).

New method of building stones' analysis used in the study of the Historical City Wall of Cluj-Napoca, Romania

P.C. Răcățăianu

"Babeş-Bolyai" University, Department of Geology, Faculty of Biology and Geology, Cluj-Napoca, Romania

Abstract: For higher classification accuracy and the indexing of the degradation and deterioration processes of building stones, a new damage mapping system, based on the Bernd Fitzner's methods of monuments' mapping, was developed to organize all the data during- and post- research. The NDMS was developed in MS Excel to synthesize the high amount of different information resulted in the damage-weathering-restoration research project of the Historical City Wall's dimension stones from Cluj-Napoca, Romania. The analysis allows identifying all visible macroscopic features of each block of the monument, numbered and noted in tables according to the rock type-, sound speed test-, moisture-, and damage mappings. Thus, the tables contain specifications about the type of rock, colour, texture, structure, deteriorations, sound speed tests, percentage of moisture, and type of alteration processes. These data are used for automatic generation of graphics to help in the exposure and the interpretation of values obtained. Special functions and formatting assigned to cells shorten and simplify the introduction of values, make it easier to link different data, avoiding the time consuming. NDMS can be updated to collect other additional data such as OM, XRD, X-ray Fluorescence, SEM, chemical analyses of building stones and mortars, climate and pollution data etc. The widescreen aspect thus obtained provides a simple but effective display of the edifice/monument/architectural element's "health condition" (a joint overview between data collected in situ, in laboratory, and resulted from the environment's particularities), combining simultaneously graphics with statistical data.

1 INTRODUCTION

1.1 *General aspects*

The main characteristic of "Project NDMS" consists in its interdisciplinarity, comprising the computer science and database management, the study of human kind past and its cultural heritage, and not lastly the Earth system science and geochemistry. All these domains join within New Database Mapping System (NDMS). At the end, the final result will consist in providing a new solution contributing to the conservation of world cultural heritage.

1.2 *Facts*

Worldwide, all natural building stones and all the natural stone monuments are affected by direct contact with the atmosphere. Complex physical, chemical and biological processes alter the stone. The decomposition of the rocks is called weathering, which cause changes in colour, texture, strength, chemical composition, or other properties of the

natural material due to the action of the weather (*Harris, 1975*). Therefore all natural building stones will be weathered, dissolved and/or eventually disintegrated into grains or sand. Also, the anthropogenic influences, such as processing of the rock by cutting or shaping, generate micro-fissures on the surface. This may accelerate weathering and later overwhelming urban exposure accelerates the decay. The presence of the binding materials (mortars) and the interactions with the natural building stone give more complexity to the research.

To understand the complex interactions that occur between building stones and the surrounding environment requires an interdisciplinary approach with the work of geologists, mineralogists, material scientists, physicists, chemists, biologists, architects and historians (*Siegesmund et al., 2002*), therefore the nature of such projects must be an interdisciplinary approach. In the field of geology, the study of the natural building stones and also their interaction with the binding elements is one of the most complex research field related to the cultural

heritage conservation. For making the conservation and/or the restoration possible, several steps have to be followed before. With an interdisciplinary approach the objective proposed for restoration or/and conservation has to be evaluated within a research project, which must provide information about: the history of the edifice and his nowadays socio-economic and cultural heritage value (by historians and architects); the construction of the edifice - original blue-prints and architectural details (by architects); the mapping of the edifice - the present condition related to the original state of the art (by geologists and architects); the construction material study (by geologists, mineralogists, material scientists, physicists, chemists, and biologists); the proposed techniques and/or solutions for further restoration/conservation in regards with the economic point of view (by geologists and architects); the restoration/conservation actions (by restorers); and the observations of the edifice's behaviour after the conservation/restoration (by geologists, mineralogists, material scientists, physicists, chemists, and biologists).

1.3 Solutions

In the recent years classical and newly developed techniques have been used to study the constructions, their weathering and damages, the interactions between the materials, and the processes that occur from these interactions. For the study of the construction material (building stone) classical methods widely used nowadays are: the monuments mapping, photogrammetry, thin section analysis, XRD bulk and clay minerals analyses, CaCO₃ content, salt analyses, chemical analyses, physical-mechanical tests, sound velocity measurements, E-module, moisture measurements, etc.. The laboratory results represent an important part of damage investigation. They are essential for preservation and conservation actions (*Fitzner & Heinrichs, 1998a*). As a conclusion of years of research and observations, *B. Fitzner and K. Heinrichs (2002)* collated a table which contains a classification of the alterations. The experience has shown that direct investigation on factors and processes of stone deterioration is quite difficult and very time, and cost consuming and the results are

often “insufficient and unsatisfactory”.

The scientific analysis, evaluation, quantification and rating of stone damages are essential for effective and economic monument preservation measures. Therefore, a non-destructive method for the monument degradation mapping has been developed (*Fitzner et al., 2002*) as a non-destructive procedure for precise registration, documentation and evaluation of lithotypes and deterioration phenomena, being well described by *Fitzner and Heinrichs (1998a, 1998b, 2002)*, *Fitzner et al. (1997)*, *Fitzner and Kownatzki (1997)*, and *Kownatzki (1997)*.

The difficulty of the problem consists in the difficulty of explaining the results by using the nowadays methods. These are consisting in large amounts of information more or less grouped in tree-like categories. For important restoration projects the volume of collected data in situ, and later the information gained in laboratory is very large. The problem remained unsolved is the standardization of the final data. Each project is different, each studied edifice is different, and the weathering processes can vary from environment from environment even for the same type of building stone. The complexity of such kind of projects requires a standardized model, which will collate and correlate all the researches, analyses, data and techniques, to offer more accurate conclusions and to reduce the time and money consuming. The end user has to access the data easily and also has to be able to correlate them with other restoration projects information for more accurate interpretation and for more effective and sustainable calculation of the costs.

2 NEW DAMAGE MAPPING SYSTEM (NDMS)

2.1 The new idea (Methods)

During a PhD study, a new mapping system (NDMS) was developed (*Fig. 1*) using MS Excel 2007, which collate the information, converting the data into statistical calculations, and producing a graph of the statistics. NDMS is strongly related with the classical monument mapping method, which guarantees results contributing essentially to precise damage diagnosis.

Figure 1: The New Damage Mapping System interface, a seven-sections Excel Sheet. Legend: 1 – the number on the map section; 2 – rock type section; 3 – hammer clash test section; 4 – moisture section; 5 – macroscopic weathering processes section; A – control and total calculation section; B – calculation section (Răcățăianu, 2010).

The monument mapping method is recognized internationally and has been applied successfully worldwide. The method guarantees: objective and reproducible mapping of lithotypes and weathering damages, quantitative evaluation of damages as function of lithotypes and monument characteristics, scientific rating of damages, information on causes and mechanisms of damage, evaluation of damage progression, damage prognosis, information for optimal application of additional investigation methods, information on necessity/urgency of preservation measures, and recommendations of appropriate preservation measures (Răcățăianu, 2010). To benefit from all measurements and to allow optimum use of the data collected, all the information are indexed by NDMS, for each block of an edifice separately and subsequently grouped in specific categories. As a consequence, the new proposed model gives the possibility of connecting all the input data, thus obtaining preliminary conclusions regarding the present state of the wall, the types of deterioration and the causes that triggered these processes. The method has been successfully used during the research of the historical town wall of Cluj-Napoca, Romania.

2.2 Study case - Historical City Wall of Cluj-Napoca, Romania. What is really the NDMS (New Damage Mapping System)?

In the study case “Historical City Wall of Cluj-Napoca, Romania” the data collected in situ, and later in the laboratory, were separated in four Excel sheets. Each sheet contains a table partly divided into 5 main

sections and 2 side sections (Fig. 1). A category, called "Total", was chosen to group the results obtained in the previous four sheets thus facilitating final analysis on the research and production of useful graphics. Thus, the analysis allows identifying all properties and all visible macroscopic features of each block of the wall, numbered and noted in the tables. The tables contain specifications about the type of rock, colour, texture, structure, degree of deterioration, the result of sound speed test (clash test mapping), the percentage of moisture measured at the surface of the rock and the alteration types of processes observed macroscopically.

To benefit from all the measurements and to allow optimum use of all data collected the information were grouped in the new database model of each block separately. The overall content of the information in the table renders an overview for the present state of the wall. As a consequence, this model gives the possibility of connecting all the input data, thus obtaining preliminary conclusions regarding the present state of the wall, the types of deterioration and the causes that triggered these processes. Thus, using MS Excel 2007, the data collected from the four locations (A/N - the Historical City Wall of Cluj was split during the research in four distinctive parts/locations) were separated in four Excel sheets (Fig. 2) and named "L1 full, L2 full, L3 full and L4 full", representing each location separately.



Figure 2: The collected data separated in four Excel sheets.

In details, The New Damage Mapping System interface is a seven-section Excel Sheet. *Section 1, Number on the map*, contains the numbers of each block as it was made from mapping, to respond to reality. Therefore, at any time identifying the block mapping table or vice versa can be done easily. Each horizontal row of the table is representing a block of stone.

Section 2, Rock type (Fig. 3), is divided into 4 columns, each representing one type of rock (building material) identified as being used to build the wall.

Rock Type			
Limestone	Sandstone	Mortar	Brick/ Other
1			

Figure 3: Rock type section

An important detail of this model “database” and spread sheet, which involves the functioning and implementation of these tables in Excel, is the association of colour with numeric values. Thus, if one block was identified as limestone, a dye cell was assigned for the right block number in a pre-established colour, yellow-orange in the case of limestone, khaki green in the case of sandstone, light blue in case of mortar and dark red in the case of bricks. This way of presenting data by associating the information with certain colours finally lead to a graphical representation, making it easier to observe evolutionary processes and the degree of this, grouping all the information that normally would fill dozens of pages and being difficult to manage and associate in one place. If the cells were filled with a certain colour graphics using only the tools (e.g. "Fill Colour") a simple coloured table were obtained, without virtually numerical value. Special formatting of the cells that allows the introducing of numerical values in cells having as result a colour was used.

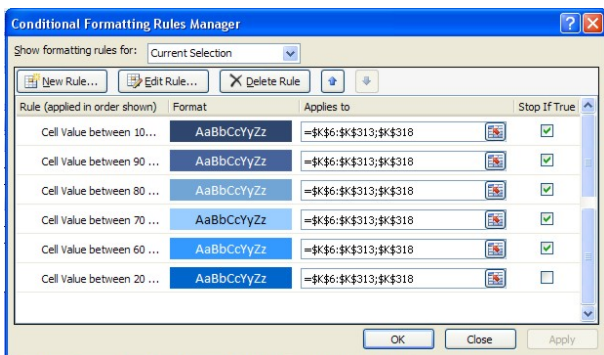


Figure 4: Conditional formatting option rules manager in MS Excel

Using the "Conditional Formatting" in MS Excel 2007 (Fig. 4) each set of cells in a column was given different properties. Therefore, the table contain only the value "1" or no value in almost every section for statistical reasons. Following this idea, special conditions were assigned to the cells in the column

"Limestone" by which, when typing the number "1" the cell will automatically show not only the numbers that it contains, but also the right colour for the text. Consequently, the result is a coloured cell that contains a numeric value "1", but the text/number entered is not visible because the cell and the text have the same colour. (Răcățăianu, 2010)

For example, a block was identified as “limestone” corresponding to the value “1”. Because all cells in column "Limestone" were attributed to the condition that at the introduction of automatic value 1 to be coloured yellow-orange, both cell and text are automatically coloured (Fig. 3), and it was not needed to use the "Fill Colour" option. If a block was not identified as “limestone”, no value was introduced, leaving the cell empty, inserting the value "1" in one of the cells in these columns (Sandstone, Mortar and Bricks) depending on its nature. The result is a graphical representation of the map with the presence of different types of rocks from bottom to top and in the same time cells containing numeric values which will help later for the statistical calculations. The same principle was applied to all the sections of the table designed to acquire data, excepting the moisture measurements section, where a simple arithmetic mean was used to obtain a unique value after several measurements.

Section 3, Hammer clash test (Sonic velocity) (Fig. 5) is structured on three columns called "OK", "Partial OK" and "Bad" and presents, in the same way as the previous section.

Hammer clash test (sound velocity test)		
OK	PARTIAL OK	BAD

Figure 5: Hammer clash test section

Section 4, Moisture measurement (1st measurement, 2nd measurement and 3rd average measurement) groups into three columns humidity values measured by hydrometer GANN at the rock surface.

Within the research project of the historical wall, several mappings have been accomplished. The mappings methods developed by Bernd Fitzner have been adapted to the specific needs of this project and of NDMS. Therefore, the data collected in situ have been used to create maps of rock types used for the construction, of mortars, of damages, and of the moisture at the surface of the wall (*Fig. 10*).

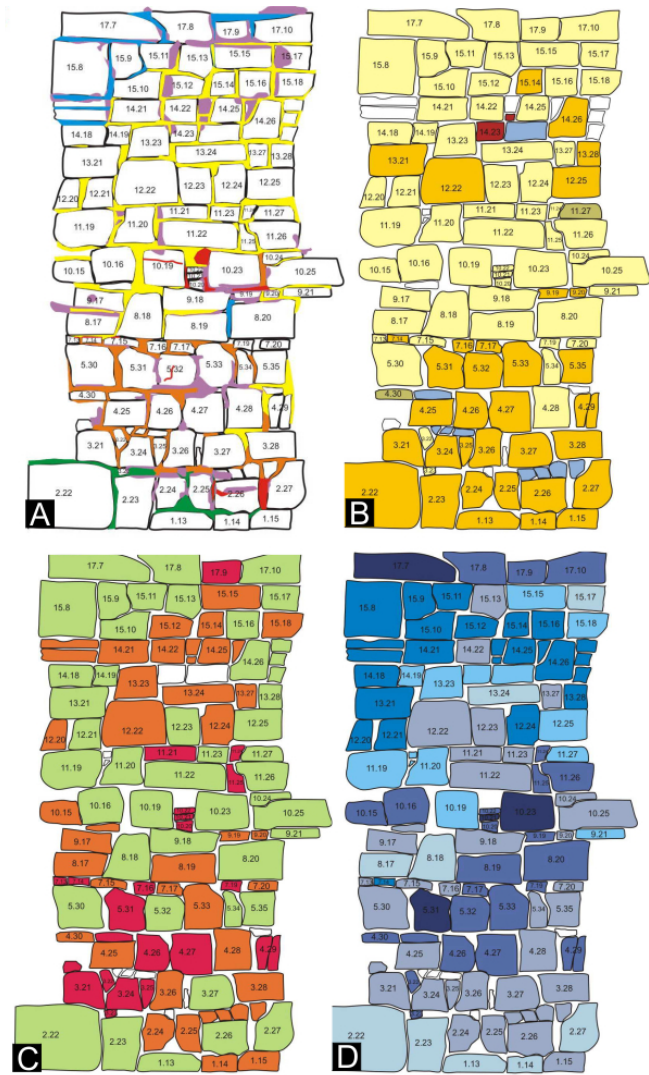


Figure 10: Examples of mappings used at Historical City Wall of Cluj-Napoca, Romania. Legend: A- Mortar type and damage mapping; B – Rock type mapping; C – Damage mapping; D – Moisture mapping, after Răcățăianu, 2010.

The mappings, according to Răcățăianu (2012), indexed all the blocks of the wall, each block being numbered. In the NDMS, the blocks have been inputted using the method described above. Then, NDMS collected the data from the mappings (by a non-automatic process), generating ‘Excel mappings type’.

Figure 11 presents an example of how NDMS generates results. The table offers a map view the

wall section mapped in Figure 10. Therefore, the bottom of the table represents the bottom of the wall and the top of the table, represents the top of the wall, as the blue arrow indicates. In other words, this is a transposition of the wall in Excel. Observing the sections A, B, C, and D of the *Figure 10*, we are able to draw interesting observations and conclusions. In section D, we noticed the increasing of the weathering processes’ incidence in the middle part. Moreover, the ‘light’ weathering processes are present all over the wall surface, while the severe weathering processes occur on the top of the wall.

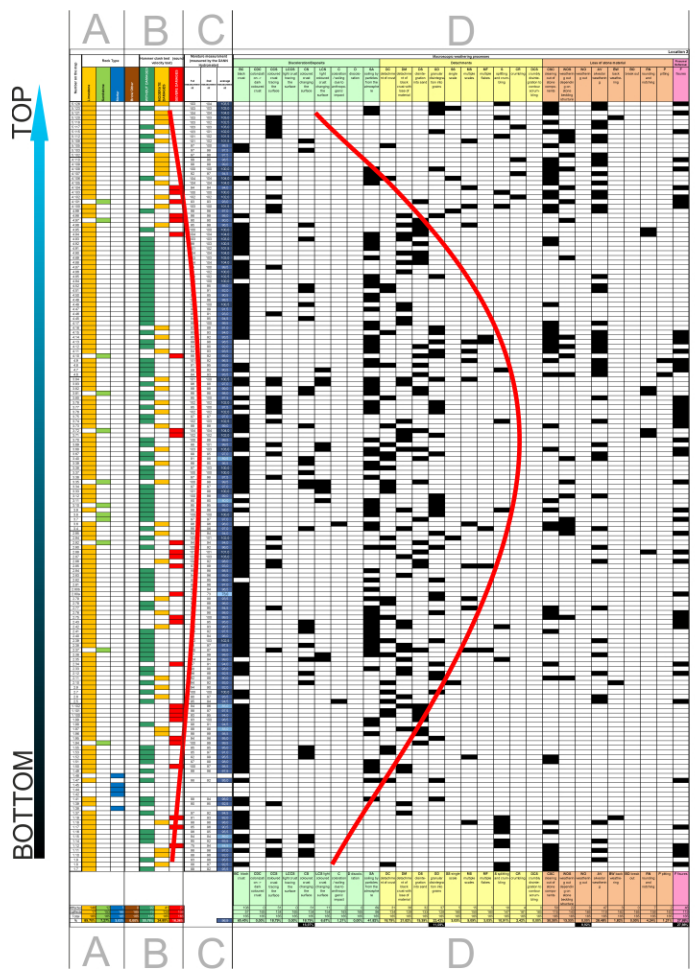


Figure 11: The transposition of the wall section mappings and measurements into NDMS. Section A collects information about the rock types, section B - about the decay ratio, section C - about the moisture content measured on the wall surface, and section D - about the incidence of the weathering processes identified in situ (after Răcățăianu, 2010).

In the same time, in section C, the present of moisture, indicated by the dark blue color, is higher on the upper part of the wall than the lower part. Not the least, the damage scale from section B, indicates the middle part of the wall as being the most affected. Concluding, the integrity of the wall is

more affected in the middle part of the wall (indicated by the red curves), where the moisture content starts to increase. On the top of the wall higher plants grow, contributing to the weathering. The constant presence of the water in the upper and the middle part provided by rain and by the higher plants' roots generates inside matrix dissolutions. Later, the insulation, the freeze-thaw cycles, and the winds generate microfissures due to the absence of the matrix, the development of secondary gypsum and because of the physical forces involved. This gives to water, to pollutants, and to dust particles easy access to the fresh rock. The cycle is restarted and the decay advance inside the rock step by step.

These conclusions have to be correlated with the chemical analyses, with the X-Ray diagrams, with the thin sections analyses, SEM pictures, salt analyses etc. to offer accurate conclusions and further solutions for restoration and/or conservation. The most important thing is that NDMS can also collect this kind of data, generating more complex 'Excel maps'.

2.4 Future work

The future work will consist in upgrading of the NDMS, and the development of a large database using a common database Management System (DBMS), such as MS Access, containing information gathered by the NDMS. Further interconnection between NDMS and MS Access, by means that MS Access automatically collects the input information from NDMS as database entries is also one of the further objectives. Therefore, the next steps will be: 1. *Upgrade* by adding new fields in the NDMS programs will allow the input of new type of information, data obtained in laboratories such as: Optical Microscopy observations (OM), quantitative XRD measurements, X-ray Fluorescence data, Scanning Electron Microscopy observations (SEM), porosity and permeability measurements, chemical analyses, climate and pollution particularities; mineralogy composition; paleontological and micro-paleontological observations depending on the natural building stone type. This will expand the area of the applicability of NDMS and will transform the simple MS Excel sheet in a virtual front-end of the database. In the same time, by extending its possibilities, new

radio buttons list-like will be used to facilitate the usage. 2. *Develop the database* by using the Link to Excel data in Access, the information collected by NDMS will consist in a database as an integrated collection of data records. MS Access will allow different the user application program to concurrently access the same database if is installed on a server or to import later the exported MS Excel data. The database will be structured as a network structure. The database has to be able to collect all data types used. 3. *Gather new data* by producing new analyses within new study cases in order to develop NDMS. 4. *Building the database* by adding available information from other available projects.

2.5 Contribution of NDMS to the conservation of cultural heritage

The contribution to the field of conservation/restoration the cultural heritage by the continued development of the NDMS is of very important value. Basically, there are no limits of the current approach in the context of the state of the art in this field because is the first attempt of a database which can connect information collected in different projects from all over the world in order to attempt standardized correlations between the types of the construction materials, the weathering processes, the environment characteristics, and the laboratory analyses. NDMS can fill the gap occurred by the non-existence of such a dedicated software, saving money, time and large amounts of work.

3 CONCLUSIONS

NDMS is a new mapping system, which collate the information, converting the data into statistical calculations, and producing graphs of the statistics. NDMS is strongly related with the classical monument mapping method, which guarantees results contributing essentially to precise damage diagnosis. NDMS can be standardized for use also on Palm PC and/or Notebook and can be upgraded with other "custom add-ons". The widescreen aspect provides a simple but effective display of the "health condition" of the objective of study and also combines the graphics with statistical data. The idea, the development, and the final

product are original, but we do hope for future collaborations with partners interested in developing of this solution. When the project will mature, the product will be available for end-users, adding a new step in the cultural heritage conservation domain. Finally, the end-user will be able to adjust NDMS according to its needs and will use the mapping system on the field, in situ, like a portable application.

ACKNOWLEDGMENTS

The financial support was provided through the Sectoral Operational Programme for Human Resources Development 2007-2013, co-financed by the European Social Fund, under the project number POSDRU 89/1.5/S/60189 with the title „*Postdoctoral Programs for Sustainable Development in a Knowledge Based Society*”.

REFERENCES

- Harris C. M. (1975) *Dictionary of architecture and construction*, McGraw-Hill, New York
- Fitzner, B. & Kownatzki, R. 1997. Erfahrungen mit der Kartierung von Verwitterungsformen an Natursteinbauwerken. In W. Leschnik & H. Venzmer (eds), *Bauwerksdiagnostik und Qualitätsbewertung, WTA-Schriftenreihe*, Heft 13, Stuttgart: Fraunhofer IRB Verlag: 157-172
- Fitzner, B., Heinrichs, K. & Kownatzki, R. 1997. Weathering forms at natural stone monuments – classification, mapping and evaluation. *International Journal for Restoration of Buildings and Monuments*, Vol. 3, No. 2, Stuttgart: Aedificatio Verlag/Fraunhofer IRB Verlag: 105-124
- Fitzner, B., Heinrichs, K. & Volker, M. 1997. Model for salt weathering at Maltese Globigerina limestones. In F. Zezza (ed), *Proceedings of the E.C. Research Workshop “Origin, mechanisms and effects of salts on degradation of monuments in marine and continental environment”, March 25-27, 1996, Bari, Italy*: C.U.M. University School of Monument Conservation: 333-344
- Fitzner, B. & Heinrichs, K. 1998a. Damage diagnosis at natural stone monuments mapping and measurements. *Proceedings of the 4th International Congress on Restoration of Buildings and Architectural Heritage, July 13-17, 1998*, Centro Internacional para la Conservación del Patrimonio, CICOP, Spain: 170-172
- Fitzner, B. & Heinrichs, K. 1998b. Evaluation of weathering damages on monuments carved from bedrocks in Petra/Jordan – a research project 1996-1999. *Annual of the Department of Antiquities of Jordan*, XLII, Amman: 341-360
- Fitzner, B. 2002. Damage diagnosis on stone monuments – weathering forms, damage categories and damage indices.– In Prikryl, R. & Viles, H.A. (ed.): *Understanding and managing stone decay, Proceedings of the International Conference “Stone weathering and atmospheric pollution network (SWAPNET)”, May 7-11, 2001, Prachov Rocks – Czech Republic*, Karolinum Press, Charles University, Prague
- Fitzner, B. & Heinrichs, K. 2002. Damage diagnosis on stone monuments - in situ investigation and laboratory studies. *Proceedings of the International Symposium of the Conservation of the Bangudae Petroglyph, Stone Conservation Laboratory*, Seoul National University, Seoul, Korea: 29-71
- Fitzner, B., Heinrichs, K. & La Bouchardiere, D. 2002. Damage index for stone monuments. In Galan, E. & Zezza, F. (ed.) *Protection and Conservation of the Cultural Heritage of the Mediterranean Cities, Proceedings of the 5th International Symposium on the Conservation of Monuments in the Mediterranean Basin, Sevilla, Spain, 5-8 April 2000*, Swets & Zeitlinger, Lisse, The Netherlands: 315-326
- Kownatzki, R. 1997. Verwitterungszustandserfassung von Natursteinbauwerken unter besonderer Berücksichtigung phänomenologischer Verfahren. *Dissertation RWTH Aachen*, Aachener Geowissenschaftliche Beiträge, Band 22, Aachen: Verlag der Augustinus Buch-handlung
- Racataianu, P.C. 2010 Dimension Stones of the Historical City Wall of Cluj-Napoca, Romania: Construction, Weathering, Damages, *PHD Thesis*, OPUS Erlangen-Nürnberg – der Dokumentenserver der Universität Erlangen-Nürnberg, 29-opus-20396/2010
- Siegesmund, S., Weiss T. & Vollbrecht, A. 2002. Natural Stone, Weathering Phenomena, Conservation Strategies and Case Studies: introduction. In *Natural Stone, Weathering Phenomena, Conservation Strategies and Case Studies*, Geological Society, London, Special Publication 205: 1-7

Gamma irradiation a chance for textile and leather heritage artefacts' conservation

Ioana Stanculescu, Valentin Moise & Corneliu Ponta

Horia Hulubei National Institute of Physics and Nuclear Engineering (IFIN-HH), Radiation Processing Centre, Magurele, Ilfov, Romania

Maria Haiducu, Steluta Nisipeanu

National Research and Development Institute on Occupational Safety Alexandru Darabont, Bucharest, Romania

Maria Geba

Moldova National Museum Complex, Iasi, Romania

Lucretia Miu, Ovidiu Iordache

National Research and Development Institute for Textiles and Leather, Bucharest, Romania

Abstract. The biocide effect of the ionizing radiation is indubitable. The method's efficiency recommends it for the disinfection of cultural heritage items. The TEXLECONS project "Improvement of occupational environment quality in cultural heritage deposits. Validation of gamma radiations treatment of textile and leather cultural goods" intends to expand the results obtained in 3 previous projects on the radiation treatment of polychrome wood and paper to leather and textiles. After the irradiation treatment bioburden and artifact changes depend on the absorbed dose. The project has two main objectives: 1. Study of the microbiological contamination of the textiles and leather heritage items, cultural heritage deposits and workplaces to establish a maximal contamination limit that will lead to a minimum required dose for treatment. 2. Study of the radiation induced degradation on heritage items that will lead to a maximum allowed radiation dose for treatment. This paper gives a brief description of TEXLECONS project.

1 INTRODUCTION

The classical approach for preservation of cultural heritage items involves the individual treatment of each item, using common disinfectants and cleaning agents but these methods necessitate mainly manual work, they are time consuming and cannot be applied for mass treatment of large quantities of items. Fumigation with different poisoning chemicals is one of the methods that can be applied for both the treatment of individual items and for mass decontamination. The use of these methods adds to the microbiological risk, the risk of using dangerous chemicals for the working personnel. Other methods like deep freezing or anoxic atmosphere are

environmentally friendlier but the treatment is not always effective against the resistant forms of the bio-contaminants: spores, eggs, pupae). Alternatively, gamma irradiation has major advantages: biocide effect guaranteed by reaching every part of the item with the right "killing dose"; fast turnaround (hours); the highest degree of penetration (mass treatment); simplicity (the material is irradiated in its transportation or storage package); can be applied to composites; the treatment does not leave any toxic or radioactive residues.

Irradiation with ionizing radiation, gamma rays or electron beams has proved to be one of the most effective disinfestations methods and a number of recent reports shows successful application of the this method for paper and wood artifacts (*Magaudda*

2004, Da Silva et al. 2006, Dettino 2007, Ponta 2008, Rela et al. 2007).

In case of irradiation treatment of cellulose there is always a concern regarding the degradation effects induced by the high energy photons and electrons. Studies performed in different countries showed that the proper choice of the irradiation dose can minimize the degradation effects and keep the efficacy of the treatment (Adamo et al. 2007, Bouchard et al. 2006, Bratu et al. 2009, D'Almeida et al. 2009, Gonzalez et al. 2002, Manea et al. 2012, Moise et al. 2010, Negut et al. 2007). The risk of artifact radioactivity after irradiation is totally excluded by the physics laws in the case of gamma rays and also by technical means in case of e-beam but the large molecules of natural polymers can be structurally affected.

There are very few reports on the ionizing radiation treatment for cultural heritage items containing leather (tanned or not) and textiles and fewer reports on the effects of ionizing radiation on the skin/leather or textile fibers from cultural heritage items.

The most spectacular applications of the irradiation treatment of items containing skin and textiles are the irradiation of the mummy of Ramses II (see references list) and the most recent treatment of Khroma baby mammoth Tran (2011) but the scientific dissemination of the results is very poor. In the case of the famous Pharaoh mummy, studies on the radiation effects were developed during two years on less valuable mummies but the results were published in a low circulation book, in French.

However the coordinating group of the project accumulated in the past 20 years a large experience on irradiation treatment of cultural heritage, in both ORIZONT 2000, PNCDI and PNCDI 2 research projects and cooperation over the time with more than 10 National Museums (see Fig.1 and Table 1). This cooperation included irradiation of samples containing leather, skin, parchment or textiles without being accompanied by testing of interesting physical and mechanical properties before and after irradiation. This lack of testing was due mainly to the reduced accessibility of state of the art analytical equipment in the '90.

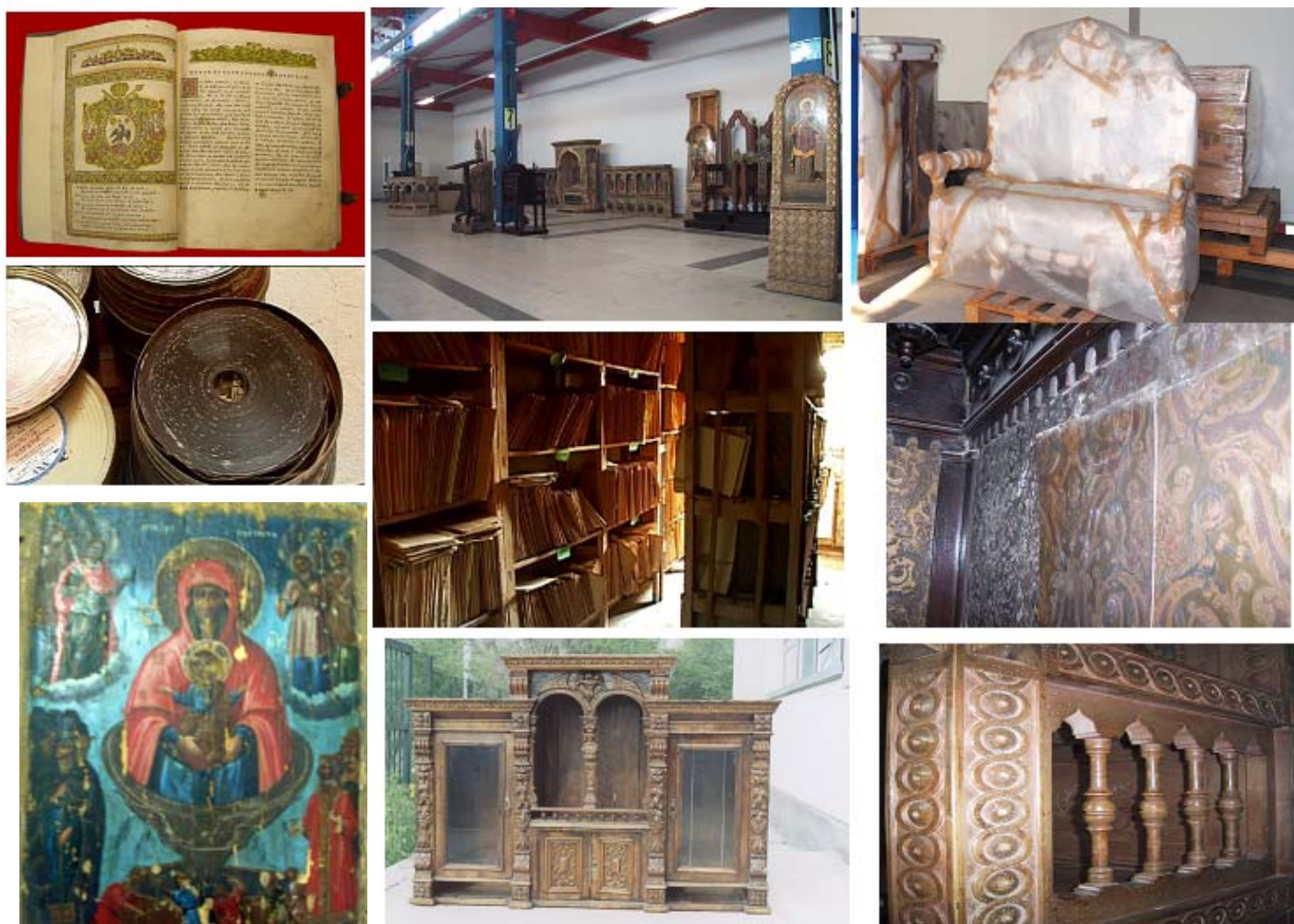


Figure. 1: Cultural heritage objects treated at IRASM

Table 1. Recent irradiation treatments performed at IRASM, IFIN-HH

No	Date	Beneficiary	Object	Volume	Ab- sorbed (kGy)
1	2002.04	Cotroceni Museum	Cupboard	1.5	6-12
2	2002.12	Izvoarele Church, PH	Iconostasis Furniture	10	1-10
3	2003.06	National Film Archive	Film	0.05	25-30
4	2005.05	T. Aman Museum	Doors Carvings	9	5.2-15
5	2005.06	National Library	Books	0.006	2.7-11
6	2005.10	Izvoarele Church, PH	Iconostasis	4.3	3-12
7	2006.04	Moldova Complex, Iasi	Icons, wood & textile objects	1.5	5-12
8	2006.05	Moldova Complex, Iasi	Furniture, Icon Parquet	0.5	2-20
9	2006.07	National Film Archive	Photographic Plates	0.1	7.7
10	2006.07	One Wood Monastery, VL	Cult objects	0.6	5.3- 12.6
11	2007.09	National Archive	Wood objects	0.25	5.1- 7.8
12	2008.11	INC DIE ICPE	Books, Revues	49.1	5.8- 8.7
13	2010.01	Bucharest City Museum	Wall paper	0.9	7.0- 9.3
14	2010.05	T. Aman Museum	Furniture	13.8	5-16
15	2010.05	IFIN-HH	Archive	15.8	6.2- 9.4
16	2010.08	T. Aman Museum	Furniture	18.5	3.5- 14.7
17	2010.09	National Film Archive	Film	0.0005	28.5- 38.2
18	2010.10	Private Collection	Old books	0.2	6.6- 8.0

Some information but also questions to be answered were gathered during the last two projects led by the coordinating group: ARCON (ctr. no 92083/2008) and DELCOM (ctr. no. 92086.2008).

Altogether leather, textiles and pigments were encountered during the study and application of irradiation treatment of paper (ARCON) and wood (DELCROM).

Same testing methods used for the characterization of gamma radiation effects of cellulose fibers and old natural pigments can be used for the development of the study of textiles and leather. The experience gained in the microbiological characterization of paper and wooden items and the characterization of storage and working conditions deposits of paper (archives) and wood will be used also. Additionally, Partner 3, National Research and Development Institute for Textiles and Leather has an extensive experience on the study of leather

degradation (natural or artificial) gained also in a recent R&D project (PNCDI 2 Parteneriate, Contract no 92-089/2008). The other two partners involved in the project are Alexandru Darabont National R&D Institute for Work Safety (Partner 1) and Moldova National Museum Complex (Partner 2).

2 OBJECTIVES

Cultural heritage goods made of organic materials: textile, wood, paper, leather, *etc.* are readily attacked by biodeteriorants: insects, fungi, yeasts, molds, bacteria *etc.*, which thrive and feed on them. Bio-deterioration is a natural process in which the metabolic activity connected with the growth of living organisms maintains the equilibrium in the matter transformation cycles. Bio-deteriorants affect all stages of textile processing and storage causing: discolouration, changes in appearance, loss of strength and elongation, partial or total destruction of the material with underlying chemical changes: oxidation state, degree of polymerization, breakdown of molecular structure *Katusin-Razem et al. (2009)*.

Biodeteriorants in items of vegetal origin are: fungi, the most active agents; the fungal genera *Chaetomium*, *Myrothecium*, *Memnoniella*, *Stachybotrys*, *Verticillium*, *Alternaria*, *Trichoderma*, *Penicillium* and *Aspergillus*; bacteria, of lesser significance, mainly the genera *Cytophaga*, *Cellulomonas*, *Cellvibrio*, *Bacillus*, *Clostridium* and *Sporocytophaga*, insects, the main families involved in textile biodeterioration are *Blattidae* (cockroaches), *Lepismatidae* (silverfish) and *Mastotermitidae*, *Hodotermitidae*, *Rhinotermitidae* (termites).

Biodeteriorants in items of animal origin: wool - keratinolytic bacteria, the most frequent agents, especially of the genus *Bacillus* (*B. Mesentericus* & *B. subtilis*), *Proteus* (*P. vulgaris*) and some species of *Actinomycetes* (*Streptomyces albus* & *Streptomyces fradiae*), *Pseudomonas aeruginosa*; - fungi, not very frequently involved, but reported those of the genera *Trichophyton*, *Fusarium*, *Chaetomium*, *Aspergillus*; - insects, cause the most serious damage of animal-derived textiles in museums; families: *Dermestidae*, *Oecophoridae* (brown house moth) and *Tineidae* (cloth moth), also *Tinea pellionella*, *Tinea bisselliella* & *Hofmannophila pseudospretella*; silk - bacteria,

predominantly: *B. Megaterium*, *Pseudomonas*, *Serratia*, *Streptomyces*, *Pseudomonas*, *Cepacia*, insects, cause most serious damage.

Fungi play a considerable role for the deterioration of cultural heritage. Due to their enormous enzymatic activity and their ability to grow at low water activity values fungi are able to inhabit and to decay paintings, textiles, paper, parchment, leather, oil, casein, glue and other materials used for historical art objects. In museums and their storage rooms, climate control, regular cleaning and microbiological monitoring are essential in order to prevent fungal contamination. Education and close collaboration of mycologists and restorers are needed to develop object specific methods for the conservation and treatment of contaminated objects.

All this biological threats will affect not only the cultural heritage artifacts but also the health of the people working with them. Due to the specific contamination of the old items (textiles and leather are usually recovered from archeological sites and graves), the problems related to the work environment may be considerable different from the usual workplaces that are dealing with biological threats (hospitals and other health care facilities). This is the reason for looking for new sanitizing methods and agents to be applied for cultural heritage storages and workplaces.

The fungicidal and bactericidal effect of the ionizing radiation is indubitable. Radiation sterilization is currently one of the few existing industrial sterilization methods used in the field of the manufacturing of medical devices and pharmaceutical products with a market share of over 50% for the single use sterile medical devices. The efficacy and efficiency of the method recommends it for the sanitization of cultural heritage items but its application is restrained due to the degradation effects encountered in the case of multiple and diverse natural polymers of the cultural items, already degraded by natural ageing or physical-chemical or biological factors.

The TEXLECONS project intends to expand the results obtained in 3 previous projects (PNC DI BIOTECH Prioritar, PNC DI 2 Parteneriate, Contract no 92083/2008, PNC DI 2 Parteneriate, Contract no 92086/2008,) for the radiation treatment of polychrome

wood and paper for two other categories of important materials for cultural heritage: leather and textile.

Leather is a totally different material from wood and paper (where cellulose is the main constituent). The collagen structure, which is generally resistant to ionizing radiation, is already altered by the tanning and ageing and there are almost no reports for the study of radiation effects on leather items.

Collagen is the main structural component of parchments and leather. Parchment structural matrix is predominantly composed as a composite of the hierarchical protein – collagen (*Kennedy & Wess 2003*). The hierarchy from the molecular to the fibrillar arrangement of collagen implies three polypeptide chains that are arranged into a triple helix to form a collagen molecule. Collagen molecular units, in their native form, are bound in a quarter staggered axial arrangement which subsequently produces a collagen fibril (*Hodge & Petruska 1963*).

To this day, 29 distinct collagen types have been characterized and all display a typical triple helix structure (*Parenteau-Bareil et al. 2010*). Collagen types I, II, III, V and XI are known to form collagen fibers. Collagen molecules are comprised of three α chains that assemble together due to their molecular structure. Every α chain is composed of more than a thousand amino acids based on the sequence -Gly-X-Y-. The presence of glycine is essential at every third amino acid position in order to allow for a tight packaging of the three α -chains in the tropocollagen molecule and the X and Y positions are mostly filled by proline and 4-hydroxyproline (*van der Rest & Garrone 1991; Prockop & Kivirikko 1995*).

Collagen consists of macromolecular chains of various kinds of amino acids and is a significant constituent of various tissues and organs. Gamma rays can destroy proteins through their high energy and peroxidated radicals. Furthermore the proteins will denature or oxidize and lose their original bioactivity function (*Yu-Chang Tyan et. al., 2002*).

Cheung et al. (2004) showed that collagen molecules are readily damaged by γ -radiation at dosages commonly used for sterilizing biomedical products. At 1 Mrad, while the reported effectiveness of the radiation at such a low dosage to completely

sterilize a material is questionable, less damage was caused to the collagen peptide backbone. Above such dosage, however, significant damage was clearly demonstrated with collagen alone and collagen in a chemically crosslinked tissue matrix. Molecular weight analysis showed a significant number of peptide bonds being cleaved by the radiation which could cause considerable changes in the long-term characteristics of the material.

After exposure of collagen to gamma ray irradiation, of more than 15KGy, a change of structure was signaled in amide I and amide II structure, which indicates the change of structure from R-NH-R' to R-NH₂, which leads to the conclusion that the decay of amide groups is provoked by gamma ray irradiation. Relatively significant decreases of amide groups have been found at gamma ray exposure doses of more than 10 KGy. The structures are not degraded linearly. Oxidation or amide degradation (broken of -C-N) generally is the cause of such degradation (*Yu-Chang Tyan et. al., 2002*).

Gamma ray degradation of collagen, results in the scission of the peptide linkage (or hydrogen abstraction) and nitride decomposition, which are combined with oxidative reactions. The irradiation sensitizes collagen-bonded surfaces (*Yu-Chang Tyan et. al., 2002*).

For textiles based on cotton, some similarities can be found both in the study of paper degradation or in sterilization of cotton sterile medical products (gauzes, bandages etc.).

Cellulose is also the main constituent of all the vegetable fibers but the behaviour under the radiation treatment may be different from the pure cellulose (Whatman paper) due to the modifications already induced by the manufacturing process and ageing. Textiles using animal origin fibers (wool) will have a different behavior, since nor cellulose nor collagen are not the main constituents.

After the irradiation treatment, both bioburden (microbial load of the items) and degradation effects (chain scission, *etc.*) depend on the absorbed dose. High radiation doses will highly decrease the bioburden (exponential decay) and low doses will produce less degradation on the irradiated materials.

Under these circumstances this project proposal establishes two main objectives:

1. Study of the microbiological contamination

of the cultural heritage items (textiles and leather), cultural heritage deposits and workplaces in order to establish a maximal contamination limit. This will lead to a minimum required dose for the treatment.

2. Study of the radiation induced degradation on cultural heritage items and this will lead to a maximum allowed radiation dose for the treatment. The tests will be performed on both recent (reference) and naturally and/or artificially aged materials. For subtracting the cumulative effects, tests will be performed both to the whole material as it appears in the cultural artifacts and to constituents, raw materials and additives.

Finally one standardized method ISO 11137-2:2006 will be used for the substantiation of the decontamination dose and validation of the irradiation treatment. The process specification for irradiation treatment will be built as the first stage of the preparation of technological transfer of the use of the irradiation technology for leather and textile cultural heritage preservation.

An important objective of the project is the training component addressing two important topics for the workers in cultural heritage deposits and laboratories:

- environmental safety of the workplace and means of reducing of the biological threats when working with highly bio-contaminated items. This topic is dedicated to all kind of workers from cultural heritage preservation workplaces.

- radiation effects on irradiated materials. This topic is dedicated specially to conservators and restorers with the goal of clarifying misunderstandings related to the irradiation process and for increasing their capability for taking decisions on the appropriateness of application of the radiation treatment for a certain category of cultural heritage items.

3 CONCLUSIONS

The partners of the consortium were chosen to cover all the topics and foreseeable problems that can be encountered during the development of the project activities. Each of the partners has extended expertise and experience in participation in partnership R&D activities. The development of the TEXLECONS project will maintain and increase the

competitiveness of Romania, as member of European Union, in the field of Cultural Heritage Preservation.

ACKNOWLEDGEMENT

This work was funded by the ANCS, **PN-II-PT-PCCA-2011-3-1742** project, "Improvement of occupational environment quality in cultural heritage deposits. Validation of gamma radiations treatment of textile and leather cultural goods (TEXLECONS)" contr. no. 213/2012.

REFERENCES

- Adamo, M., Brizzi, M., Magaouda, G., Martinelli, G., Plossi-Zappalà, M., Rocchetti, F., Savagnone, F. 2001. Gamma Radiation Treatment of Paper in Different Environmental Conditions: Chemical, Physical and Microbiological Analysis. *Restaurator* vol. 22, 107131.
- Bouchard J., Methot M, Jordan B. 2006. The effects of ionizing radiation on the cellulose of woodfree paper. *Cellulose*, vol. 13 (5), 601-610.
- Bratu, E., Moise, I.V., Cutrubinis, M., Negut, D.C., Virgolici, M. 2009. Archives Decontamination by Gamma Irradiation. *Nukleonika* vol. 54 (2), 77-84.
- Cheung, D.T., Perelman, N., Tong, D., Nimni, M.E. 1990. The effect of γ -irradiation on collagen molecules, isolated α -chains, and crosslinked native fibers. *Journal of Biomedical Materials Research*, 24(5): 581-589.
- D'Almeida, M.L.O., Barbosa, P.d.S.M., Boaratti, M.F.G., Borrelly, S.I. 2009. Radiation effects on the integrity of paper. *Radiation Physics and Chemistry* vol. 78 (7-8), 489-492.
- Da Silva, M., Moraes, A.M.L., Nishikawa, M.M., Gattic, M.J.A., Vallim, de Alencard, M.A., Brandao, L.E., Nobrega, A. 2006. Inactivation of fungi from deteriorated paper materials by radiation. *International Biodeterioration & Biodegradation* vol. 57 (3), 163-167.
- Dettino, B.M.A 2007', Tratamento de salvaguarda em situação de emergência: a atuação do IEB em acervo cedido pela Justiça Federal de São Paulo, *Revista do IEB* vol. 44, 275-306.
- Gonzalez, M. E., Calvo, A. M., Kairiyama, E. 2002. Gamma radiation for preservation of biologically damaged paper. *Radiation Physics and Chemistry*, vol. 63 (3-6), 263-265.
- Hodge A.J., Petruska J.A. 1963. Recent studies with the electron microscope on ordered aggregates of the tropocollagen molecule, London, London Academic Press.
- ISO 11137-2:2006, Sterilization of health care products -- Radiation -- Part 2: Establishing the sterilization dose
- Katusin-Razem, B., Razem, D., Braun, M. 2009. Irradiation treatment for the protection and conservation of cultural heritage artefacts in Croatia, *Radiat. Phys. Chem.*, 78 729-731.
- Kennedy, C.J., Wess T.J. 2003. The structure of collagen within parchment – a review. *Restaurator Int J Preservation Library Archival Mater* 24:61-80.
- Magaouda, G. 2004. The Recovery of Bio-deteriorated Books and Archive Documents Through Gamma Radiation - Some Considerations on the Results Achieved. *Journal of Cultural Heritage* 5 (1):113118.
- Manea M., Moise I.V, Virgolici M., Negut C.D, Barbu O.H., Cutrubinis M., Fugaru V., Stanculescu I. R., Ponta C.C. 2012. Spectroscopic evaluation of painted layer structural changes induced by gamma radiation in experimental models, *Radiation Physics and Chemistry*, 81, 160-167
- Moise, I.V., Virgolici, M., Stanciu, C., Nisipeanu, S., Balan, Z. 2010. The treatment with ionizing radiation: A chance for the future of archives, *Restitutio - Buletin de Conservare-Restaurare*, vol. 3, 130-142.
- Negut D.C., Ponta C.C., Georgescu R. M., Moise I.V., Niclescu Gh., Lupu A.I.M. 2007. Effects of gamma irradiation on the colour of pigments, *Proc. SPIE Int. Soc. Opt. Eng.*, 6618, 66180R
- PNCDI BIOTECH Prioritar (2004-2006): "Produse si tehnologii pentru protectia (conservarea) obiectelor de patrimoniu impotriva agentilor biologici daunatori (microorganisme: bacterii, mucegaiuri, ciuperci, alge etc.; insecte: molii, carii, diferite specii de gandaci etc.)". CO National R&D Institute for Chemistry and Petrol-chemistry Bucharest.
- PNCDI 2 Parteneriate, Contract no 92083/2008 (2008-2011): ARCON - A chance for the future of the archives: Conservation by irradiation. CO Horia Hulubei National R&D Institute for Physics and Nuclear Engineering (IFIN-HH). Partners: CEPROHART SA, Alexandru Darabont National R&D Institute for Work Safety, Braila Museum.
- PNCDI 2 Parteneriate, Contract no 92086/2008 (2008-2011): Cultural Heritage conservation by salvation treatments of large volumes. Study oriented on decontamination by gamma irradiation of polychrome wood. CO Horia Hulubei National R&D Institute for Physics and Nuclear Engineering (IFIN-HH). Partners: National Institute for Wood, Astra National Museum Complex Sibiu, Moldova National Museum Complex.
- PNCDI 2 Parteneriate, Contract no 92-089/2008 (2008-2011): ETNO PEL: Techniques for Investigation, Assessment, Conservation and Restoration of Ethnographic Collagenous Materials. CO - National R&D Institute for Textiles and Leather (INCDTP). Partners: National R&D Institute for Electrical Engineering, National R&D Institute for Optoelectronics, University Politehnica of Bucharest National Center for Consultancy, Bucovina Museum Center of Suceava, - National Museum Center Astra of Sibiu, National Museum Dimitrie Gusti
- Ponta, C. C. 2008. Irradiation Conservation of Cultural Heritage, *Nuclear Physics News* vol. 18:1, 22-24.
- Prockop, D.J., Kivirikko, K.I. 1995. Collagens: Molecular biology, diseases, and potentials for therapy. *Annu Rev Biochem* 64:403-434.
- Ramses II - Les Films du Scribe (<http://www.lesfilmsduscribe.com/Ramses2themovie/index.html>)
- Rela, P.R., Gomes, F.F., Thomé, L.E., Kodama, Y. 2007. Recuperação de um acervo: uso da Radiação Gama (Cobalto 60) na descontaminação de objetos do acervo do Instituto de Estudos Brasileiros USP. *Revista do IEB* vol. 45, 285-272.
- Parenteau-Bareil, R., Gauvin, R., Berthod, F. 2010. Collagen-Based Biomaterials for Tissue Engineering Applications, *Materials* 3:1863-1887.
- Tran K., ARC-Nucléart: a workshop for conservation of cultural heritage using gamma irradiation. Croatian National Workshop, Zagreb 4-5 October 2011 (http://www.hr-z.hr/res/dbfiles/1319102882/3_q_k_tran_radijacijski_post_upci_u_zastiti_predmeta_kulturne_bastine_u_francuskoj.pdf)
- van der Rest, M., Garrone, R. 1991. Collagen family of proteins. *FASEB J.* 5:2814-2823.
- Tyan, Y.-C., Liao, J.-D., Lin, S.-P., Chen, C.-C. 2003. The study of the sterilization effect of gamma ray irradiation of immobilized collagen polypropylene nonwoven fabric surfaces, *J Biomed Mater Res A.* 67(3):1033-43.

The study of archaeological ceramic samples from Satu Mare County, Romania

E. Nagy, B. Kocsis, R. Barabás, Zs. Molnár-Kovács

Babeş-Bolyai University, Cluj-Napoca, Romania

M. Guttmann

Transylvanian Museum Society, Cluj-Napoca, Romania

Abstract: The article presents the study of the material composition and structure of some archaeological findings from four different sites (Andrid, Berveni, Carei, Pir) in Satu Mare county. In terms of chronology, the ceramics from Andrid belong to the Early Bronze Age, while the findings from Berveni, Carei and Pir belong to the Middle Bronze Age. Samples were collected from each location and the aim of the analyses was to gain information about the possible raw materials, production technology and conditions used by the ancient potters. The samples were analyzed by optical microscopy (OM), scanning electron microscopy and energy-dispersive X-ray spectroscopy (SEM-EDX) X-ray diffraction (XRD) and Fourier transformed infrared spectroscopy (FTIR). Analyses concluded that the raw material of the ceramics was based on kaolin and feldspars, silicium dioxid (sand) and some calcite were detected as thinners. Some picks in the FTIR suggest the presence of organic materials coming probably from the use of the pottery. The studied samples show different burning temperatures confirmed by the mineralogical composition determined with the above methods, but this temperature is above 600°C for each sample.

1 INTRODUCTION

1.1 *Archeological background*

In the region of the river Eriu, Bronze Age settlements have been discovered in the years after 2000. These settlements were rich in artifacts. Four of them were analyzed, selected randomly regardless of the different age and resources. The four sites are: Andrid, Berveni, Carei and Pir from Satu Mare county. The majority of the artifacts are simple pottery, but the sample from Andrid contains etched line pattern. In terms of chronology, the ceramics from Andrid belong to the early Bronze Age (3500-2000 BC), which takes part of the culture from Sanislău, while the artifacts from Berveni, Carei and Pir belong to the Middle Bronze Age (2000-1600 BC), representing the Otomani culture.

1.2 *The geological study of the archaeological sites*

Analyzing the geological map of the environmental region of the river Eriu and plain of

Carei it can be observed that is mainly characterized by sandy and gravelly soil. Besides, the region of Berveni it is characterized by marsh, while in the case of Carei and Pir red clay and loess can be also found. The sedimentary rocks of the river Eriu cannot be disregarded; it contains yellowish-red clay, sandy and fine-grained clay.

2 ANALYTICAL METHODS

2.1 *Sample characterisation*

2.1.1 *Macroscopic description of the samples*

The macroscopic observation of the samples was performed with a Nikon SMZ 645 stereomicroscope. Their detailed description can be found in *Tabel 1*. The color of the ceramic shows similarities, varying from shades of gray to black, probably due to reducing firing atmosphere. A thin brownish crust can be observed on the artifacts surface (<1 mm), having a color. The matrix of the samples is relatively homogeneous, without the presence of any specific fragment aggregates.

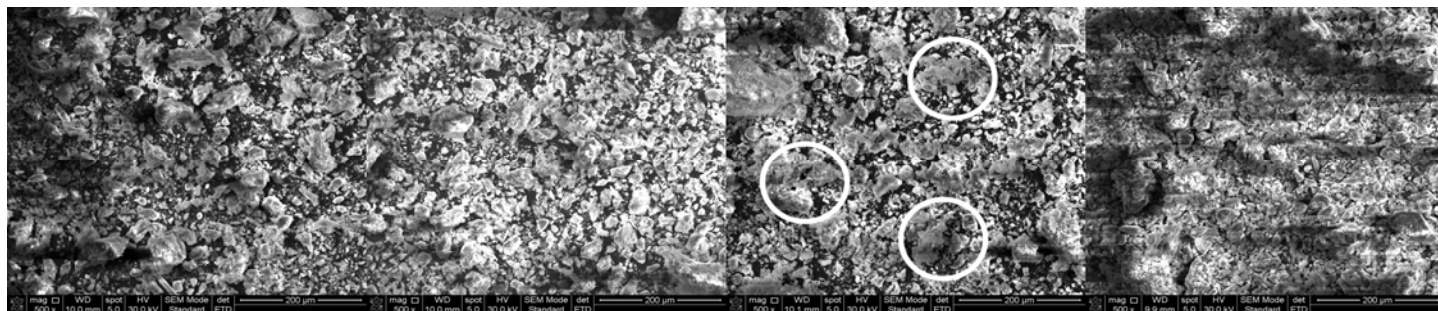


Figure 1. The SEM images of sample I., III., IV. and II. (500x)

The structure and granulometry of the matrix is variable from fine/ medium-grained to rough-grained. The diameter of the particles varies in a wide range up to 1-2 mm. Furthermore, it can be observed the presence of quartz grains, mica and clastic pottery. The values of porosity varies within a limited interval (between 0.5 x 1.5 and 2.0 x 3.0 mm), which is valid for the large, oblong-shaped pores (located parallel to one another) and for the secondary pores with irregularly shape. The production technology can be defined by the shape of the pores; in our case must have been plastic pressure.

2.1.2 Sample characterization by optical microscopy

Analyses were carried out with Nikon Eclipse E200 microscope on thin sections; microphotographs were taken with a Nikon FDX-35 camera. Based on granulometry, the samples can be divided into two groups: medium grained, as lutito-silto-arenitic type and coarse grained as lutito-arenito-siltic type of ceramics. Each sample contains clastic pottery, occupying 2-3 % of the matrix. The elements of the matrix appear in micro-crystalline and also in amorphous-micro-crystalline form. This characteristic of the matrix, and also the dominant nature of illite, the presence of kaolinite and montmorillonite suggest that the firing temperature does not reach too high values. The main components of the samples are: quartz, mica (muscovite and biotite), agglomerations of iron-oxide (predominantly hematite), the plagioclase group belonging to feldspars and also epidote, garnet, zircon. It also exist calcite in the samples, which also suggests a lower firing temperature than 850-900 °C.

2.2 Scanning electron microscope (SEM) and energy-dispersive X-ray spectroscopy (EDX)

The SEM-EDX measurements have been performed by Philips XL30 ESEM-FEG device.

Based on the SEM images the samples can be classified according to their grain morphology into three categories. To the first group belong samples I. and III., because in their material structure grains are individual which reflects a lower firing temperature. Sample IV. represents the second category. In some places – indicated with white circles in *Figure 1* - the observed particle fusion suggests higher firing temperatures than for the first group. Finally, the structure of sample II, representing the third group, indicates the highest firing temperature because the grains are stuck together. With the evaluation of the EDX spectra it can be observed that sample I. mainly contains silicon, oxygen and aluminum (aluminum silicates), the weight percentages are above 10%. Furthermore, in moderate percentages (3-10%) contains iron (usually in form of oxide) and carbon.

Compared to the principal components, it appears a very low amount (0-3%) of potassium, calcium, phosphorus, magnesium, titanium and sodium. The content of sample IV is similar to sample I., but there is a deviation in the average substances, which refers to iron and potassium and besides does not contain phosphorus, like the other samples. The composition of samples II and III is the same; the components are identical, only the amount of them is different. The SEM images in the case of these samples suggest that the structure is dissimilar which implies that the firing temperature is not the same.

Sample II is different from the other three due to its sandwich structure, which means that the outer layers of the ceramics fragment is light brown and the core it is black. The difference is probably due to the firing conditions, mainly the atmosphere in the oven.

2.3 X-ray diffraction (XRD)

A Shimadzu XRD 600 device was used for the XRD measurements. The X-ray diffraction studies

confirm the results of optical microscopy. All four samples mainly contain quartz, plagioclase (albite-anorthite) and also mica (signals appear at 10 and 5 Å). The presence of highly birefringent mica indicates that firing temperatures could not pass 900°C. The accuracy of the composition is also confirmed with the microscopic studies. The clay minerals suffer thermal conversion; their presence can be identified only by the lines at 4.5 and 2.6 Å. This fact also confirms that the firing temperature did not exceed 900-950 °C.

The signal at 3.03 Å confirms the presence of calcite in the samples. However, the ubiquity of iron-oxides (hematite and goethite) is more difficult to be identified because their signals overlap with the signals of other clay minerals.

2.4 Fourier transform infrared spectroscopy (FT-IR)

The type of the device used for the FT-IR measurements was Jasco FT-IR 615. During of the evaluation process it can be observed the absence of Al-OH bond at the wavelength 915 cm⁻¹ and OH bonds absence at 522 cm⁻¹, whereby it can be esteemed that the firing was above 600°C. This valuation is also confirmed on the FT-IR spectra by the absence of signals 3700 cm⁻¹, 915 cm⁻¹ in case of samples I. and II. and the weakening of bands at 1163 cm⁻¹ at sample III., and 1161 cm⁻¹ in case of sample IV. By rising the temperature the silicate structure collapses and this occurrence is accompanied by a broad symmetric band, which appears at 1030 cm⁻¹ for red clay, while for white clay at 1080 cm⁻¹. This band can be found at 1032 cm⁻¹ on the spectra of sample I. For samples II and III the signal is at 1034cm⁻¹, whilst in case of sample IV reappears at 1041 cm⁻¹.

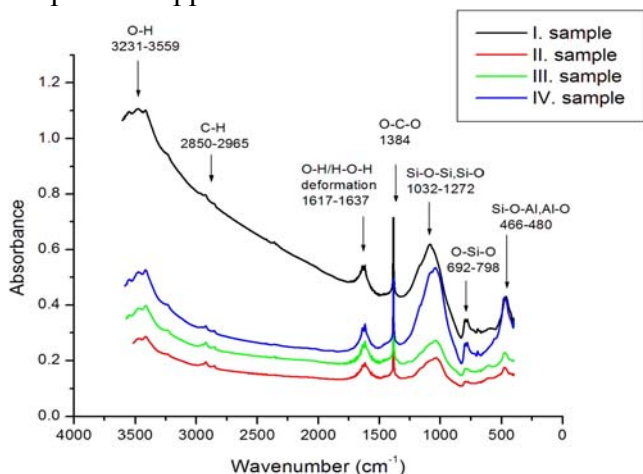


Figure 2: The absorption spectra of the samples in reference to

the entire measurement interval (4000-40 cm⁻¹).

Table 1: Evaluation of the identified bands.

Bond type	Collation
O-H	Kaolinite, Calcite, Illite, Mica, Montmorillonite
C-H	-
O-C-O	Calcite
Si-O-Si, Si-O	Kaolinite, Feldspar, Mica, Montmorillonite, Plagioclase , Epidote , Garnet
O-Si-O	Quartz
Si-O-Al, Al-O	Kaolinite, Feldspar, Illite

3 RESULTS SUMMARY

As the result of investigation it was concluded that all four samples (deriving from archeological ceramic artifacts founded at Andrid, Berveni, Carei and Pir) can be derived from the same raw material. Nevertheless slight variations exist, proved by the EDX analysis. The identified crystalline clusters are: quartz, mica (muscovite and biotite), the agglomeration of iron oxide (hematite predominates), epidote and garnet, zircon, and the plagioclase group belonging to the feldspar silicates as well. The embayed grains are represented by quartzite, mica and limestone. Clastic pottery is a component part of all samples. The authenticity of the results is proved collectively by the X-ray diffraction review, optical microscope and FT-infrared studies. The geological map also supports the presence of these raw materials in the area, but the demonstration of it requires the analysis of soil. Elements of matrix appear in micro-crystalline or amorphous-microcrystalline form, illite is predominant, however kaolinite and montmorillonite are present as well. From these facts can be concluded that the firing temperature was not too high. About the manufacturing method of ceramics primarily it can be said that due to greyish-black color of sample they used reductive atmosphere, moreover according to the shape of the pores they manufactured it with plastic pressure. Some of the samples have a noticeable thin layer (<1 mm) on the

outside which indicates in situ transformations, not the alteration of the firing conditions. For the plasticity of the clay the potters used sand, namely quartz or rather calcite. By the same token, they could use organic derivatives of plants or animals, which could explain the organic peaks in the IR spectra, nevertheless those could be subsequent impurities. The four artifacts differ from each other by the firing temperature, demonstrated by the FT-IR spectra and the SEM images also, although in all cases the firing temperature is higher than 600 °C but did not reach 800 °C.

ACKNOWLEDGEMENTS

We would like to render thanks to Dr. Veress Erzsébet for her useful observations. We gratefully acknowledge the work of the scientists performing the analyses, Prof. Dr. Marcel Benea (optical microscopy and evaluation of the XRD spectra) and Dr. Liliana Bizo (SEM_EDX and FTIR).

REFERENCES

- [1] Molnár-Kovács, Zs. A bobáldi régészeti ásatások jegyzőkönyve (Notes of the archaeological excavations in Berven) (unpublished)
- [2] Ovejanu, I.; Candrea, B. & Crăciunescu, V. 2011 Harta Geologică a României scara 1: 200 000 (The Geological Map of Romania), Facultatea de Geografie, Universitatea din București, Institutului Geologic al României (IGR).
- [3] Pataki B et al. 2011 Az FTIR spektroszkópia alkalmazhatósága régészeti kerámiák eredetvizsgálatában, Bitay, E. (Ed) FMTÜ XVI, EME-Cluj, : 239-242.
- [4] Ravisankar, R. et al. 2001 Spectroscopic techniques applied to the characterization of recently excavated ancient potteries from Thiruverkadu Tamilnadu, India, In Microchemical Journal, Vol. 99, 370-375.
- [5] D. Barilaro et al: Spectroscopic techniques applied to the characterization of decorated potteries from Caltagirone (Sicily, Italy), Journal of molecular structure, 2005, 827-831 old.
- [6] Adriana S. Cavalheri et al.: Vibrational spectroscopy applied to the study of archeological ceramic artifacts from Guarani culture in Brazil, Vibrational Spectroscopy, 2010, 164-168 old.
- [7] Bhaskar J. Saikia, Gopalakrishnarao Parthasarathy: Fourier transform infrared spectroscopic characterization of kaolinite from Assam and Meghalaya, Northeastern India, Scientific Research, 2010, 206-210 old.
- [8] Kevin D.O. Jackson: A Guide to identifying common inorganic fillers and activators using vibrational spectroscopy, The internet journal of vibrational spectroscopy, 1998, Volume 2, Edition 3.
- [9] Janey M. Cronyn: Régészeti leletek konzerválásának alapjai, Magyar Nemzeti Múzeum Kiadó, Budapest, 1996, 134-148. old.

This proceeding contains a part of the contributions to The Third Balkan Symposium on Archaeometry, organized in Bucharest, on 29 - 30 September 2012, by The National Institute of Research and Development for Optoelectronics – INOE and The National VillageMuseum „Dimitrie Gusti” from Romania.

The Symposium continues the tradition of previous Balkan Network of Archaeometry scientific meetings, the first being held in Ohrid - Republic of Macedonia in 2008 and the second in Istanbul – Turkey in 2010.

The event created – as previous editions, too - a frame for professional debates of ideas, for the most recent results reporting, and an opportunity for new advanced projects elaboration. This collection of papers have been submitted by representative groups from Balkans and other countries (Belgium, Italy, Egypt etc.) with strong traditions in Cultural Heritage investigation and archaeological researches.

This proceeding was published with the support of the project PN-II-PT-PCCA-2011-3.2.-0356 (WATCH)

ISBN - 13 978-973-88109-9-0

